THE SYNTHESIS OF DIMETHYLDIHYDROCYCLOPENT[a]PYRENE, ION(1-) AND ITS METAL COMPLEXES AND THE INTERPRETATION OF THEIR ^{1}H NMR DATA

by

Nasr A. Khalifa
B.Sc., University of B.C., Canada 1985

A Dissertation Submitted in Partial Fullfilment of the Requirement for the Degree of

ACCEPTED
FACULTY OF GRADUATE STUDIES

DOCTOR OF PHILOSOPHY

_____ DEAN

in the Department of Chemistry

DATE 1991-03-04

We accept this thesis as conforming to the required standard

Dr. R. H. Mitchell

Dr. K. R. Dixon

Dr. P. R. West

Dr. W. W. Kay

Dr. L. T. Scott

Supervisor: Dr. Reginald H. Mitchell

ABSTRACT

The synthesis of *trans*-11b,11c-dimethyl-11b,11c-dihydro-7H-cyclopent[a]pyrene, **109**, from *trans*-10b,10c-dimethyl-10b,10c-dihydropyrene, **32**, was achieved in six steps in an overall yield of 29%. Deprotonation of **109** gave the first annuleno-fused cyclopentadienide, *trans*-11b,11c-dimethyl-11b,11c-dihydrocyclopent[a]pyrene, ion(1-), **101**. Experimental and theoretical proton NMR results for the anion in the presence and absence of the counter cation were analysed. The cyclopentadienyl anion, when fused to **32**, has 53% of the effective bond-fixing ability of benzene fused to the same system. In terms of benzene resonance energy units, cyclopentadienyl anion has an effective resonance energy of 0.53.

Metal complexation of the cyclopent[a]dihydropyrene, **101**, was investigated, and gave the first two cyclopent-fused large annulene metal complexes, [6a,7,8,9,9a-μ^5]-*trans*-11b,11c-dimethyl-11b,11c-dihydrocyclopent[a]pyrene-pentamethylcyclopentadienylruthenium(II), **139**, and [6a,7,8,9,9a-μ^5]*trans*-11b,11c-dimethyl-11b,11c-dihydro-cyclopent[a]pyrene-tricarbonylmanganese(I), **141**. Experimental and theoretical ^{1}H NMR results for the two complexes were analysed. Ruthenocene, when fused to **32**, was found to be 1.38 times more bond-fixing than benzene itself. Similarily, cyclopentadienylmanganesetricarbonyl is 1.33 times more bond-fixing than benzene. In terms of benzene resonance energy units, the two complexes have effective experimental resonance energies of 1.42 and 1.36, respectively.

The diamagnetic susceptibility, X, of a cyclopenta-dienylruthenium moiety, with the center of anisotropy located at the metal atom, was calculated as -330×10^{-36} m^3 per molecule. The same parameter for a manganese tricarbonyl moiety, with the center of anisotropy being

located at 3.2 A^{o} down from the manganese atom, was calculated as -635×10^{-36} m^3 per molecule.

An X-ray structure determination of **32** was finally achieved some 25 years after its first synthesis. The structural data confirm the planarity and lack of bond alternation in the bridged annulene, indicating that it is aromatic.

Examiners:

Dr. R. H. Mitchell, Supervisor (Department of Chemistry)

Dr. K. R. Dixon (Department of Chemistry)

Dr. P. R. West (Department of Chemistry)

Dr. W. W. Kay (Department of Biochemistry)

Dr. L. T. Scott (External Examiner)

TABLE OF CONTENTS

LIST OF TABLES

LIST OF FIGURES

LIST OF ABBREVIATIONS

^{13}C NMR	carbon-13 nuclear magnetic resonance
Cp	cyclopentadienyl
Cp^*	pentamethylcyclopentadienyl
DIBAL	diisobutylaluminium hydride
DMDHP	*trans*-10b,10c-dimethyl-10b,10c-dihydropyrene
DMF	dimethylformamide
DMSO	dimethyl sulfoxide
IR	infrared
^{1}H NMR	proton nuclear magnetic resonance
br	broad
s	singlet
d	doublet
t	triplet
q	quartet
dd	doublet of doublets
m	multiplet
ppm	parts per million
MeLi	methyllithium
mp.	melting point
ms.	mass spectrum
CI	chemical ionization
EI	electron impact
Ph	phenyl
RE	resonance energy
THF	tetrahydrofuran
UV	ultraviolet

ACKNOWLEDGEMENTS

I would like to express my sincere thanks to Professor R. H. Mitchell for his encouragement and guidance throughout the course of this work.

A special word of thanks goes to Mrs C. Greenwood for recording some of the NMR spectra reported in this thesis and Dr. D. McGillvary for recording the mass spectra. I am indebted to my colleagues and friends for their suggestions and support.

Finally, I would like to thank the University of Victoria and the Department of Chemistry for financial support which made this work possible.

To the two women in my life

my wife Grace and my mom Rukeya

CHAPTER ONE

INTRODUCTION

1.1 Prologue

One of the most difficult and yet fascinating problems in chemistry is the definition of aromaticity. At the turn of the nineteenth century, the term aromatic was used to describe a structurally diverse group of compounds which have a common property, a fragrant smell. The discovery of benzene by Faraday[1] in 1825 and its subsequent synthesis by Mitscherlich[2] in 1833, made the term synonymous with being benzenoid, ie. derivative of benzene.[3] This hydrocarbon exhibits low reactivity and undergoes substitution rather than addition reactions that are normally described for unsaturated hydrocarbons containing double bonds.

The first attempt to bridge between theory and experiment to explain the properties exhibited by benzene was put forward by Bamberger[4] who suggested that these were concerned with the hexavalent nature of the benzene nucleus. Armit and Robinson[5] later reformulated the concept in electronic terms by relating these "aromatic" properties to the presence of a closed loop of π-electrons. It was not until 1931 that the first real bridge between theory and experiment was formulated. On the basis of molecular orbital theory, Hückel[6] extended

the concept of aromaticity beyond the aromatic sextet by introducing his famous rule, which states that *planar monocyclic completely delocalized conjugated hydrocarbons will be aromatic when the ring contains (4n+2) π-electrons*. In molecular orbital terminology, structures that have a particularily stable arrangement of occupied π-molecular orbitals are called aromatic.

At the time when Hückel introduced the rule, there were only two neutral species to which it could be applied: benzene, [6]annulene, and cyclooctatetraene, [8]annulene. Thus, the rule initiated a systematic search for higher homologs of benzene, leading to an enormous contribution to the growth of synthetic as well as theoretical organic chemistry. Structures **3-6** are

1

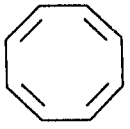

2

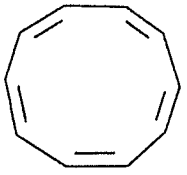

3a

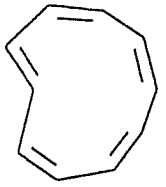

3b

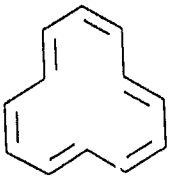

4

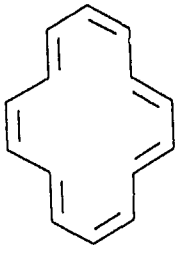

5

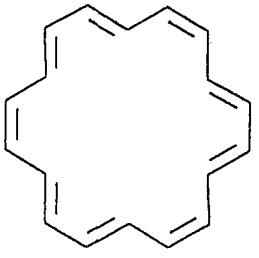

6

examples of such homologs. The first homolog to be synthesised was [18]annulene, **6**.[7] The molecule is unfortunately conformationally mobile and is more prone to polymerize than to undergo electrophilic substitution reactions. It can, however, be rendered rigid by bridging. Planar or near planar "frozen" 18 π-ring systems, porphyrinoids, as stable derivatives of the annulene have recently been reviewed by Vogel.[8]

While the (4n+2) π-electron rule remains the center piece of any discussion of aromaticity, it presents difficulties when applied to some conjugated systems. The rule explicitly demands planarity as a prerequisite for aromatic character. It is also valid rigorously only for monocyclic conjugated annulenes. For sometime now, however, it has been obvious that aromatic compounds will tolerate considerable deviations from planarity without losing their aromaticity. Well studied examples of these systems include the paracyclophanes, in particular, [2,2]paracyclophane, **7**. The hydrocarbon is a three dimensional aromatic compound which contains bent benzene rings. As a whole, it essentially behaves as a single π-electron system as demonstrated by its photoelectron spectrum.[9]

The two geometric isomers **8** and **9** are interesting cases. Both are bridged [14]annulenes. The distance between the inner bridge hydrogen atoms in **8** is 1.78 A^{O}, one of the shortest distances of non-bonded hydrogens

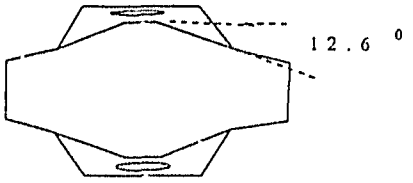

7

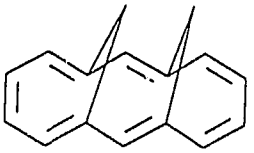

8

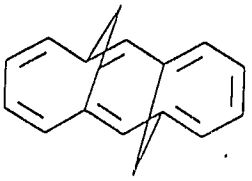

9

reported.[10] The contact between the two atoms is partially relieved through an increased dihedral angle between the two bridges (26.6°).[11] In compound **9**, the dihedral angle is 75° leading to very little π-orbital overlap. Compound **8** is about 63 kJ/mol more strained than the anti isomer, **9**. The latter is a cyclic polyolefin, while the former is an aromatic molecule, even though it contains a somewhat bent annulene ring. Apparently, aromatic character is obtained at the expense of steric compression between the inner hydrogen atoms.

Hückel's aromaticity rule is inadequate in classifying polycyclic conjugated systems, since it does not take into consideration internal double bonds. The perimeter model of Platt[12] and polycyclic version of

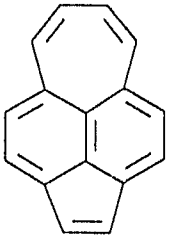

10

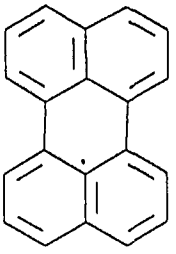

11

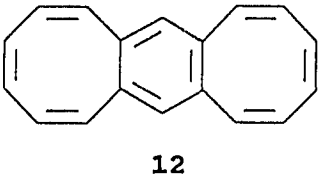

12

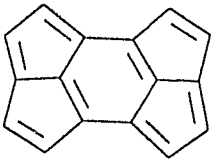

13

Volpin[13] and π-electron enumeration of Randic[14] has extended the rule to these polycyclic compounds. Thus, hydrocarbons such as **10** and **11** fall under the aromatic category whereas **12** and **13** do not.

Perhaps one of the most important contributions of Hückel's theory is the prediction of a new and stable class of compounds, namely the charged annulenes. It predicted cycloheptatrienyl cation, $C_7H_7^+$, **14**, to be a stable charged aromatic. The cation was prepared as far back as 1891 by Merling, but in the absence of theoretical support its structure was not verified.[15] The first reported synthesis of the cation was carried out by Doering and Knox in 1954.[16] Their studies of this 6 π-[7]annulene cation proved the above prediction.

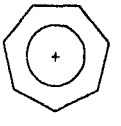

14

15

Studies of the isoelectronic negatively charged species **15** date back to 1900.[17] This 6 π-[5]annulene is also aromatic by Hückel's definition. An extensive number of charged monocyclic and polycyclic compounds are now known. These have been reviewed by a number of authors.[18] More about the properties of such systems will be discussed below.

1.2 Criteria For Aromaticity:

Aromatic molecules have the appearance of being unsaturated but nevertheless behave chemically unlike alkenes or alkynes. Benzene is stable to oxidation, is reluctant to undergo hydrogenation, and undergoes electrophilic substitution rather than addition. Thus substitution, rather than addition, is considered as a chemical guide to the aromaticity of the species. The notion of "aromatic" in this context should, however, be viewed with caution. Naphthalene, **16**, is unreactive towards dienophiles and only under forced conditions does it react with maleic anhydride. On the other hand, anthracene, **17**, reacts readily with the reagent to give the Diels Alder adduct **18**. Phenanthrene, **19**, adds bromine across the 9,10 double bond to give the dibromide **20**.

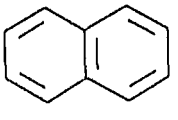

16

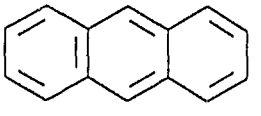

17

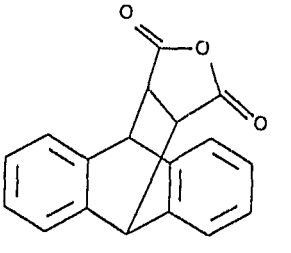

18

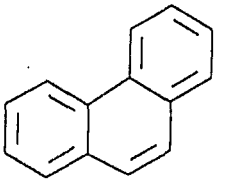

19

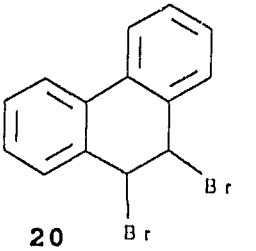

20

In the case of charged systems, the notion of a stable aromatic must also be viewed with care. Although some of these ions are stable at room temperature, and can be isolated as salts, e.g. **14** and **15**, the vast majority of aromatic ions are synthesized under rigorously controlled conditions. The ability to undergo electrophilic substitution as in the neutral aromatics no longer applies to these systems. Cyclopentadienyl anion reacts with electrophiles to produce substituted cyclopentadiene. Prolonged treatment of tropylium cation with concentrated deuteriosulfuric acid or with a solution of aluminum bromide in the above acid does not effect deuterium exchange. Under these conditions, benzene undergoes deuterium exchange almost instantaneously and even saturated hydrocarbons undergo rapid exchange.[3]

Therefore, the classical criteria for aromaticity such as lack of reactivity and stability are not as useful since these properties depend on differences in energy between ground and excited states and not on the ground state energy itself. Thus, when a molecule does not undergo electrophilic substitution it can not be ruled out as an aromatic. Other energetically favourable pathways are readily available to the molecule under consideration. A similar problem arises with the use of electronic spectra as a criterion for aromaticity.[19] The uv/visible spectrum is not simply a property of the

ground state of the molecule, but is characteristic of the energy differences between that state and the excited state. The spectrum is therefore not a suitable means of distinguishing the presence or absence of aromaticity.[20] It is, however, useful for comparing molecules that are closely related in structure, such as the benzenoid polycyclic hydrocarbons, and is often an excellent indicator of the way in which the system has been perturbed.

The delocalization of π-electrons lowers the energy content of the aromatic molecule relative to the hypothetical bond-localized structure. A theoretical parameter, called resonance energy, has been suggested as a suitable criterion for determining the aromaticity of a compound. However, the choice of a model is critical. The Hückel molecular orbital, HMO, method using ethene or cyclohexene as a model system does not satisfactorily account for differences in resonance stabilization of the (4n) and (4n+2) π-electron systems. Indeed, the HMO treatment grossly overestimates resonance stabilization for higher annulenes. The change of the model from a cyclic polyene to an acyclic one, adopted by Dewar, using the Pople-Pariser-Parr (PPP) approximation gives more reasonable values, termed Dewar resonance energy (DRE). The calculations suggest that at higher n, the annulenes will become non-aromatic possessing zero resonance stabilization.[21] Hess and Schaad's[22] use of the HMO

calculation method with the new reference, produced resonance stabilization values that mirror those of the PPP results.

In order to compare systems with different numbers of π-electrons, Hess and Schaad[22] suggested the use of the term resonance energy per π-electron (REPE) as a more suitable parameter than the total resonance energy. Table 1 contains the REPE's for a few systems as calculated by Dewar using the PPP method and by Hess and Schaad using the HMO method.

Table 1: Calculated REPE of selected conjugated compounds

Number	compound	REPE / β	
		Dewar	Hess-Schaad
21	[4]annulene	-0.136	-0.268
1	[6]annulene	0.120	0.065
16	naphthalene	0.093	0.055
22	fulvene	0.006	-0.002
23	azulene	0.017	0.023

Later modifications of resonance energy, RE, calculations based on different definitions of the hypothetical reference energy include those by Herndon[23] (RE from

Kekule structures) and Aihara[24] and Trinajstic[25] (RE from graph theory). The use of graph theory for resonance energy calculations has an advantage over Dewar's method in that it can be applied to ions and radicals. The topological resonance energy[25] of **15** is calculated as 0.094(β) whereas that of **14** as 0.032(β).

Carbon-carbon bond length is a ground state property that could be used as a criterion to determine aromaticity. Benzene has all bonds equal at 1.398 A^{o}. Thus in theory, aromatic systems should have equal bond lengths which should approach that of the benzene C-C bond. In reality, however, carbon-carbon bonds in higher annulenes are not all equivalent, and variation in the bond lengths, but not alternation, is normally the rule rather than the exception as illustrated for phenyl-tropylium cation, **24**,[26] ethano-bridged [14]annulene, **25**,[27] and [18]annulene, **6**.[28]

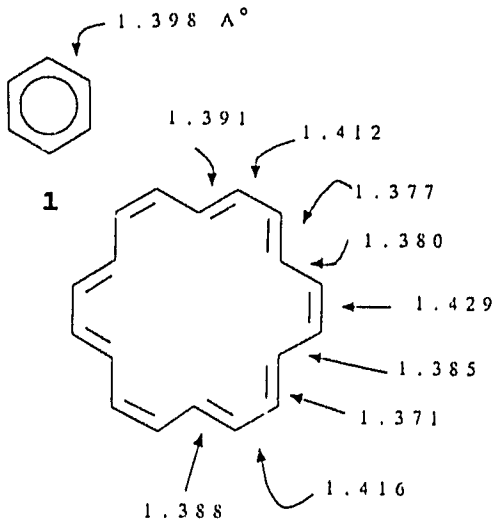

1

6

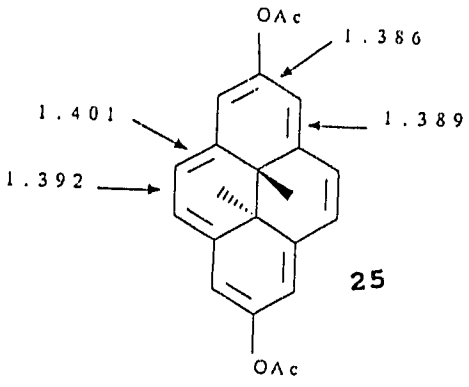

25

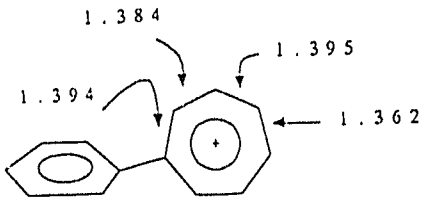

24

The determination of C-C bond lengths is, however tedious and requires laborious work since it involves preparation of suitable crystals and therefore can not be used as a routine criterion. Molecular mechanics coupled with π-SCF orbital calculations may prove useful since it can predict bond alternation.

Another criterion for determining aromaticity is bond orders. The concept relates to the valency multiplicity between atoms in molecules. The quantity has a physical significance that is associated with the binding power of a bond since the product of the coefficients of adjacent bonded atoms may be considered as a bond electron density

$$p_{rs} = \Sigma_J \, n_j c_{jr} c_{js} \quad \ldots\ldots\ldots\ldots (1)$$

where

n = no. of electrons in the J^{th} molecular orbital.

c_{jr}= coefficient of atom r in the J^{th} M.O.

Benzene has a bond order of 0.667 whereas a perfectly delocalized [14]annulene has a value of 0.642. The bond orders of 1-2 and 2-3 bonds in naphthalene have values of 0.725 and 0.603, respectively. A range of bond orders where a system might be classified as aromatic is difficult to determine.[29] Nevertheless, as we will see later in this chapter, bond orders about a conjugated system are a very good indicator of bond fixation.

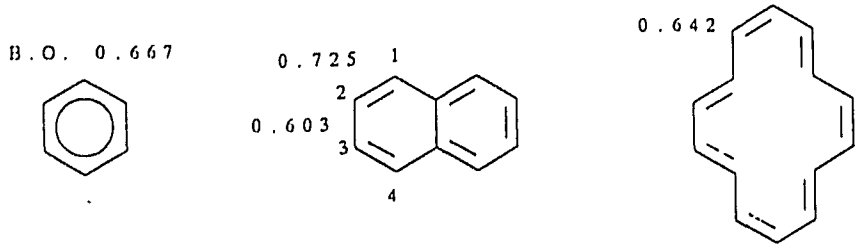

Perhaps the most popular, and appealing to the experimental chemist, of aromaticity criteria is nuclear magnetic resonance (NMR) spectroscopy. An aromatic compound is characterized by its diatropicity or the ability to sustain an induced diamagnetic ring current. Qualitatively, this ring current can be viewed as the circulation of the electrons in a delocalized π-system under the the influence of a magnetic field in an NMR spectrometer, as shown in Figure 1. The ring current is responsible for the large magnetic anisotropy in these systems.

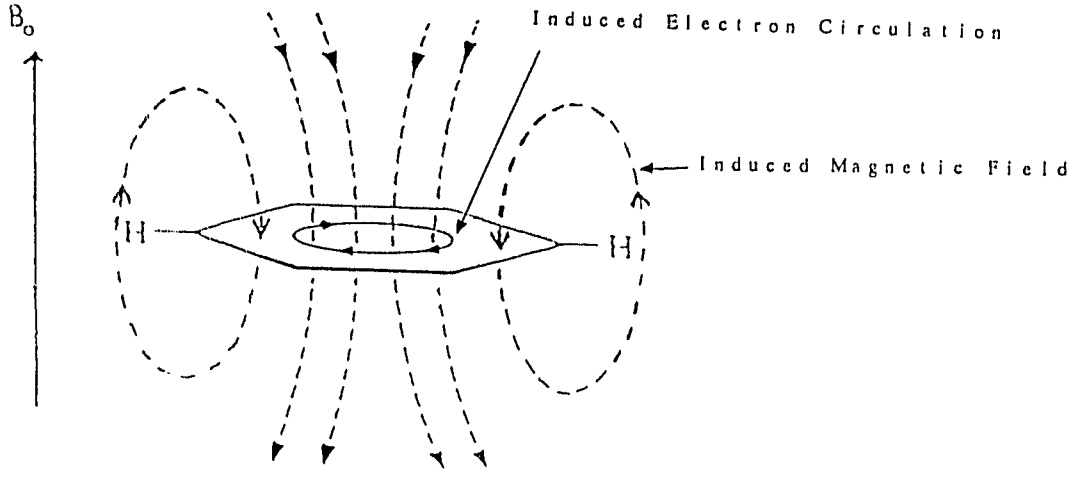

Figure 1: Ring current origin in aromatic compounds.

The model in Figure 1, in which the π-electrons precess in a donut shaped cloud extending over the ring can be used to explain the deshielding of aromatic protons in their proton NMR (^{1}H NMR) spectra. An aromatic proton in the plane of the ring experiences a ring current field that enhances the applied field; hence its resonance occurs at a lower field than might be expected. A proton held over the aromatic ring, on the other hand, experiences an upfield shift. In the case of [4n]annulenes, a generated paramagnetic ring current has the opposite effect. Annulenes that sustain a paramagnetic ring current are referred to as paratropic. Table 2 has selected examples of proton chemical shifts for a number of (4n+2) and (4n)annulenes.

Table 2: Proton chemical shifts (δ) of (4n+2) and (4n)annulenes in ppm.

Annulene	Number	Outer Protons	Inner Protons	Ref.
[6]	**1**	7.27	---	30
[8]	**2**	5.70	---	31
[10]	**3a**	5.66	---	32
	3b	5.84	---	32
	26	7.27-6.95	-0.52	33
[12]	**27**	5.5-5.2	6.06	34
	28	4.69-3.88	4.75	35

Table 2 continued,

Annulene	Number	Outer Protons	Inner Protons	Ref
[14]	**5a**	7.88	-0.61	36
	5b	6.82	3.55	36
	29	8.95-8.30	---	37
	8	8.0-7.0	0.9, -1.2	11a
	9	6.33-6.20	2.48,1.88	11b
	30	8.77-8.04	-4.53	38
	31	8.74-7.50	-2.06	39
	32	8.67-7.98	-4.25	40
[16]	**33**	5.09-4.77	5.68,8.30	41
[18]	**6**	9.25	-2.88	42
	34	9.55-9.30	-6.54- -7.96	43
[20]	**35**	9.35-7.15, 6.08-5.35	4.52	44
[22]	**37**	9.65-8.50	-0.40,-1.20	45
[24]	**36**	8.62-8.36, 6.19-5,70	4.04	44
	38	8.99, 6.27-5.75	4.11	46

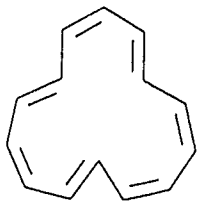

5b

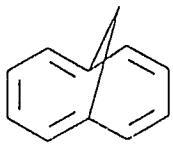

26

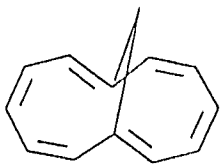

27

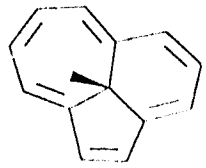

28

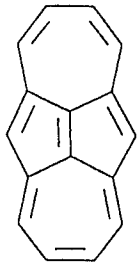

29

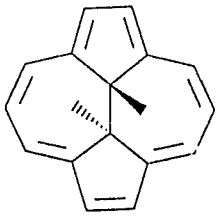

30

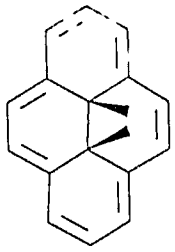

31

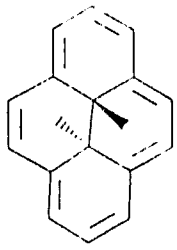

32

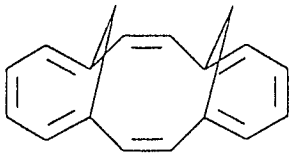

33

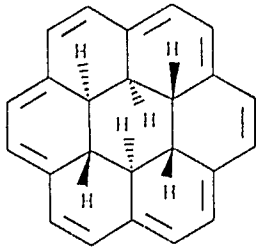

34

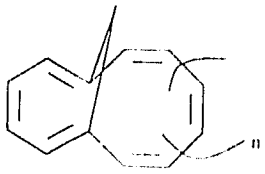

n=5 35
n=7 36

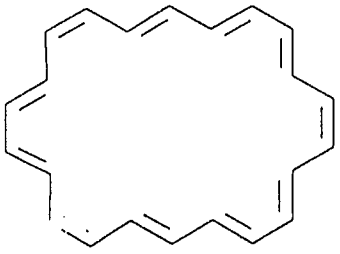

37

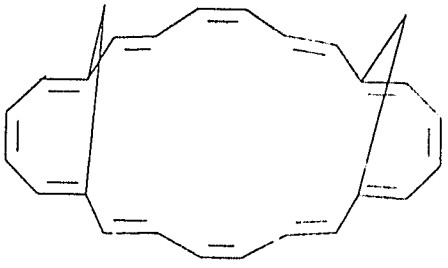

38

Planar annulenes exhibit strong diatropicity since the maximum degree of π-electron delocalization is related to the planarity of the conjugated system. One method of locking the conformational mobility is methylene bridging such as the case in Vogel's annulenes, of which **8**, **9**, **26**, **27**, and **33** are examples. The compound **26** exhibits aromatic character as seen from its ^{1}H NMR data from Table 2, whereas the open form is extremely reactive and not diatropic at all.[32,33]

Ethano-bridging also renders planarity to conformationaly mobile annulenes. Boekelheide's [14]annulenes are examples of such bridging. The enhancement in the ring current due to bridging is apparent in the dramatic increase in the internal methyl chemical shift changes in going from the flexible [14]annulene, **5a**, to **30**, **31**, and **32**. The internal protons of **5a** resonate at δ -0.61 ppm. The cis compound **31** has its internal methyl protons resonating at δ -2.06 ppm, about 2.2 ppm lower than the trans isomer **32** due to its being slightly bent (it exists in a saucer shaped form).[39,40]

The introduction of acetylene units in a conjugated system increases its rigidity and in some cases its tropicity. Sondheimer's[47] and Nakagawa's[48] annulenes are representatives of such systems.

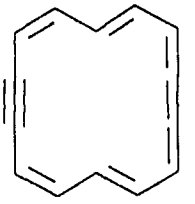

39

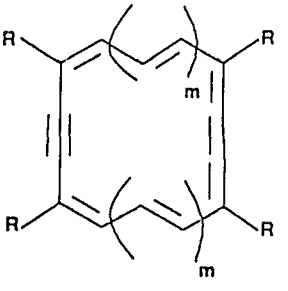

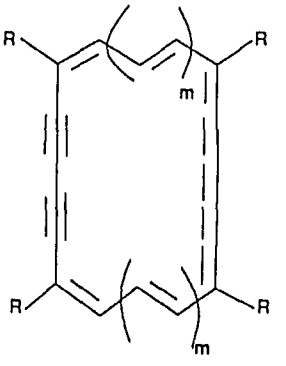

40	**m=1**
41	**m=2**
42	**m=3**
43	**m=4**
44	**m=5**

45	**m=1**
46	**m=2**

The rigidity of **39** is indicated by the high field ^{1}H NMR signal of its internal protons at δ -5.48 ppm.[49] Nakagawa's tetrasubstituted didehydro- and tetradehydroannulenes **40-44** and **45-46** are also essentially planar . As can be seen from Table 3, the chemical shift shielding of the internal protons progressively decreases as m increases, suggesting a gradual loss of diatropicity as the annulene becomes larger.

Table 3: ^{1}H NMR Chemical shift values of some didehydro- and tetradehydroannulenes[50] in ppm.

Annulene	outer protons	inner protons
40	9.42	-4.39
41	9.82-9.32	-3.61
42	9.16-8.76	-0.83
43	8.23-7.93	+1.9
44	7.5	+3.5
45	9.86	-4.89
46	10.16-9.67	-3.44

It should be noted here that diatropicity (or paratropicity) is not the only magnetic property of conjugated systems that has been related to aromaticity. Diamagnetic susceptibility exhaltation, DSE, is such a property. The term was introduced by Dauben et al[51]

$$DSE = X_m - X_{m'} \quad \ldots\ldots\ldots\ldots(2)$$

where X_m is the experimentally determined molar susceptibility of the compound and $X_{m'}$ is the estimated molar susceptibility for the corresponding theoretical cyclic polyene calculated from increments by means of a localized multiple bond model. A value of DSE higher

than zero indicates that the compound is aromatic whereas a value lower than zero classifies it as antiaromatic. The contribution of fully delocalized π-electrons to the magnetic sucseptibility is termed London diamagnetism. Aihara[52] correlated the value for X_π (the diamagnetic susceptibility of a conjugated system = DSE) to the resonance energy of the system.

Although the DSE method is empirical in character, its disadvantages include requirement of a large sample of the compound under investigation and the assumption of a model theoretical polyene. Aihara's correlation might however render the criterion more useful since it relates the value of DSE to a calculated parameter.

Of the criterion mentioned above, none can be exclusively counted to classify aromaticity, and none when violated are good enough to discount the property. Perhaps the most inclusive definition up to date is that of Garratt in which an aromatic compound is defined as *a cyclic diatropic system with a positive calculated Dewar resonance energy in which all the ring atoms are involved in a single conjugated system.*[19]

Garratt's definition above is by no means comprehensive. With the advent of new computer software, more criteria and criticism of the concept of aromaticity will likely be introduced. Indeed, with the utilization of sophisticated calculations, theoretical chemists never cease to induce imagination in experimental chemists.

References 53 and 54 offer some insight in new measures of quantitative aromaticity.

1.3 Charged Conjugated Systems:

π-conjugated anions and cations represent an important branch of chemistry in that their study allows linking between theory and experiment, and are therefore of interest to the spectroscopist as well as the theoretical and synthetic chemist. In accordance with Hückel's rule, charged conjugated systems with (4n+2) π-electrons are aromatic and those with (4n)π-electrons are not. Indeed, cyclopentadienide anion, **15** and cycloheptatrienyl cation, **14**, are both aromatic. Their infrared (IR) and raman spectra are simple, as expected for molecules of D_{5h} and D_{7h} symmetry.[3]

In principle, it should be possible to convert (4n+2)annulenes into (4n)-systems by adding or subtracting two electrons (and vice versa). This change in total π-electrons should lead to opposite ring currents in the neutral and charged annulenes and manifests itself in chemical shift values. Indeed, nuclear magnetic resonance spectroscopy is the most convenient method in the study of these charged systems. It enables a complete and in most cases unambiguous structure elucidation of the charged species. A striking example is that of the ethano-bridged [14]annulene, **32**.[55]

The aromatic compound bears its methyl substituents within the 14 π-electron cloud placing them in the center of the magnetic ring current, which strongly shields them from normal chemical shift values. The internal protons of **32** appear at δ -4.25 ppm, some 5.2 ppm shielded from those of the non-delocalized model **47**.[55] the paratropic species **48**, a result of adding two electrons to **32**, exhibits a very pronounced paratropic ring current. Its internal methyl protons, Table 4, resonate at +21 ppm, about 20 ppm downfield from the model.[56]

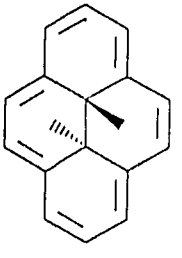

32

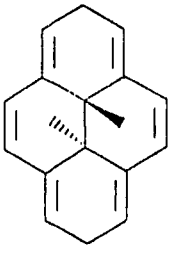

47

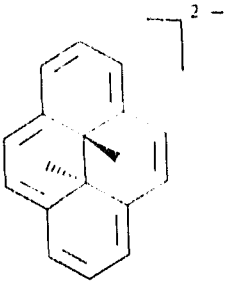

48

Chemical shift-electron density correlations, introduced first by Schneider et al,[57] allow an estimate of experimental charge densities in the case of carbon-13 NMR parameters. The proton chemical shifts in the NMR spectra can be related to the diatropicity and paratropicity of the system. For each negative or positive charge introduced in the conjugated species, an overall change of approximately 10.7 ppm is incorporated to account for that charge.[58,18a] In the case of carbon,

an overall charge correction of approximately 200 ppm is incorporated.[18b,59]

In its proton NMR spectrum, anion **15** shows a singlet at δ 5.57 ppm while cation **14** exhibits a signal at δ 9.28 ppm. The chemical shift of the protons is in reasonable agreement for a system with a diamagnetic ring current of a comparable magnitude to that of benzene, having one fifth (in the case of **15**) or one seventh (in the case of **14**) unit charge at each carbon atom.[57b,58] The carbon-13 spectra for **14** and **15** are singlets at 156.1 and 102.8, respectively. After charge correction, these shifts are comparable to that of benzene (128.8 ppm).

Charged annulenes **14** and **15** are examples of small symmetric annulenes, where the charge distribution is uniform judging by their NMR and IR spectra. In larger charged annulenes, however, there is a non-uniform charge distribution. Therefore, the local π-charge density in these systems is the main factor influencing the individual carbon-13 chemical shifts[18b] and care must be exercised when interpreting chemical shift changes. In negatively charged annulenes, charge alternation may result.[18f] A representative example is that of dianion **62**, where the carbons 1 and 6 appear at 163.7 ppm. In the parent compound **26**, they appear at 114.6 ppm. The significant deshielding in the paratropic species is attributed to development of positive charge at these two carbons.[70]

Table 4: Chemical shift values for selected charged annulenes (in ppm).

Annulene	Outer Protons	Inner Protons	Ref
49	11.1	---	60
50	10.68	---	61
48	-3.19,-3.96	21.0	56
51a	2.22-0.01	---	37
b	5.68-4.40	---	62
52	5.70	---	31
53	7.16-6.28	-6.44	63
54	10.70	-4.48,-4.10,-2.58	64
55	9.6-8.3	-0.3,-1.8	65,66
56	11.81,11.02,10.56	-5.71,-2.29	67
57	6.8-5.4	-0.7,-1.2	68
58	3.56,2.83,2.70	11.95,8.50	18e
59a	1.50,1.04	23.33	18b
b	8.95,7.95	-8.97	18b
60	9.52,8.21	-7.97	69
61	-0.85- +0.17	11.96	18f
62	3.07,1.59	11.64	70

49

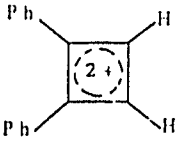

50

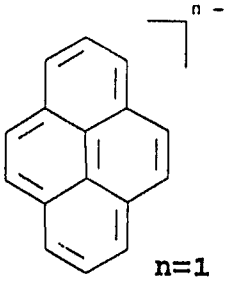

n=1 51a
n=2 51b

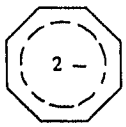

52

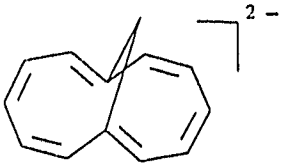

53

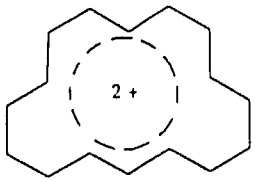

54

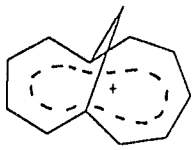

55

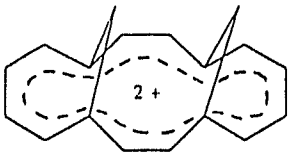

56

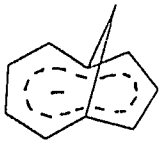

57

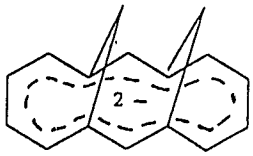

58

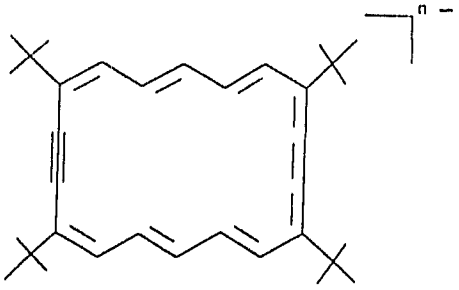

n=2 59a
n=4 59b

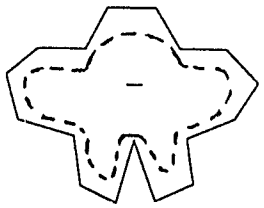

60

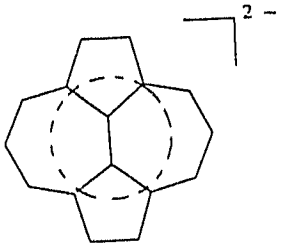

61

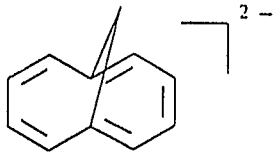

62

In multiply charged ions, a greater resonance energy is experienced, as compared to the corresponding isoelectronic neutral system, on attaining a delocalized state.[71] This is inferred by the remarkably high diatropicity of these charged annulenes as can be seen from examples included in Table 4. The effect is also present in some singly charged annulenes. The internal protons of 18 π-[17]annulenyl anion **60** resonate at δ -7.97 ppm, Table 4, whereas those of the corresponding isoelectronic neutral [18]annulene **6**, Table 2, resonate at δ -2.88 ppm. Such contrast between neutral and charged annulenes is a new feature in the study of aromaticity.[18b,64,69,72] Kuwajima's calculations using the PPP-π-electron model to reproduce the effect, emphasizes the electronic origins of aromaticity[72], hence the importance of valence bond, VB, structures in these systems.

1.4 Annelation Probed by Dimethyldihydropyrene:

trans-10b,10c-Dimethyl-10b,10c-dihydropyrene, DMDHP, called *trans*-15,16-dimethyldihydropyrene by Boekelheide[40,55], is a stable aromatic compound which is strongly diatropic. It has an almost planar rigid skeleton, held by the ethano bridge, that is little strained and as such acts as a stereochemically fixed [14]annulene. The parent [14]annulene, **5**, made by

Sondheimer[73] is unstable and is conformationally mobile at ambient temperatures, with the inner and outer protons exchanging environments. Its internal protons resonate at δ -0.61 ppm at -126°C.[36]

DMDHP bears its internal methyl substituents within the 14 π-electron cloud, placing them in the center of the magnetic current. The internal methyl protons are well insulated from the π-system, 3 bonds, and their chemical shift does not change significantly upon substitution with a variety of groups at a number of positions. The chemical shifts of the internal methyl protons for a number of derivatives of **32** are presented in Table 5.

Table 5: Internal δCH_3 for substituted DMDHP.

Compound	Substituent	position	δCH_3	Ref
63	Br	2	-4.07,-4.08	74
64	$COCH_3$	2	-4.03	75
65	$C(Ph)_3$	2	-3.92,-4.03	75
66	NO_2	2	-4.03	75
67	DMDHP	2	-3.68,-3.77	76
68	CH_3	2,7	-4.09	77
69	Br	2,7	-4.02	75
70	$COOCH_3$	2,7	-3.92	77
71	*t*-Bu	2,7	-4.06	78
72	$OCOCH_3$	2,4,7	-3.83	55

It can safely be concluded from Table 5 that the internal methyl chemical shift mainly depends on the strength of the diamagnetic current and hence on the degree of delocalization of the π-electrons of the 14 π-periphery.[79] These protons appear at δ -4.25, some 5.2 ppm shielded from those of the non-delocalized model **47**. The chemical shift shielding of the inner protons of the parent *trans*-dihydropyrene **73**[80] is somewhat larger, 8.3 ppm, as compared with the reference **74**[32a], and hence provides a larger range of shielding than DMDHP. However, because the internal hydrogens can readily eliminate to yield pyrene **75**, the parent **73** proves less suitable than **32** for any studies involving a change in the extent of delocalization of the π-electrons in the periphery.

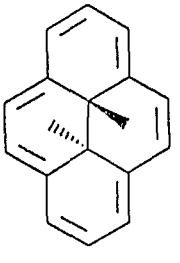

32

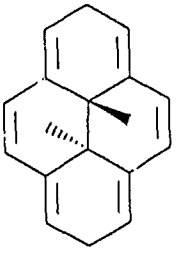

47

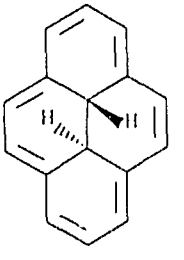

73

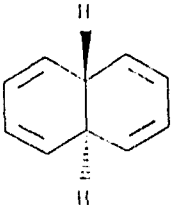

74

The phenomenon whereby a benzene is fused to another annulene is termed benzannelation. Annuleno-annulenes are the products of annelated annulenes with other rings

than benzenoid ones. Thus naphthalene **16** is considered a benzobenzene whereas compound **76** is a benzopyrene. Compounds **78**[81] and **79**[82], made by Sondheimer are examples of annulenoannulenes.

Table 6: Chemical shifts of inner protons of some annelated annulenes (in ppm).

Compound	Chemical shift	Ref
77	5.2-4.2	83
78	3.82	81
79	1.42	82
80	4.99	84
81	0.81-0.71	80
83	-3.45	80

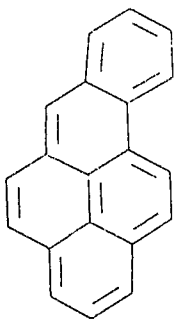

76

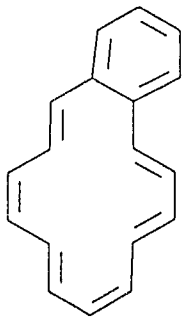

77

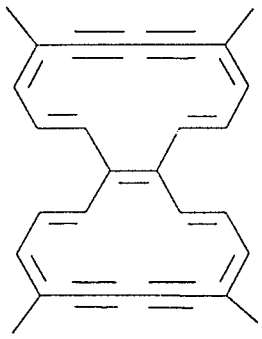

78

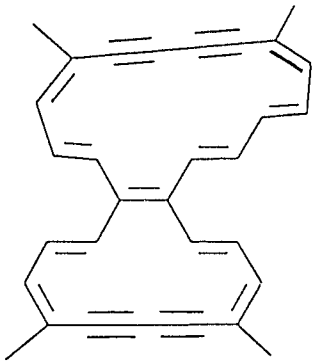

79

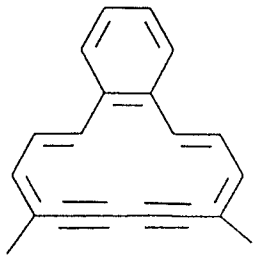

80

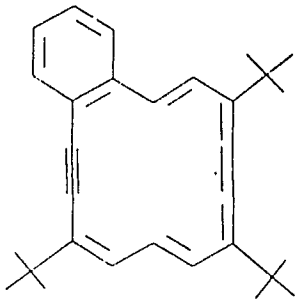

81

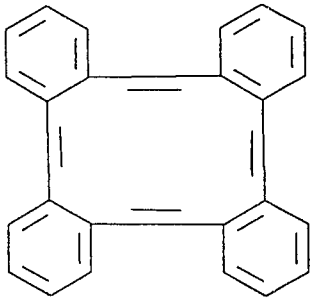

82

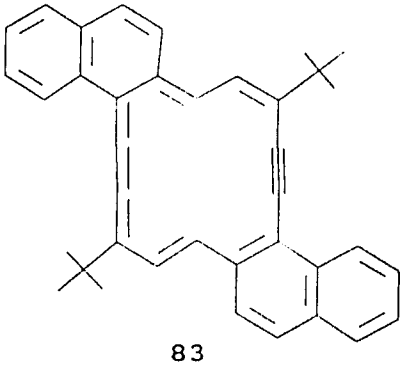

83

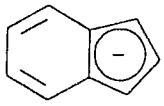

84

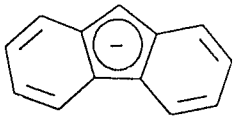

85

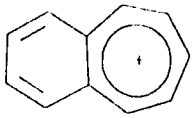

86

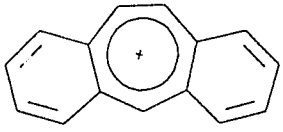

87

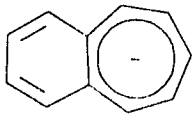

88

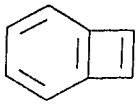

89

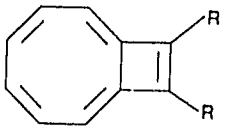

90a R = H
90b R = Ph

When an annulene is benzannelated, its aromaticity is reduced.[85] In the compounds **77** and **80** , it is lost as can be deduced from their proton NMR shifts (Table 6). In compounds such as **82**, one of the first benzannelated derivatives of higher annulenes to be made, the compound is not planar and thus changes to proton shifts are difficult to determine.[86,87] Because of the properties mentioned above, DMDHP has been very effectively used as a probe for ring current effects due to benzannelation.[85] To understand some of these effects, however, a short discussion of the properties of fused annulenes is in order.

In general, conjugated polycyclic systems can be classified according to three different types of fusion:

1. The fusion of a (4n+2) π-ring with a second (4n+2) π-ring where each component contributes to the aromatic character and thus the diamagnetic ring current is reduced in each ring. The effect on NMR data when (4n+2)annulenes are benzannelated has been reviewd by Mitchell[80], and for annuleno-annulenes has been reviewed by Nakagawa.[50]

2. The fusion of a (4n+2) π-ring with a paramagnetic (4n) π-system resulting in contradictory aromatic and anti-aromatic character to the entire system. Compound **79** is representative of this class. Examination of the inner

protons of the 14-membered ring, Table 6, shows that the 16-membered ring makes a paratropic contribution, the inner protons being at higher field than in **78**. Other examples of this mode of fusion include benzocycloheptatrienyl anion **88** and benzocyclobutadiene **89**. In the case of the latter, the benzene protons resonate at δ 6.26 and 5.78 ppm, whereas those of the four membered ring resonate at δ 6.36.[88]

3. The fusion of two paratropic (4n) π-systems yielding two paratropic contributions. Examples of this mode of annelation are rare due to the instability of the products. However, bicyclo[6.2.0]decapentaene, **90a**, can be isolated and is planar.[89] It is characterized by a long transannular bond (which avoids a 4 π-ring contribution). In the diphenyl derivative, **90b**, this bond is equal to 1.535 A^{o}.[89b]

Even though a considerable amount of effort has been devoted to the synthesis and study of benzannulenes and annelated dehydroannulenes of both the (4n)- and (4n+2)-electron series, especially by Sondheimer[81,82], Staab[83], Boekelheide[43], Nakagawa[50], and Mitchell[85], very little work has been done on annelated charged systems. The use of an annelating benzene ring is mainly used in the relevant known systems to stabilize the charged derivative.[18a] Indenyl anion **84** is a benzofused cyclo-

pentadienide whereas fluorenyl anion **85** is a dibenzofused cyclopentadienide. The indenyl anion and the benzofused cycloheptatrienylcation **86** are isoelectronic with naphthalene, whereas **85** and **87** are isoelectronic with phenanthrene. Since the charged moieties **14** and **15** are both aromatic, one would expect them to affect the aromaticity of the annelating ring. The only indicator for the effect present in such compounds is the alternance parameter Q. On the basis of PPP-πSCF calculations, Günther has shown that this value, defined as the ratio of π-bond order in the fused six membered ring, may be used as a guide to the diatropicity of the ring.[90] The larger the value of Q, the less delocalized the six membered ring is. Thus for a molecule of the type **91**, the bond orders are estimated from the vicinal H-H coupling constants $^3J_{H-H}$ using the equation;

$$P_{mn}(SCF) = 0.104\ {}^3J_{mn} - 0.120 \quad .....(3)$$

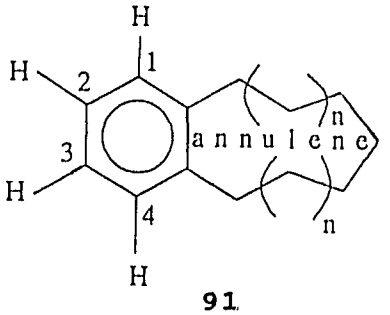

91

For delocalized (4n+2)annulenes, the ratio of P_{12}/P_{23} is > 1.10 and for delocalized (4n)annulenes, it is < 1.04, whereas localized systems of either type exhibit values

between 1.04 and 1.10. Table 7 presents a selected number of these values.

Table 7: Alternance values for some benzannulenes[90,91]

Compound	J_{12}(Hz)	J_{23}(Hz)	Q
benzene	7.56	7.56	1.00
naphthalene	8.28	6.85	1.25
indenyl anion	8.05	6.46	1.24
bcht	7.83	7.36	1.08
bt	8.37	7.05	1.22
bcot	7.73	7.29	1.07
$bcot^{2-}$	8.51	5.80	1.58

bcht = benzo-cycloheptatriene

bt = benzo-tropylium

bcot = benzo-cycloctatetraene

As mentioned earlier, DMDHP is an excellent probe for studies of benzannelation effects on ring current changes.[85,92] The internally methyl substituted benzo[a]pyrene, **92**[93] and the symmetrical benzo[e] derivative **93**[94] were synthesized by Mitchell et al and the chemical shifts of the internal methyl protons of the two derivatives are δ -1.62 ppm and -1.85 ppm respectively. Subtracting these values from the possible

maximum shielding of 5.22 ppm gives a shielding value of 2.80 and 2.53 ppm, implying a reduction of the ring current by about 50%. The small difference between the two results probably represents an anisotropy difference due to the different positions of fusion of the rings.

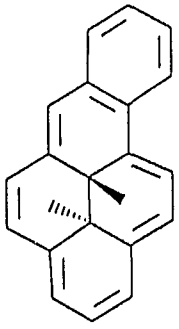

92

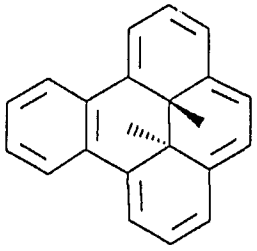

93

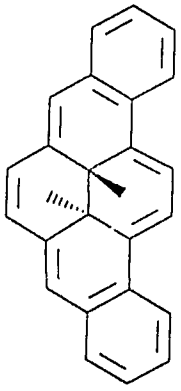

94

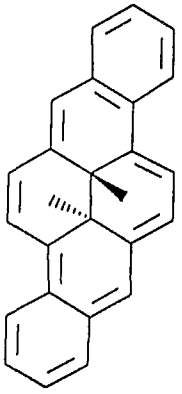

95

A more dramatic result is obtained on fusing two benzene rings to the dihydropyrene system. In the case of the dibenzo[a,h] derivative, **94**, the two benzene rings apparently cooperate to reduce the ring current in the macrocyclic ring. The methyls appear at δ +0.02 ppm, shielded by 0.95 ppm indicating 18% of the ring current of **32**.[79] The chemical shift of the internal methyls in the case of dibenzo[a,i] derivative, **95**, is at δ -3.58 ppm, suggesting a reduction of only 13% in the ring current. Only one of these benzene rings can be benzenoid and they thus *oppose* each other.

To qualitatively correlate the changes in the ring current with those of chemical shift shielding, $\Delta\delta$, the average deviation of π-SCF bond order from the expected

Hückel value of 0.642, Δr, for a perfectly delocalized [14]annulene for each macrocyclic ring of **92-95** was plotted against the chemical shift shielding of the internal methyl groups.[92] The correlation here being theoretically valid due to the dependence of ring current on bond orders[95], ie. ring current is maximum when bond orders are equal around a perfectly delocalized annulene. Measured or calculated deviations from the perfectly delocalized annulene thus provide a quantitative measure of ring current changes, taken here as the shielding of the internal methyl protons.

The result is a straight line plot from which the following equation is obtained:

$$\Delta\delta = 5.533 - 27.52\,\Delta r \quad \ldots\ldots\ldots (4)$$

The correlation proved valuable in two respects. Firstly, if bond orders can either be calculated or measured using equation 3 or π-SCF calculations, then the chemical shift shielding could be predicted. Secondly, a measured chemical shift can be used to comment on the average bond order deviations and hence on ring current changes due to annelation. Table 8 includes some of the predicted and observed chemical shift values for the internal methyl groups for a number of bezannelated dihydropyrenes.

Table 8: Predicted and observed δCH_3 for some fused DMDHP

Compound	δCH_3(predicted)	δCH_3(observed)	Ref.
96	-2.75	-2.78	92,96
97	-3.97	-4.19,-4.28	92,96
98	-1.25	-0.74	92,97
99	-3.84	-3.32	98

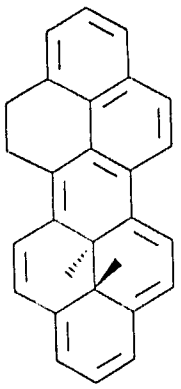

96

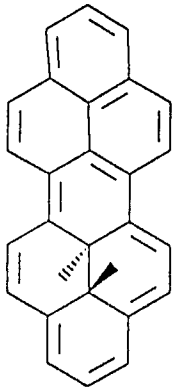

97

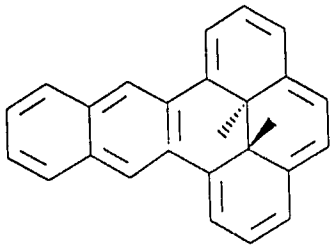

98

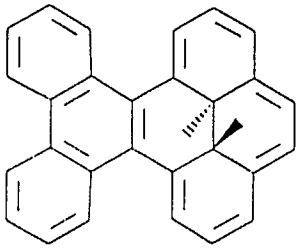

99

The agreement is surprisingly good considering the anisotropy effect of the annelating rings through space, is ignored. In the molecule **100**, proton E is the farthest from the annelating ring and is thus least affected by its anisotropy. Recently[99], a quantitative correlation that relates the internal methyl ring current chemical shift, δ_{RCM}, to that of the ring current chemical shift of proton E, δ_{RCH}, for a number of annelated DMDHP derivatives has been derived. The

following equation, which represents a straight line plot, was obtained:

$$\delta_{RCM} = -2.60\ \delta_{RCH} - 0.029 \quad \text{.....(5)}$$

where,

$$\delta_{RCM} = 0.97 - (\delta CH_3)\ , \quad \text{and}$$

$$\delta_{RCH} = 6.13 - \delta_E$$

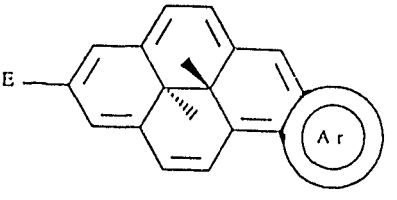

100

The value of 0.97 is the chemical shift for the model **47** and 6.13 is that of an annulene in the absence of any ring current effect.[29,100] Two important observations from the equation can be drawn. Firstly, the value 2.60 implies that the internal methyl protons in DMDHP are about 2.6 times more sensitive to ring current changes than the external protons. Secondly, it provides a sound check for anisotropy effects on the internal methyl chemical shifts.

Thus, the ethano-bridged [14]annulene **32** proves an excellent probe for studies of annelation as well as anisotropy effects for neutral aromatics To investigate the suitability of the system for studies of fused

charged systems, we decided to synthesize the cyclopentadienide fused dimethyldihydropyrene, **101**, and to study the effect of its annelation on ring current reduction in comparison to benzene. π-SCF calculations predict the internal methyl chemical shift for **101** at δ -2.54 ppm. The substitution of this value in equation 4 leads to a predicted chemical shift for proton E at δ 7.49 ppm in the absence of anisotropy or charge effects.

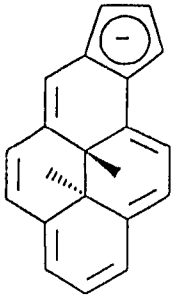

101

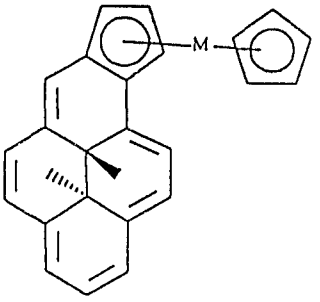

102

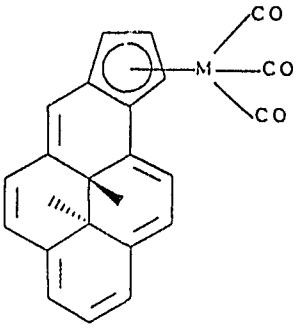

103

Metallocenes are classified as 3-dimensional aromatic compounds.[101,102] Therefore, their fusion to another aromatic moiety should affect its aromaticity. Facile reduction of the double bonds of the benzene ring in indenyl metallocenes indicates the large extent to which the π-bonds of the six membered ring are fixed.[103] This implies that metallocenes are more bond fixing than benzene itself. Synthesis of the target **101** would allow access to metallocene synthesis and would thus permit comments on the effect of fusing them to the [14] π-aromatic system. It would also access synthesis of fused

cyclopentadienyl metal carbonyls, which are also 3-dimensional aromatic systems.[104] In either case, targets **102** and **103** would also permit some understanding of the metal ligand bond anisotropy as well as additional information on the source(s) of the upfield chemical shift associated with metal complexation to aromatics.

CHAPTER TWO

SYNTHESIS

2.1 Retrosynthetic Route to 101:

A retrosynthetic analysis of the target **101** is presented in Scheme 1, which involves three retroroutes. A common feature in all of the routes is the sulfur extrusion step. Thiacyclophanes have been extensively used in the preparation of novel conjugated aromatic compounds.[105]

Scheme 1:

Retroroute 1:

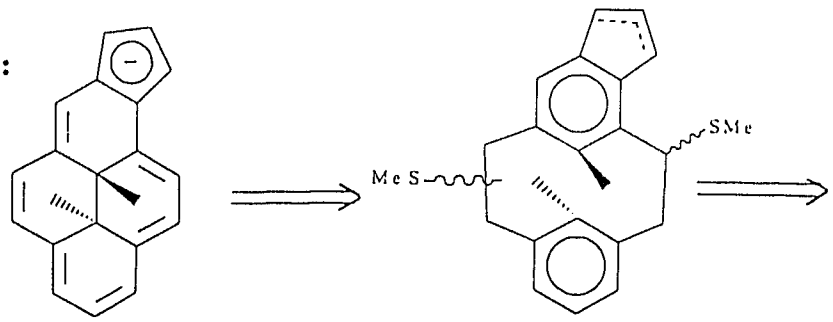

101

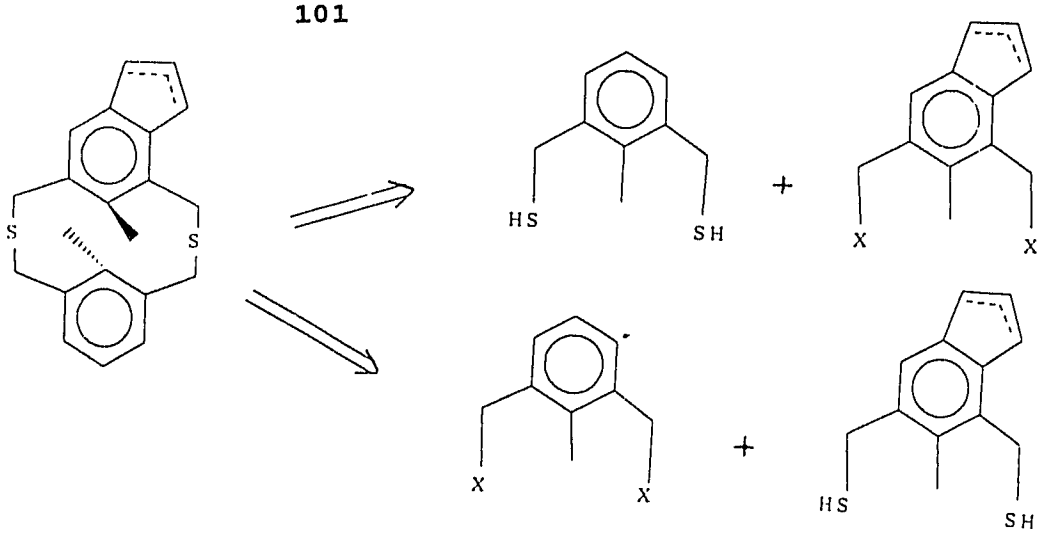

Retroroute 2:

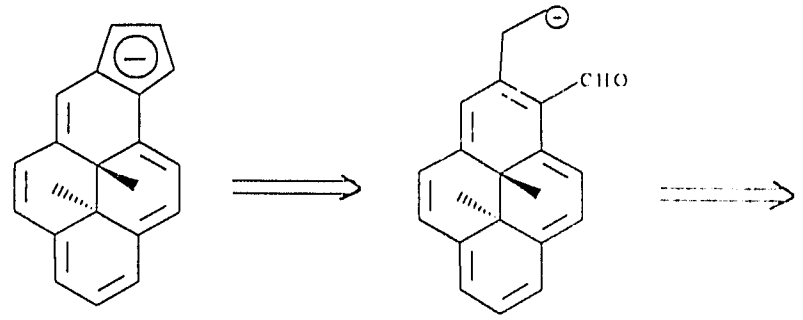

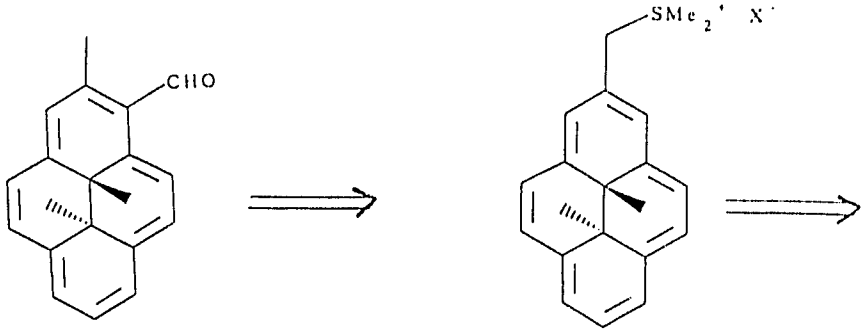

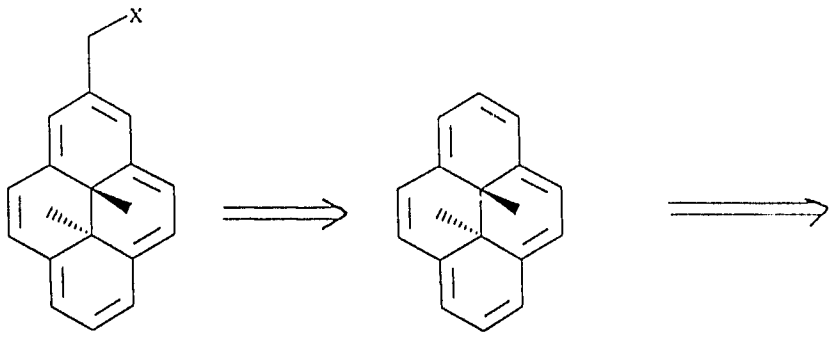

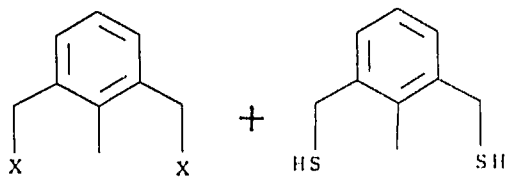

Retroroute 3:

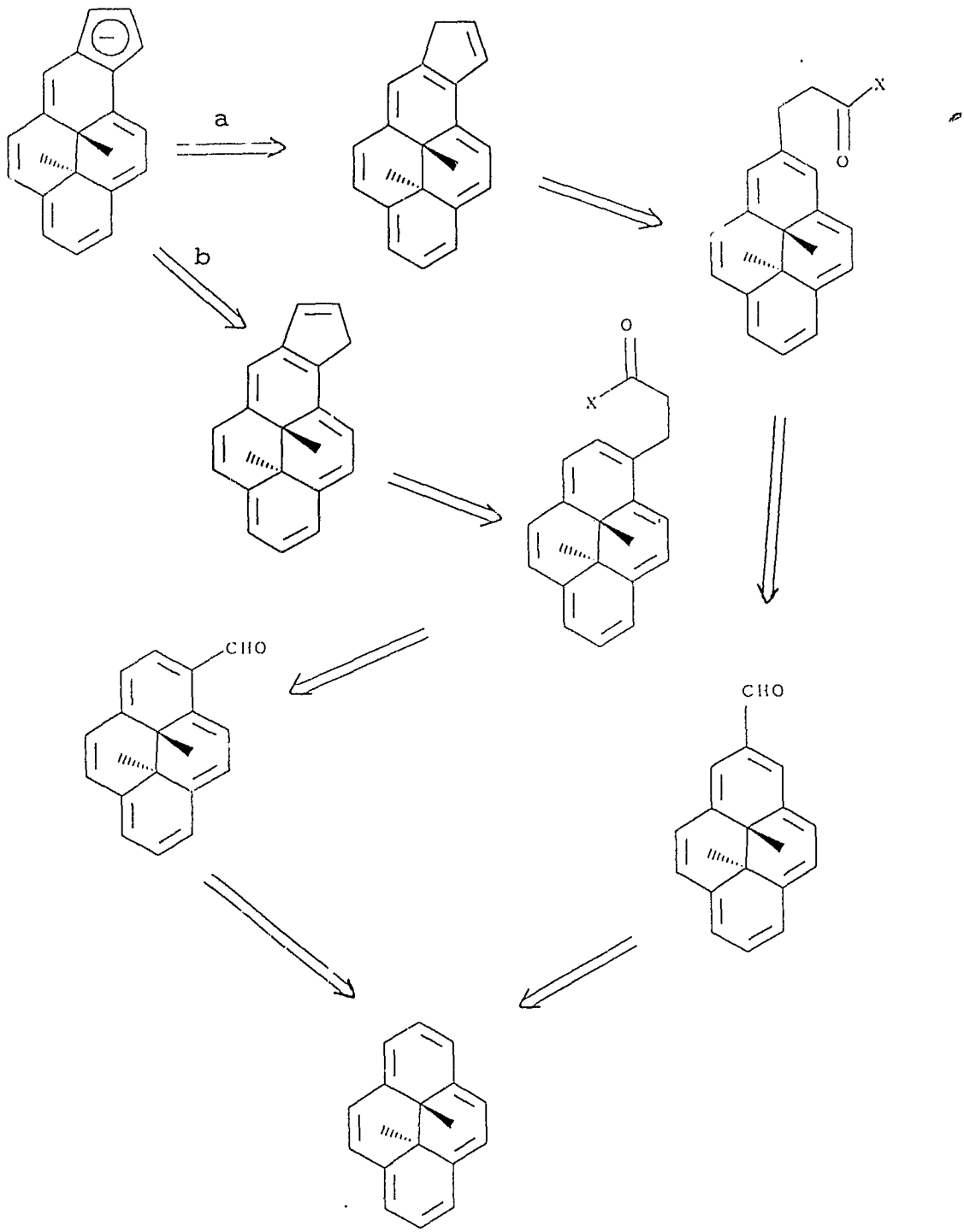

The Boekelheide-Mitchell route, which essentially involves a Stevens or Wittig rearrangement followed by Hoffmann elimination, has been successfully used in the synthesis of **32** and its derivatives **92-95** via the cyclophanes **104-107.**

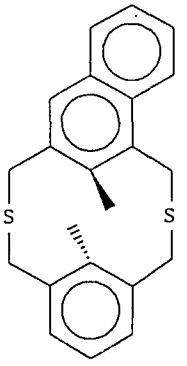

104

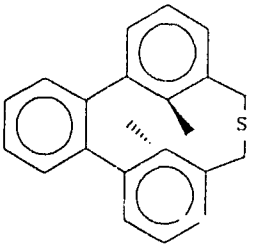

105

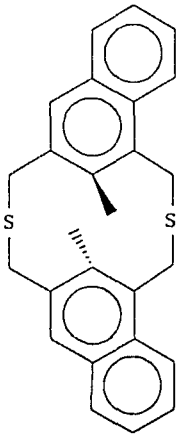

106

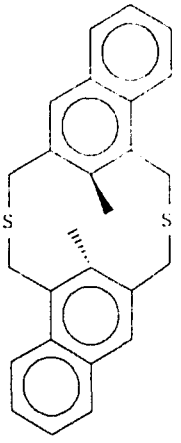

107

Yields of derivatives **92-95** via the thiacyclophane route are however low because of the large number of steps. With this in mind, retroroute 1, which involves the synthesis of the five-membered ring at an earlier stage, whilst probably certain to succeed, is lengthy and not very elegant. Retroroute 2 involves a number of

functional group interconversions, one of which the ortho functionalization is unpredictable. Retroroute 3 looked to be the most promising and most predictable of all three routes. Both cyclopenteno-dmdhps **108** and **109** are precursors to the anion **101**. The retrosynthetic route 3b presents a problem due to the position of substitution at the aromatic nucleus. The highest electron density in **32** is located at positions 2 and 7.[106] Friedel-Crafts formylation of **32** mainly results is substitution at these two positions. A small percentage of the formylated isomer at position 4, the next highest position in electron density, is also obtained.[75] Therefore, route 3b did not appear to us as feasible as 3a. We therefore decided to follow route 3a in our pursuit of the target **101**.

2.2 Synthetic Route to Target 101:

trans-10b,10c-Dimethyldihydropyrene is most conveniently synthesised by the following sequence[105];

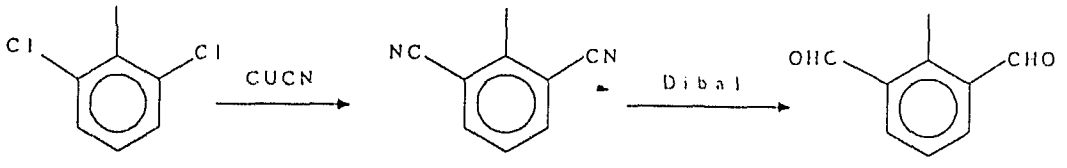

110 **111** **112**

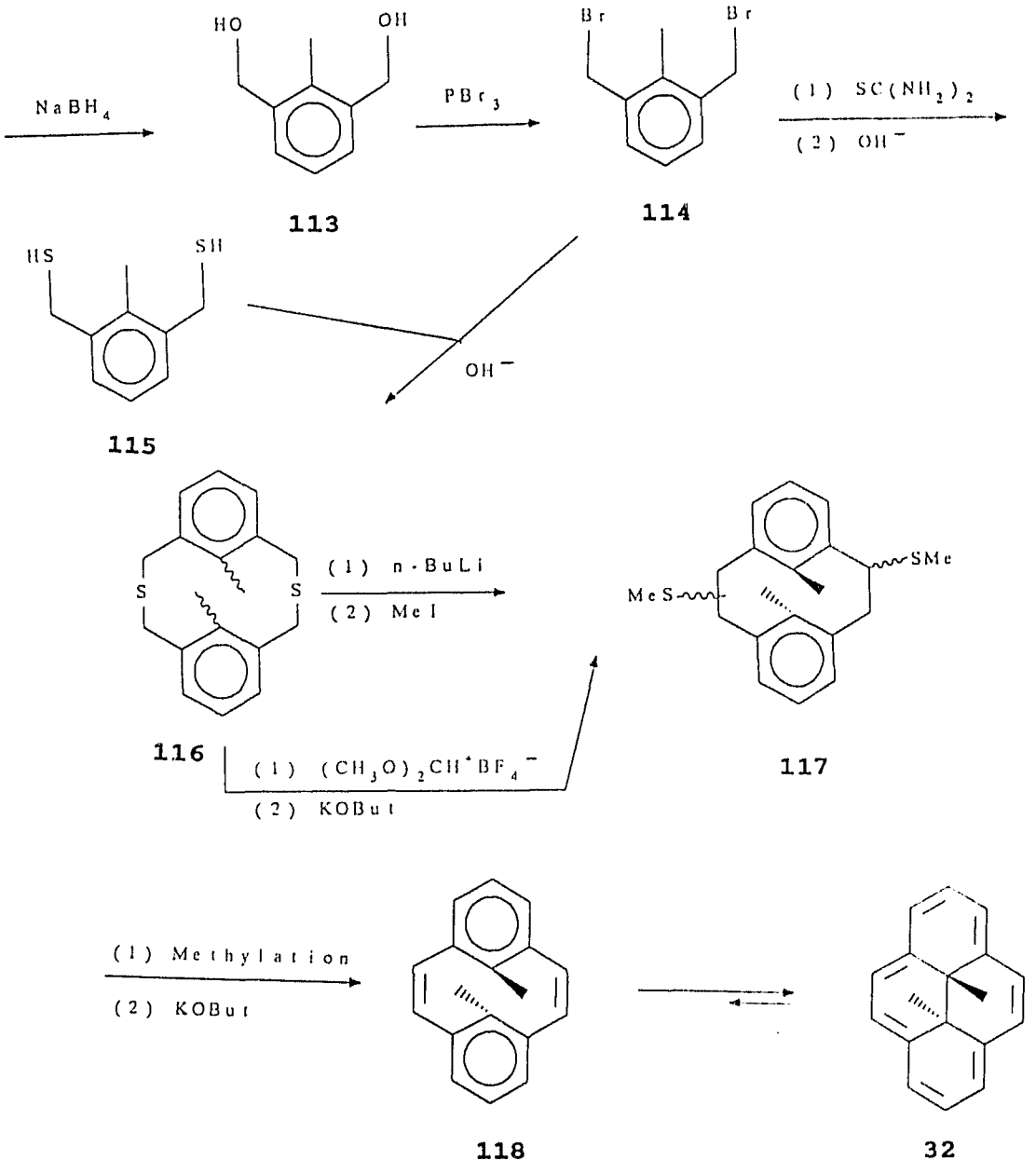

In our hands, the overall yield from the sequence was usually 25-30%. When large amounts of the diol **113** were made, it was sometimes difficult to obtain a completely dry sample. Therefore, under these circumstances, the dibromide **114** was obtained by reacting the diol with hydrobromic acid in the presence of sulfuric acid. The yields of **114** were comparable to,

although always lower than, those of phosphorus tribromide treatment, ranging between 80-85%.

The cyclophane **117** was synthesised using either the Wittig or Stevens rearrangement. It was always obtained as a mixture of two stereoisomers which could be separated by column chromatography.[105] It was found, however, that the Stevens product was always more pure than the Wittig rerrangement product. The separation of the two isomers was not normally carried out (only for characterization). The cyclophanediene **118** was obtained as a colorless solid after column chromatography at 0°C. However, samples of **118** were quickly tainted with green, due to its facile conversion to **32**, as indicated by the 60 MHz ^{1}H NMR of a sample of **118**. The cyclophanediene proton spectrum exibits a multiplet at δ 7.15-6.50 ppm (3H), a singlet at δ 6.22 ppm (4H), and another singlet at δ 1.51 ppm.

Synthetic Scheme 2 describes the route to the target **109**. The first reported synthesis of the intermediate 2-formyl-*trans*-10b,10c-dimethyldihydropyrene, **119**, utilized stannic chloride and n-butyl dichloromethyl-ether.[75a] A possible isomer, the 4-formyl derivative, **120**, was not reported. Two years later[75b], however, using the same procedure, the isomer **120** was reported in 18% yield. Our use of titanium tetrachloride as Lewis acid instead of stannic chloride slightly improved the yield of **119**. The compound was isolated in 75% yield as

Scheme 2:

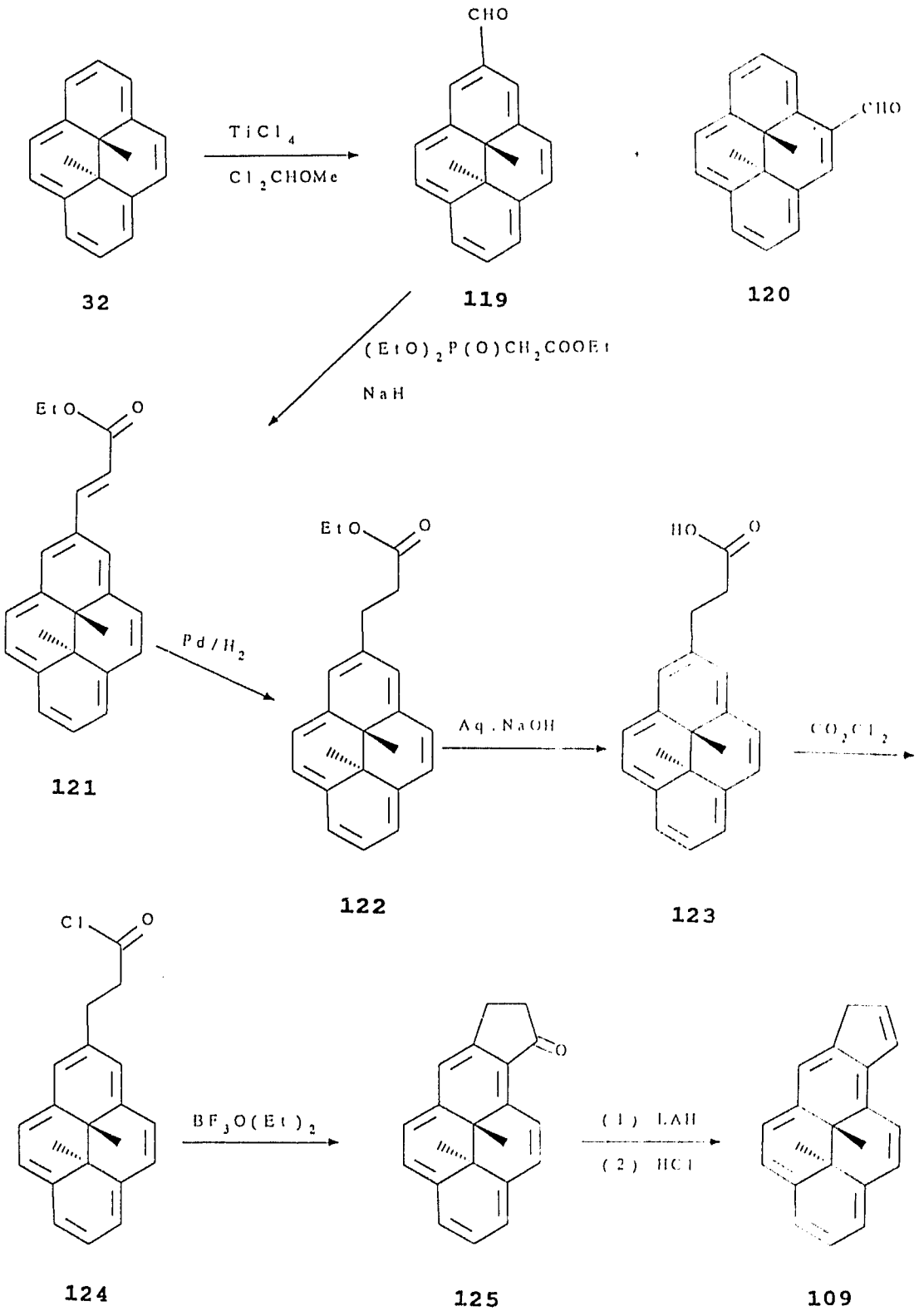
CHO
TiCl4
Cl2CHOMe
CHO
32
119
120
(EtO)2P(O)CH2COOEt
NaH
EtO
O
Pd/H2
EtO
O
Aq. NaOH
HO
O
(CO)2Cl2
121
122
123
Cl
O
BF3O(Et)2
O
(1) LAH
(2) HCl
124
125
109

dark red plates, mp 129-130 ^{o}C (literature 129-131 ^{o}C). Isomer **120** was isolated in 20% yield as dark green needles, mp 109 ^{o}C (literature 107-108 ^{o}C).

Chain-elongation by the Wittig-Horner reaction with triethylphosphonoacetate led exclusively to the trans-ester **121** in almost quantitative yield (ms. m/e 330). Recrystalization of **121** from ether-pentane gave dark-red plates, mp 146-147 ^{o}C. In its proton NMR, the internal methyl chemical shifts appeared as two singlets at δ -3.85 and -3.87 ppm. Reduction of the double bond was achieved in 86% yield. The saturated ester **122** was isolated as dark green gummy solid, m.s. m/e 332. All attempts to crystallize it failed. Both proton and carbon NMR spectra are confirmatory of the ester (see experimental). In its IR spectrum, the carbonyl stretch at 1730 cm^{-1} was normal for saturated esters. Its mass spectroscopy exact mass was found to be 332.168, while the calculated mass was 332.178.

Hydrolysis of the ester proceeded smoothly and gave the acid **123**. Chromatography of the product over silica gel with diethylether as the eluant gave pure **123** in 90% yield, ms. m/e 304, CI M+1 305. Recrystalization from cyclohexane-petroleum ether gave analytically pure **123** as dark green short needles, mp 165 ^{o}C. Its internal methyl protons appeared as two singlets at δ -4.19 and -4.20 ppm in its proton NMR spectrum. In the IR spectrum, the carbonyl stretch frequency was at 1683 cm^{-1}.

The cyclization step to making the ketone **125** proved not to be trivial. Treatment of saturated esters such as **126** with HF should lead to cyclization.[107] However, when the ester **122** was treated with liquid hydrogen fluoride no traces of **125** were detected. Instead, extensive decomposition of the starting material had resulted.

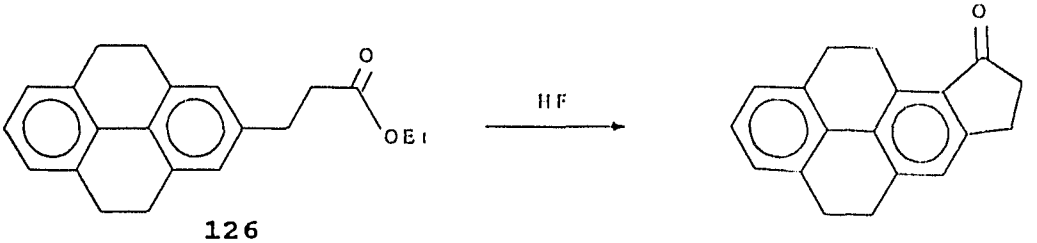

126

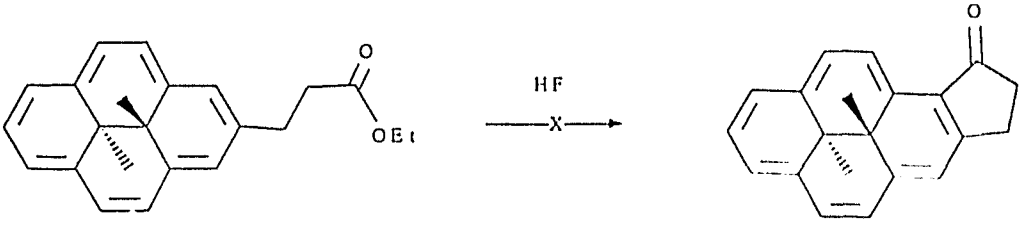

122

The saturated acid was also treated with polyphosphoric acid (PPA) as described for other aromatic systems[108], e.g. the PPA treatment works well for the paracyclophane **127**[109];

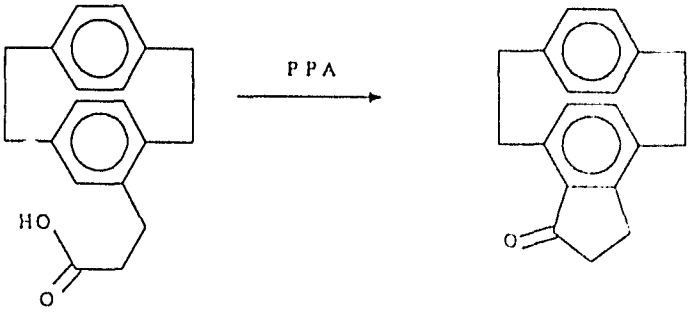

127

However, in this case no product was detected and extensive decomposition resulted. Treatment of the acid **123** with hydrogen fluoride[110] also resulted in decomposition, although not as extensive as in the case of the ester **122**. Still, no traces of the ketone product **125** were detected at the end of the reaction.

After these discouraging results, we decided to use milder conditions for the cyclization process. We thus decided to synthesise the acid chloride derivative **124**. Treatment of the acid **123** with thionyl chloride lead to extensive decomposition. In the presence of HMPA, which acts as a scavenger for protons in the reaction[111], decomposition still occurred. Treatment of the acid with aluminum chloride/sodium chloride mixture[112] at 150 ^{o}C resulted in traces of **124** (its IR carbonyl stretch was at 1802 cm^{-1}). Further heating at this temperature, however, resulted in decomposition. At higher temperatures, a black tar was obtained. No rearrangement products were detected. At high temperatures, DMDHP, **32**, is known to rearrange to **128**.[75b]

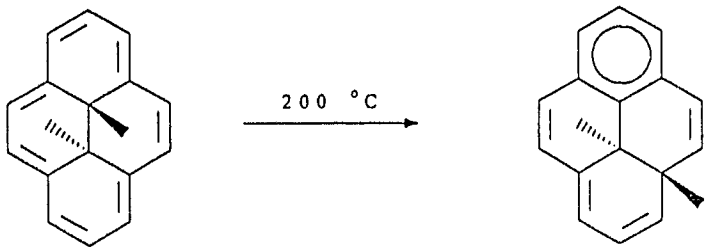

128

The acid chloride was finally obtained using a milder reagent. The infra red spectrum of the product upon treatment of the acid with excess oxalyl chloride in dry dichloromethane for six hours showed only one carbonyl stretch at 1802 cm^{-1}. The stretch at 1683 cm^{-1} due to the acid was absent. Further treatment of the acid chloride with BF_3-etherate in dry CH_2Cl_2 yielded the target **125** in about 63% yield (ms. m/e 286). The IR spectrum of the product showed a very sharp stretch at 1670 cm^{-1}. Recrystalization of the product from cyclohexane gave dark green thin plates, mp 210-211 ^oC.

When the ketone was stirred at room temperature with lithium aluminium hydride in dry THF for about 1.5 hours, followed by treatment with 15% sulfuric acid, low yields of the cyclopenteno-dmdhp **109** were obtained (ms. m/e 270). Replacement of sulfuric acid by a less strong acid, 20% hydrochloric acid, resulted in a drastic improvement in the yield. Recrystalization of **109** from cold methanol gave small dark green plates, mp 114-116^oC. In its ^1H NMR spectrum, the internal methyl protons appear at δ -4.15 and -4.16 ppm. The small shift from δ -4.25 (**32**), indicates that fusion of a cyclopentadiene to dimethyldihydropyrene does not perturb its ring current. Cyclopenteno-dmdhp **109** is not very stable. Even at 0 ^oC, decomposition usually resulted after two days. Owing to this instability, samples of **109** were always chromatographed using pentane as the eluant prior to its use in

subsequent steps. For spectroscopic purposes, generation of the anion **101** was accomplished in dry deuterated THF by treatment of **109** with potassium hydride in a glove bag under argon. The resulting intense red solution was then filtered into an NMR tube which was previosly flushed with argon. In the hopes of generating a cation free sample of **101**, treatment of the anion in deuterated dimethylsulfoxide led to extensive decomposition of the sample and no useful spectra could be obtained. The objective was, however, accomplished by using the crown ether 2,2,2-cryptan. For preparative purposes, precursor **109** was always treated with methyl lithium under argon.

2.3 Attempted Syntheses Of Iron-DMDHP Complexes

Having generated the anion **101**, our attention was now directed towards the synthesis of fused-dimethyl-dihydropyrene complexes. Our initial goal was to synthesize the targets **129a** and **130**. The most widely used method for the synthesis of complexes such as **129a** is to react the anion with ferrous chloride in dry THF. In the case of mixed complexes, the two anions are added together or separately.[113] Thus, ferrocene, **131**, is synthesised by reacting anion **15** with $FeCl_2$ and indenyl ferrocene, **132**, is made by reacting the same reagent with a mixture of anions **15** and **84**. In the second case, ferrocene is also produced.

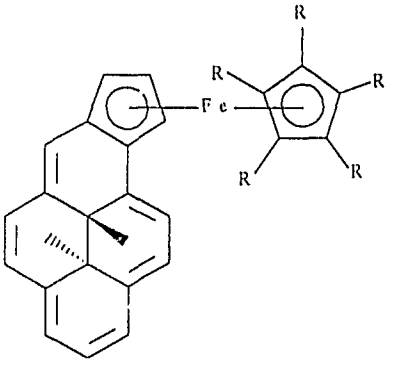

R=H **129a**
$R=CH_3$ **129b**

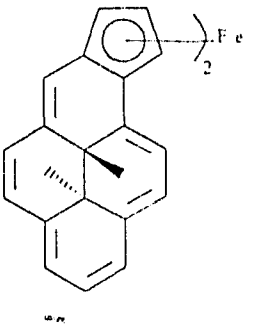

130

A solution of the anion **101**, was generated in dry deaerated THF under argon at -78 ^{o}C, after which it was warmed to room temperature and stirred for a further 15 minutes. The solution was then transferred to a flask containing a suspension of ferrous chloride (one equivalent) followed by the addition of one equivalent of lithium cyclopentadienide. The approach failed to yield the intended target **129a**. The only product detected after work-up in an air free atmosphere was ferrocene (proton NMR in $CDCl_3$: a singlet at δ 4.05 ppm). The yield was 70% based on CpLi. When a solution of the anion was added to ferrous chloride and stirred for 0.5 hour followed by the addition of CpLi, again the only organometallic product detected was ferrocene. No starting material could be recovered.

The revese addition approach also did not work. Thus, when lithium cyclopentadienide was added to a suspension of ferrous chloride, stirred for 0.5 hour and then followed by the addition of **101**, the only product

detected was ferrocene. Treatment of a solution of the anion **101** with a suspension of ferrous chloride (0.5 equivalent) did not yield any traces of the target **130**.

The use of the complex $FeCl_2$.2THF as a substitute for $FeCl_2$ dramatically improves the yields of some metallocenes.[114] We thus decided to treat the anion **101** with $FeCl_2$.2THF using the same procedures as above. Unfortunately, the change of the reagent did not improve on the negative results. No traces of either the targets **129a** or **130** could be detected. Variations in the reaction temperatures did not change these negative results.

Discouraged by these results, a search for an alternative route to ferrous chloride treatment was sought. In 1985, Manriquez et al[115] reported the synthesis of the intermediate $[Cp^*M(acac)]^+$, Cp^* = pentamethylcyclopentadienide. This intermediate was used to generate metallocenes in reasonably good yields. In the case of the pentamethyl substituted ferrocene, the yield was 86%.[115] We thus generated ferrous diacetyldiacetate by reacting the complex $FeCl_2$.2THF with acetylacetone, followed by a base as reported in literature.[116] The reagent (M = Fe) was prepared as described by Manriquez and was used *in situ*. Treatment with one equivalent of **101** did not however yield any traces of the organometallic target **129b**. Attempts to generate **130** as desribed in the reaction below also ended in failure. It

was hoped that an intermediate such as **133** would result from the treatment of a solution of **101** with $Fe(acac)_2$. Unfortunately, no organometallic products could be detected at the end of the reaction. No confirmatory spectra for **133** could be obtained suggesting that it is either extremely sensitive or that it may not have been formed in the first place.

Faced with the above negative results, we attempted to synthesise a stable derivative of the anion in the hopes that it could serve as a precursor for further reactions. We thus attempted the synthesis of the thalium target **134**. Stable thalium salts of both **15**[117] and **84**[118] are known. To a solution of KOH and thalium sulfate at 90 ^{o}C was added an equivalent amount of **109**

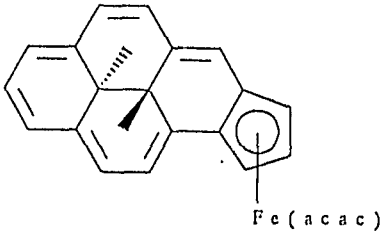

133

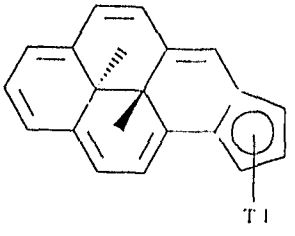

134

and the mixture was vigorously stirred using a mechanical stirrer for one hour. Upon cooling the mixture, no precipitate, as is the case when generating the thalium salt of **84**, was formed. Extensive decomposition of the organic substrate had resulted. No thalium salt could be

detected when the reaction was carried out under a temperature range from 25-85 ^{o}C.

2.4 Synthesis Of Ferrocenes Using Photolysis

para-Xylene iron cyclopentadienyl cation, **135**, synthesised by the treatment of ferrocene with $Al/AlCl_3$ in para-xylene[119], can be used to deliver an iron-Cp^+ fragment to a number of aromatic substrates. Photolysis of a solution of **135** and cyclophane **7** in dichloromethane yields the complex **136** in 85%.[120] The presence of any electronically rich aromatic species will effect the displacement of p-xylene. It is therefore reasonable to assume that a species such as the anion **15** would effect the displacement. This is indeed the case. When a solution of **135** and **15** in dry DMF was stirred at room temperature, traces of ferrocene are detected in the product. The change in the solvent here is due to solubility problems. Photolysis of the same reaction mixture for 4 hours, using a reflector 150W flood lamp, resulted in 80% yield of ferrocene. When the reaction was repeated using indenyl anion **84**, two fractions were obtained after chromatography of the product over basic alumina. The first fraction was ferrocene, followed by indenyl-ferrocene **132** (yield 69%). Recrystalization of the second fraction from pentane gave red-violet crystals

of **132** whose ^{1}H NMR spectrum agrees with that in literature.[113c]

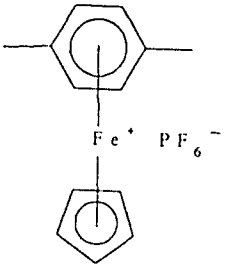

135

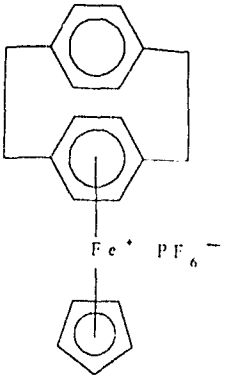

136

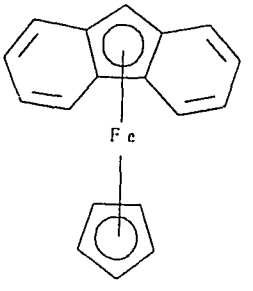

137

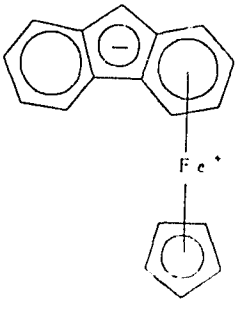

138

Attempted synthesis of the corresponding fluorenyl-ferrocene **137** as described above resulted in failure. No traces of the other possible isomer **138** could be detected.[121] The isomer **138** has a characteristic green color. It should be noted here that treatment of fluorenyl anion with ferrous chloride and cyclopenta-dienyl anion fails to yield **137**. Heating the benzene complexed isomer **138** in toluene at 80 ^{o}C yields flourenyl-ferrocene in good yield.[122] When we attempted to repeat the photolysis reaction as above using a solution of the anion **101** in DMF, a similar negative

result was obtained. The only organometallic product detected was ferrocene.

Our failure to synthesize ferrocene-fused dimethyldihydropyrene may have its origin in the charge distribution in the anion **101**. The aromatic 14-annulene is electron withdrawing. Therefore, its fusion to the anion **15** results in the reduction of the charge density in the anion. A π-SCF calculation revealed to us that 40% of the charge resides on the 12 remaining carbons of the macroring. Tetracyanocyclopentadienide[123] and penta(methoxycarbonyl)cyclopentadienide ions[124] do not form ferrocene on treatment with $FeCl_2$ in consequence of the delocalization of the negative charge over the electron accepting substituents. The derivatives obtained are iron(II) salts. The iron(II) tetracyano-cyclopentadienide salts are involatile and extremely air sensitive. These properties indicate an ionic and not a μ^5-complexed iron. Similarily, in the case of anion **101**, iron(II) salts might be formed. Our inability to isolate these salts is indicative of their extreme reactivity.

2.5 Synthesis Of Other Metal Complexes

Following the discouraging results in our attempts to obtain fused ferrocene-dmdhp complexes, our attention was focussed on generating complexes of other metals. We thus decided to investigate the synthesis of a fused

ruthenocene. Due to the increased stability of pentamethylcyclopentadienyl complexes over the unsubstituted cyclopentadienyl complexes, we turned our attention to synthesising the ruthenocene complex **139**. The reagent of choice was the oligomeric species $(Cp^*RuCl_2)_n$, **140**.[125] It is synthesised by refluxing ruthenium trichloride hydrate and pentamethylcyclopentadiene in ethanol. In refluxing methanol, the product is less soluble in organic solvents than that obtained in ethanol as a solvent, suggesting a higher degree of polymerization.[125a]

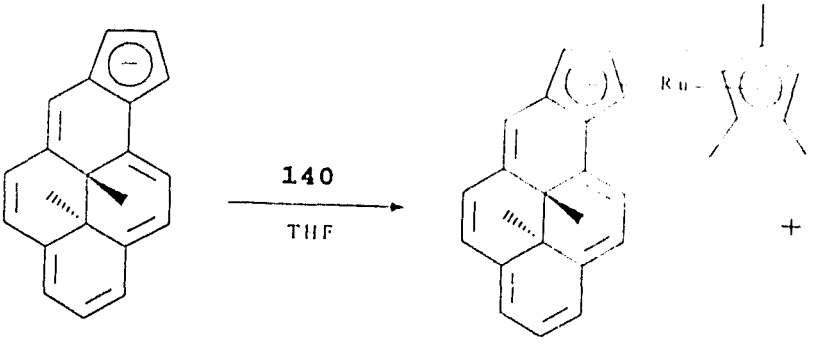

139a

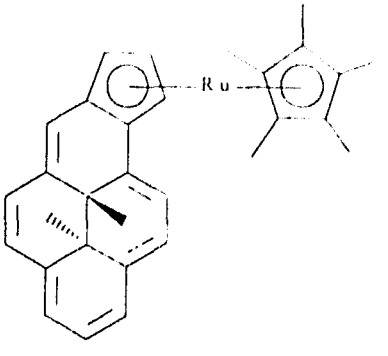

139b

The anion **101** was generated in dry deaerated THF at -78 ^{o}C, after which it was warmed to room temperature and stirred for a further 15 minutes. The reagent **140** was then added. The reaction mixture was stirred at room temperature for 30 minutes after which it was heated to 40 ^{o}C for an extra 15 minutes. The solvent was evaporated from the cooled mixture and the solid residue taken up in cyclohexane and chromatographed over basic alumina. Evaporation of the solvent led to a solid residue with a distinctive rosy-violet appearance, ms. CI M+1 506. Proton NMR of the chromatographed product indicated the presence of two isomers: *anti*-ruthenocene **139a** and *syn*-ruthenocene **139b**. The ratio of the former to the latter from ^{1}H NMR integration of the internal methyl signals is 3.7 : 1. The overall yield of the two isomers was 70%. Several attempts to separate the two isomers were not successful. Complications arise due to the air sensitivity of the product. The internal methyl protons of the major isomer appear at δ -0.548 and -0.691 ppm, while those of the minor isomer resonate at δ -0.473 and -0.820 ppm.

Following this success, we turned our attention to generating the tricarbonyl cyclopentadienyl-fused target **141**. Dipyridine tricarbonyl manganese(I) bromide appeared to be a suitable reagent.[126] It can be synthesized by refluxing manganese pentacarbonyl bromide in absolute ethanol in the presence of 2 equivalents of

pyridine.[127] The reagent can also be prepared from the bromide using pyridine as a solvent.[126a] To our surprise, treatment of the anion **101** with the reagent failed to produce the target **141**. However, treatment of the anion with manganese pentacarbonyl bromide in dry THF for 10 minutes followed by heating the mixture at 40 ^{o}C and then cooling to room temperature yielded **141** in 61%. Chromatography over basic alumina using cyclohexane as the eluant, followed by cold evaporation of the solvent yielded **141** as a dark brown solid, ms. m/e 408, CI M+1 409. Similar to the complex **139**, two structural isomers

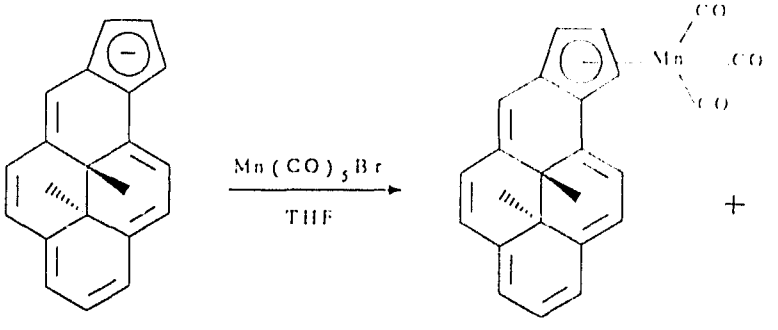

141a

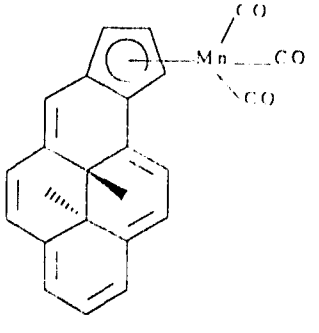

141b

were detected from its ^{1}H NMR in a ratio of 2.5 : 1. The methyl protons of the major isomer appear at δ -0.728 and -0.784 ppm. The internal methyl protons of the minor isomer **141b** were at δ -0.670 and -0.976 ppm.

Several attempts to separate the two isomers met with failure. Fractional crystalization also failed to separate them. The isomers are air sensitive and the reaction work-up was always done in the absence of air. The same work-up procedure was used in the preparation of the comlpex **139**.

CHAPTER THREE

RESULTS AND DISCUSSION

3.1. CYCLOPENTADIENYL FUSED DIMETHYLDIHYDROPYRENE

3.1.1 Introduction:

As discussed earlier in chapter one, the concept of aromaticity and its origin remains a center of discussion in the development of both theoretical and experimental chemistry. Nevertheless, no one can argue the case of benzene not being an ideal aromatic. The molecule possesses a positive resonance energy, has a D_{6h} structure with bonds equal to 1.398 A^{O} and it sustains a diamagnetic ring current. It is of no surprise that the concept itself is frequently discussed in terms of the benzene molecule. Thus an aromatic compound is one that has a positive Dewar resonance energy, shows little bond fixation, i.e. variation from benzene bond length, and most of all sustains the diamagnetic ring current invoked for the benzene case.

The choice of other aromatic compounds as a standard for comparison is indeed rare. Haddon's[29,95] calculation of the aromatic character, k, as a measure of aromaticity, using HMO theory with allowance for bond alternation, is indeed unique in that the calculations utilized parameters for dimethyldihydropyrene, **32**, and

not those of benzene. To derive k, the integration parameter β has to be parametized, and the use of 32 rather than benzene renders much smaller errors in the calculations of k for a series of annulenes. Table 9 lists the k values for a selected number of these annulenes.

Table 9: Aromatic character, k, for selected annulenes

Annulene	Aromatic character, k
[10][1]	0.768
[12]	0.582
[14][2]	1.000
[16]	0.729
[18]	0.837
[24]	0.805

1: 1,6-methanoannulene, 2: dmdhp.The rest are non-bridged

When discussing stability of annulenes, comparisons between benzene and other annulenes are always mentioned. Thus, in simple Huckel terms, the resonance energy of benzene is calculated as,

$$RE = E_{\pi} - E_{\pi loc}$$
$$= 6\alpha + 8\beta - (6\alpha + 6\beta)$$
$$= 2\beta$$

For another annulene, such as [8]-annulene, the same parameter is,

$$RE = 8\alpha + 9.6\beta - (8\alpha + 8\beta)$$
$$= 1.6\beta$$

The resonance energy per electron, REPE, for benzene is thus 0.33β whereas that for [8]-annulene is 0.20β. Thus, in simple Huckel terms, cyclooctatetraene still possesses stabilization energy.

The model system for benzene in the above calculation is three ethene molecules, whereas that for [8]-annulene is four ethene molecules. In π-SCF calculations, mentioned in the introduction[21], the model for both is changed to an acyclic polyene, giving an improvement in the results, ie. cyclooctatetraene is now predicted to have a destabilization energy in agreement with experiment. In these calculations, however, no mention of the resonance energy of cyclopentadienyl anion is cited. As a matter of fact, no charged annulenes were considered for the calculations. The difficulty, of course, arises due to the presence of the negative charge in the odd numbered annulene. A similar neglect of charged annulenes also occurs in the calculations done by Hess and Schaad using the HMO method but utilizing the new polyene reference.[22]

The difficulty in comparing a neutral system such as benzene to an isoelectronic charged system such as cyclopentadienyl anion arises due to the choice of

comparable models. The calculated resonance energy for the anion **15** , in terms of a simple HMO method, uses pentadienyl anion as a reference is,

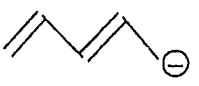

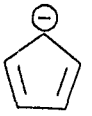

$RE = 6\alpha + 5.46\beta - (6\alpha + 4\beta)$ $RE = 6\alpha + 6.47\beta - (6\alpha + 4\beta)$

$= 1.46\beta$ $= 2.47\beta$

$(REPE = 0.24\beta)$ $(REPE = 0.41\beta)$

Thus, the reference for the anion **15** is only two ethene units compared to three units for benzene.[128] Therefore, the REPE values for both aromatics, when used to relate the extent of their comparable stability, should be used with caution. A more direct means by which the relative stability of the two compounds may be compared is to use the absolute Huckel resonance energies. This term for cyclopentadienyl anion is calculated as $2.47\beta - 1.46\beta = 1.01\beta$. The corresponding parameter for benzene is then $2.00\beta - 0.99\beta = 1.01\beta$. The two parameters are equal suggesting that in terms of HMO theory the cyclopentadienyl anion is as aromatic (stable) as benzene itself.

The first comparisons between REPE of benzene and that of anion **15** were only introduced with Aihara's calculations in 1975.[24] These were theoretical calculations based on graph theory. Other calculated REPE values for both aromatics are listed in Table 10.[95]

Table 10: REPE values (β) for benzene and **15**

	Dewar	HS	AI	AII/GMT	Haddon[95]
Benzene	0.120	0.065	0.060	0.046	0.061
Anion **15**	?	?	0.070	0.053	0.071

Dewar: Dewar and de Llano (ref. 21)

HS: Hess and Schaad (ref. 22)

AI: Aihara (ref. 24)

AII/GMT: Aihara (ref. 24), Gutman, Milun, and Trinajstic (ref. 25)

In all cases, the REPE for anion **15** is greater than that of benzene, the ratio being about 1.2. A larger value can be calculated from a simple mathematical manipulation using Haddon's correlation of the ring current to resonance energy, assuming that, from chemical shift charge correlation[57], both molecules bear a ring current of similar magnitude.

$$RC = 3SRE / \pi^2$$

$$S(\text{benzene}) / S(\text{cyclopentadienyl}) = 1.2 \quad , \text{ hence,}$$

$$REPE(Cp) / REPE(\text{benzene}) = 1.4$$

There are other methods that relate the aromaticity (stability) of other systems to benzene. The difficulty

with those methods is that they are usually limited to neutral annulenes. The HOMO-LUMO gap of Zhou and Parr,[54] the aromatic induced solvent shift[129], and the barrier to rotation of a tricarbonyl group[130] all use neutral aromatics.

As mentioned earlier, equalization of bonds around the π-periphery increases the aromaticity of the annulene. Moreover, if this annulene is fused to another aromatic, mutual bond fixation results. Thus, if a series of annulenes is fused to that annulene, a relative scale can be set up in which the aromaticity is directly related to the effective bond fixing ability (EBFA) of the fused aromatic. In the case of benzene and cyclopentadienyl anion, this parameter will provide us with an experimentally determined comparison when experimental parameters are used to calculate EBFA.

From our model molecule **100**, the experimental value for EBFA can be calculated in a number of ways. As we have seen in chapter one, the chemical shifts of the internal methyl protons are an excellent indicator of bond alternation manifested in the reduction of the ring current in the macroring. Therefore, these chemical shifts should serve as excellent indicators of the effective bond fixing ability of the fused aromatic. We will define the parameter as follows,

$$EBFA = (4.25 + \delta CH_3) / 2.63 \quad \text{---------- (6)}$$

where the value 2.63 is the difference between the chemical shift of **32** (-4.25 ppm) and the chemical shift of the internal methyls in the benz-fused **92** (-1.62 ppm). A second method is to include the coupling constants of the type a and b in the calculation of EBFA. The value of EBFA may be calculated as follows,

$$EBFA = a_1 - a_2 / 2.47 \quad \text{------(7a)}$$

$$EBFA = b_1 - b_2 / 2.35 \quad \text{------(7b)}$$

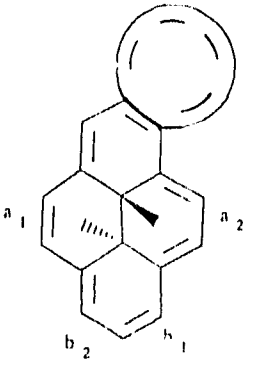

where the values 2.47 and 2.35 are the corresponding coupling constant differences for **92**. Since the magnitude of bond fixing is, however, more accurately manifested when a larger number of bonds is included, the values obtained from 7a and 7b may not be conclusive. A better value might be calculated from the average differences as in equation 7c,

$$EBFA = 1/2 \{(a_1 - a_2)/2.47 + (b_1 - b_2)/2.35\} \quad \text{---- (7c)}$$

We will thus use these equations to calculate the relative EBFA of the anion **15** to that of benzene using the proton NMR data for the newly synthesized anion **101**.

3.1.2 Properties of The Anion 101

3.1.2.1 Physical Properties:

Cyclopentadienyl-fused dimethyldihydropyrene, **101**, which we will call cp-dmdhp, is an intense red charged aromatic. It is relatively stable at room temperature provided that the solvent is dry and the anion is kept under argon or nitrogen. Decomposition is usually noticeable after about two hours of its generation. To our knowledge, cp-dmdhp is the first cyclopentadienyl fused large annulene.

3.1.2.2 Experimental and Theoretical Internal Methyl Chemical Shifts:

As we mentioned previously, the internal methyl chemical shift was calculated, using π-SCF calculations, as -2.54 ppm. Table 11 lists the calculated π-SCF bond orders for the anion. To simulate the presence of a counter cation, a metal cation was placed at a distance of 1.4 A^{o} from the Cp ring. In this case, the cation draws out about 15% of the negative charge. Bond orders for the complexed anion, **101b**, are listed in the same table.

Table 11: Calculated π-SCF bond orders for anion **101**

Bond	P_μ ($x10^3$)	
	101a	**101b**
a	540	542
b	712	710
c	565	572
d	710	703
e	565	581
f	701	688
g	577	598
h	706	693
i	568	585
j	702	691
k	573	585
l	710	710
m	532	526
$\Delta P_\mu = \Sigma P^\mu - 642$	961	848
m	13	13
$\Delta r = P_\mu / m$	73.9	65.2
δCH_3cal	-2.54	-2.77
δCH_3found	-3.14, -3.19	-2.83, -2.88

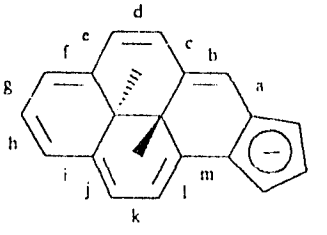

101a

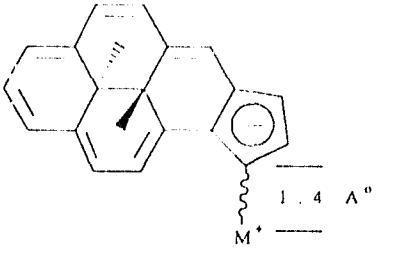

101b

The chemical shift calculated in Table 11 for the anion **101b** agrees well with that found experimentally. Hence, equation 4 (Mitchell equation) apparently works well for bond fixations resulting from neutral aromatic compounds as well as the negatively charged anion **15**.

At a first approximation, the chemical shift calculated for anion **101a** is in good agreement with the experimental chemical shift. However, the difference of 0.63 ppm is significant enough that an explanation for its origin is needed. A difference due to geometrical changes is not a factor here. Since the difference value is due to a shielding factor, the most probable cause is that involving a negative charge.

To verify this, we looked for a model that would enable us to calculate the shielding due to the through space interaction between a cyclopentadienyl anion and a similar set of protons. The anion **142**[131] seemed to us as the best choice. Figure 2 shows selected proton chemical shift values for the model along with those for the corresponding benzene analogue **143**.[132]

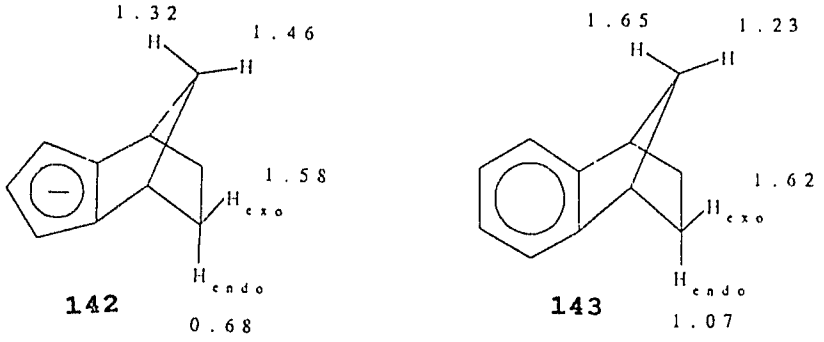

Figure 2: Effect of the negative charge on H_{endo} in **142**.

In going from the parent bicyclo[2.2.1]heptane to **142** and **143**, it is reasonable to assume that no significant geometrical changes have occured. This is verified by the molecular mechanics output. Thus, any substantial changes in the chemical shifts are essentially due to the shielding (deshielding) effects of the fused aromatic ring. In going from the parent hydrocarbon to the benz-fused **143**, the chemical shift of the endo proton is the least affected. It only experiences a shielding difference of 0.04 ppm.[132b]

To test the applicability of the MMX/PCMODEL3[133] calculations regarding the anisotropy effects of benzene, we employed the Memory equation[134] for which the parameters used were those obtained from the molecular mechanics output. The parameters were determined by querying the MMX output structure file in the display mode of the PCMODELPI. The calculated anisotropy effect of the benzene ring was indeed found to be comparable (<0.05 ppm).

From chemical shift-electron density correlations, Dailey had determined that the ring current chemical shift for an aromatic hydrocarbon is given by[135]

$$\sigma_1 = 0.63k_b \, (a_1 / a_2)^2 \, I_I \qquad \text{---------(8)}$$

where k_b is the entry in the Johnson and Bovey tables for the appropriate proton ring center distance, a_1 is the

radius of the ring in question and a_2 is the radius of the benzene ring. The symbol I_I is the ratio of the ring current intensities for the ion and benzene. Since the ratio a_1/ a_2 is less than one and assuming that the value for I_I is approximately one, the anisotropy correction due to the aromatic anion at the endo proton is less than 0.05 ppm.

Thus, from the above estimations, we can conclude that any differences in the chemical shifts of the endo proton in going from the parent to the benz-fused derivative **143** and the cyclopentadieno-fused **142** are essentially due to the charge effects. In the anion **142**, this proton resonates at 0.68 ppm. The same proton resonates at 1.07 ppm in **143**. Therefore, the shielding difference of 0.39 ppm can be used as the effective shielding value introduced due to a through space interaction between the endo proton and the cyclopentadienyl anion.

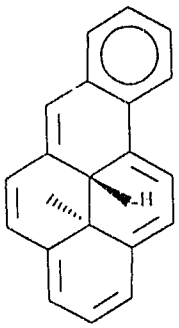

σ_{Ar} = -0.047 ppm

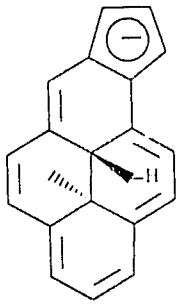

σ_{Ar} = < -0.05 ppm

Again, using the Memory equation, we calculated the anisotropic effect of the benzene ring on the internal methyl protons in **92**. The effect is indeed very small (<0.05 ppp). Using the same approach, the parameters for the internal protons of the anion **101** were also determined. The calculated anisotropy effect is also negligible (<0.05 ppm).

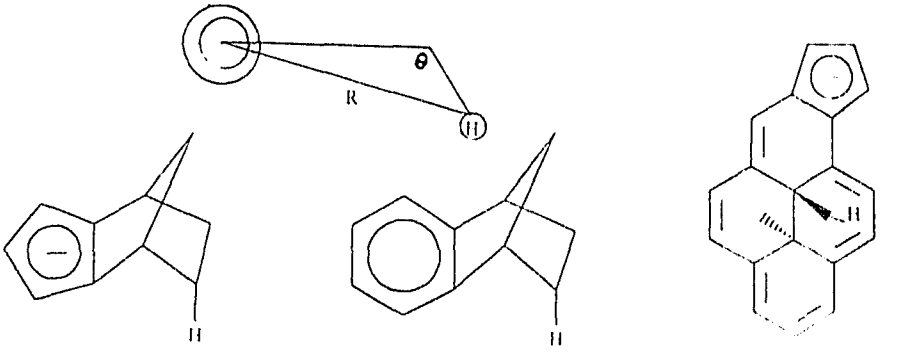

R=4.2 A^{O}, θ=103^{O} R=4.4, θ=99 R=4.6, θ=108

Figure 3: Comparison of parameters θ and R for **142**, **143** , and **101**.

To test how the spatial orientation of the endo proton in the two species **142** and **143** compared with the internal methyl protons of the anion **101**, we decided to use the parameters R and θ as explained in the figure above. Fortunately, these parameters are apparently, to a first approximation, similar. Thus, a comparison of the anisotropy effect of the anion on both the endo proton in **142** and the internal protons in **101** is valid. Hence, we can safely conclude that the chemical shift

shielding of the negative charge on the internal methyl protons in **101** is about 0.40 ppm.
The effective chemical shift of the internal methyls is therefore,

$$\text{Effective } \delta CH_3 = -3.17 + 0.40 = -2.77 \text{ ppm} \quad \text{-----(9)}$$

This value is in good agreement with that calculated from the π-SCF output (-2.53 ppm). Moreover, the effective value is in complete agreement with that calculated for the complexed anion **101b**. It is also in very good agreement with the experimental chemical shift (-2.85 ppm). This leads us to conclude that the difference between the experimental internal methyl chemical shift of the anion **101a** and **101b** , equal to 0.32 ppm, is primarily due to the shielding effect of the negative charge.

3.1.3 Coupling Constants-Chemical Shifts Correlations

Gunther's equation (3) relates bond orders to coupling constants in aromatic benzenoids. As we have seen in chapter one, it also works for dihydropyrenes. Thus by determining the coupling constant, J, we can calculate the corresponding bond order, P.

$$P = 0.104\ {}^3J - 0.120 \quad \text{----------(3)}$$

The experimental proton NMR spectra, along with the simulated spectra for the aromatic region for both **101a** and **101b** are included on the next page. The chemical shifts are listed in Table 12. Table 13 lists the coupling constants obtained from the simulated spectra. As can be seen from the latter table, the internal methyl chemical shift of the anion **101a**, calculated from the measured coupling constants, is in good agreement with the experimental one.

Table 12: Experimental chemical shifts for anion **101**

Proton	Anion **101a**	Anion **101b**
A	8.35	8.25
B	7.71	7.70
C	7.59	7.57
D	7.41	7.39
E	6.83	6.90
F	7.58	7.55
G	7.70	7.61
H	7.92	7.79
J	7.43	7.30
K	7.10	6.97
L	6.76	6.67
CH_3	-3.17	-2.85

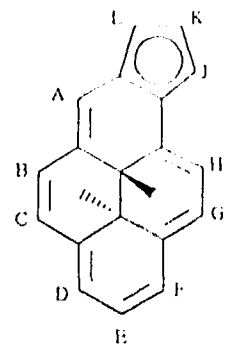

101a

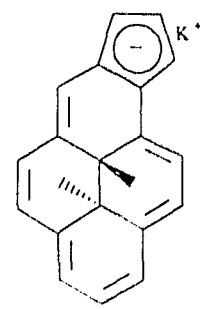

101b

a.

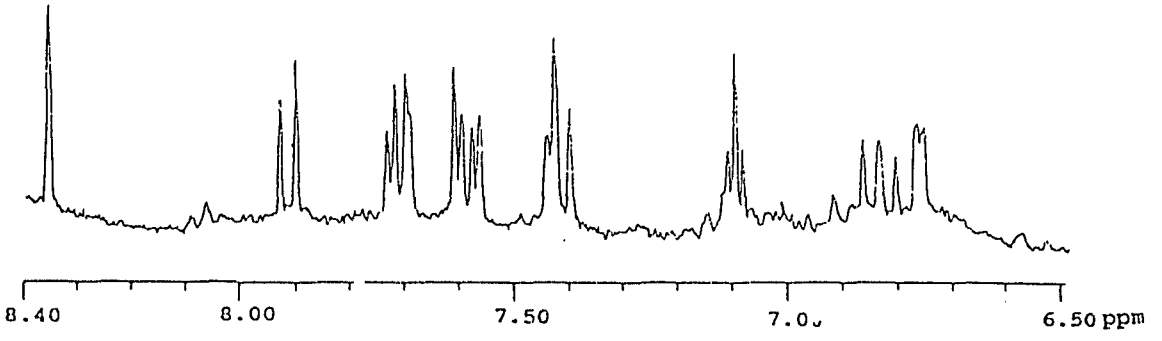

b.

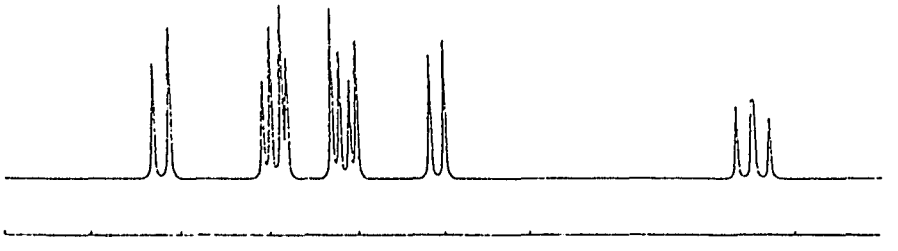

Figure 4: Proton NMR spectra (aromatic region) for anion **101a**. a. Experimental (250 MHz). b. Simulated

a.

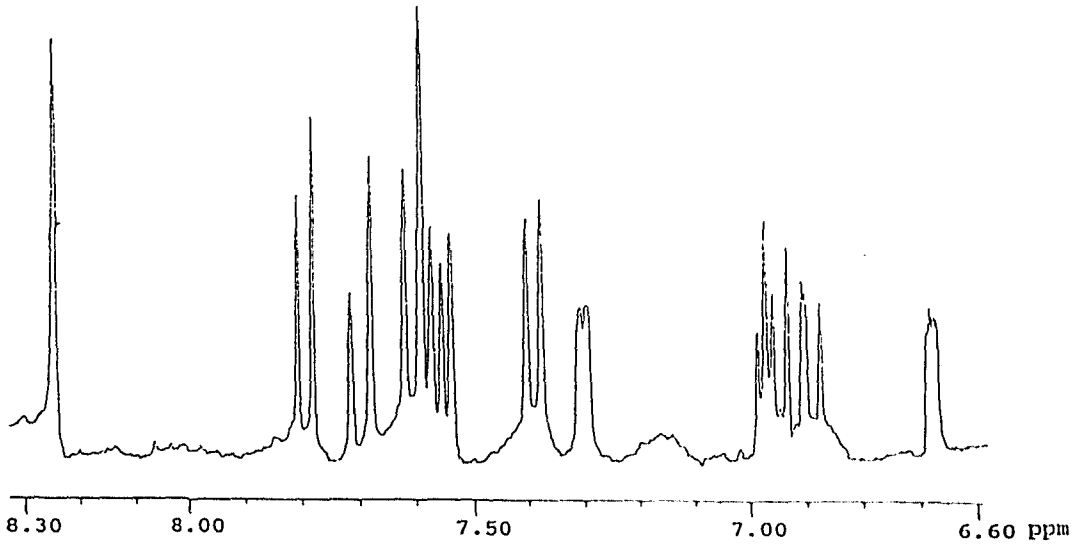

b.

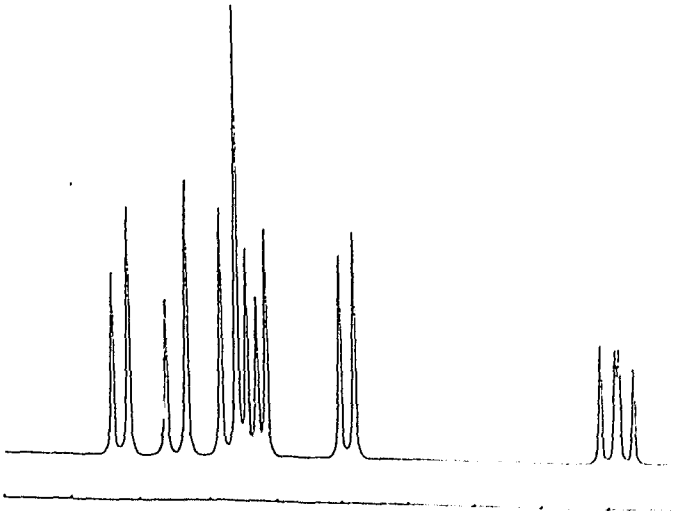

Figure 5: ^{1}H NMR spectra (aromatic region) for anion **101b**
a. Experimental (250 MHz). b. Simulated

Table 13: Calculated chemical shifts from experimental and theoretical bond orders

	101a			**101b**		
Bond	J (Hz)	P_{NMR}	$P_{\pi-SCF}$	J (Hz)	P_{NMR}	$P_{\pi-SCF}$
BC	8.33	746	710	8.70	785	703
DE	6.78	585	577	6.62	568	598
EF	7.87	698	706	8.40	747	693
HG	7.05	613	573	7.14	622	585
Δr		61.6	67.2		85.5	53.4
δCH_3(calc)		-2.87	-2.74		-2.21	-3.09
δCH_3(found)		-3.17			-2.85	
Effective δCH_3			-2.77			

This chemical shift is also almost identical to the calculated effective chemical shift. Thus it is apparent that the shielding effect due to the negative charge is almost offset by the effects of the diffused charge on the calculated bond orders. In other words, the difference between - 3.17 and - 2.87 (= 0.30) seems to have resulted from an increase in Δr caused by an increase in electron density at these bonds.

In the presence of the counter cation, the agreement is not good. The calculated chemical shift is - 2.21

ppm, some 0.64 ppm less shielded than the experimental value. The chemical shifts of the external protons of the macroring are not significantly different when compared with **101a**, the largest difference being 0.12 ppm. If we consider that each electronic charge introduces 10.7 ppm[58,18a], we can correct for the presence of partial charges at the macroring carbons. The electron density values were obtained from the π-SCF output. In the case of the free anion, about 40% of the negative charge resides on the 12 carbon atoms of the 14 π-annulene (the two carbon atoms that are a part of the fusion bond are excluded here). In the case of the anion **101b**, only 18% of the charge is delocalized on the 12 carbons. Figure 6 shows the chemical shift corrections due to these partial charges.

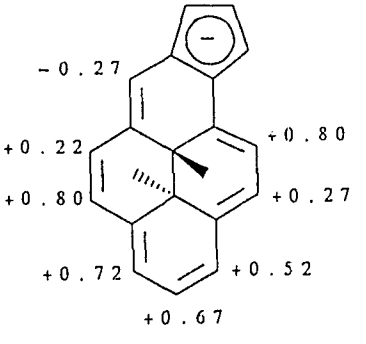

101a

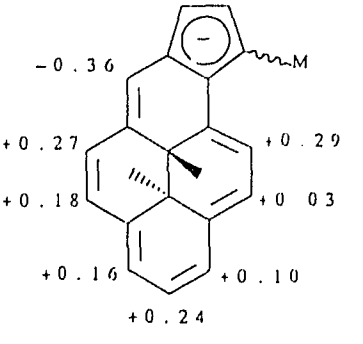

101b

Figure 6: Chemical shift correction due to partial charges (+ shielding, - deshielding)

As can be seen from the figure, magnitudes of the shielding effects due to the fused negative charge are quite different in each of **101a** and **101b**. There is less charge delocalized in the case of **101b**, hence we would expect the coupling constants J_{BC}, J_{EF}, J_{DE}, and J_{HG} to actually be smaller in **101b** than in **101a** based on electron densities alone. This is only true for J_{DE}. The largest difference in J and hence the bond order ($P_{NMR} - P_{\pi\text{-SCF}}$) is found in the bonds BC and EF. This apparent abnormality may have its cause in the effects of the counter cation or in geometrical changes in the molecule. Since the later factor is very unlikely, the large differences are primarily due to the presence of the positive charge in the medium. As is the case for the indenyl salts[136], the cation is expected to be located in the vicinity of the 5-membered ring. However, it (the cation) must also be interacting with another cp-dmdhp anion in solution. This secondary anion-cation intermolecular interaction may be the cause for such large differences, leading to the 0.64 ppm shielding difference between the calculated chemical shifts for **101b**. It should be noted that in π-SCF calculations, such interactions are not accounted for.

3.1.4 The Mitchell Equation, Revisited

When equation 4 was derived, the bond orders of **32** were all parameterized to 0.642. This value is the Huckel bond order for a perfectly delocalized 14-annulene, and is derived without allowing for any interactions between distant atoms. The π-SCF output allows for such interactions.

The π-SCF bond orders for **32** are listed in Table 14. These bond orders are slightly different from the Huckel value. Therefore, an equation that includes these differences may be slightly better. So, in the hopes of improving the previous equation (4), especially for fused dmdhp systems which show only fair agreement between experiment and theory, we set to recalculate the bond order differences. We used the same molecules that were used in the original derivations. Table 14 lists the chemical shift shielding ($\Delta\delta$) as a function of bond fixation (Δr), taking Δr for dimethyldihydropyrene as zero.

The equation obtained is a straight line plot (Figure 7, $R_c = 0.992$), in the form,

$$\Delta\delta = 5.404 - 0.02656\ \Delta r \qquad \text{----------(10)}$$

We used this new equation to recalculate the internal methyl chemical shifts for a number of annelated dmdhps. Table 15 lists the results of the calculations.

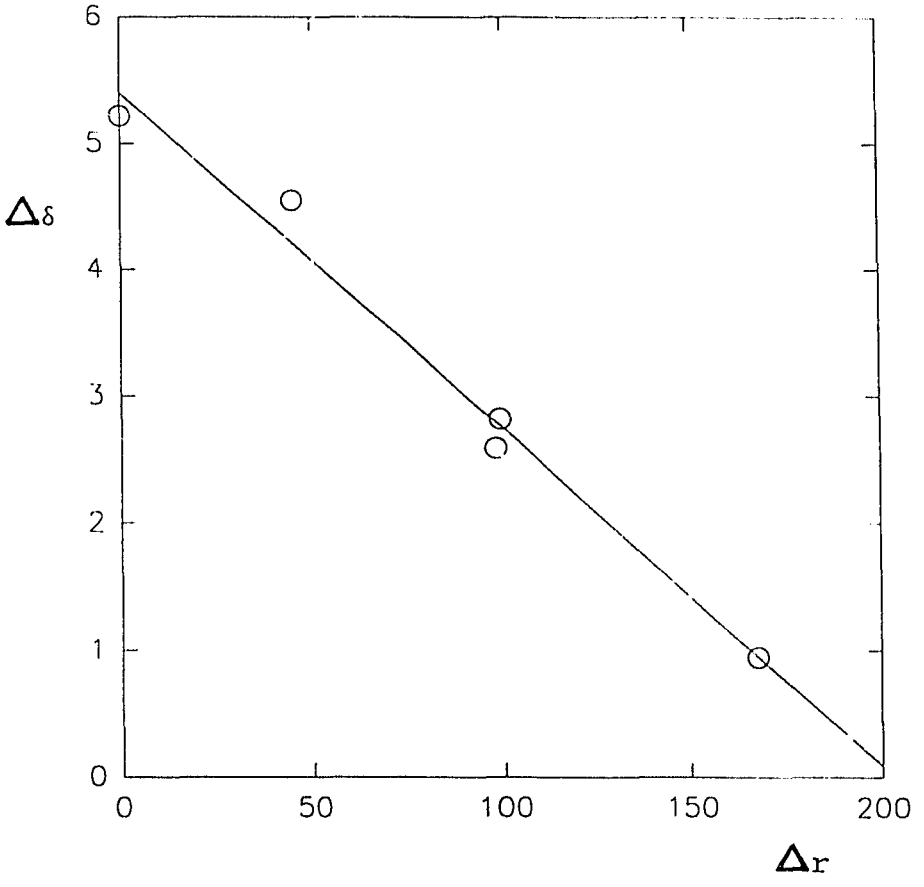

Figure 7: Chemical shift shielding ($\Delta\delta$) as a function of bond fixation (Δr).

$$\Delta\delta = 5.404 - 0.02656\ \Delta r \text{ ----------(10)}$$

$$R_c = 0.992$$

Table 14: Chemical shift shielding as a function of bond fixation for fused DMDHPs (bond orders given for **32**)

Compound	Δr	$\Delta\delta$ (ppm)
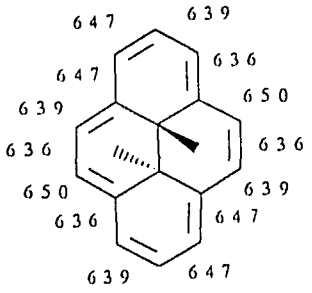 **32**	0.00	5.22
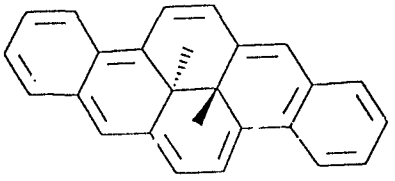 **94**	44.83	4.55
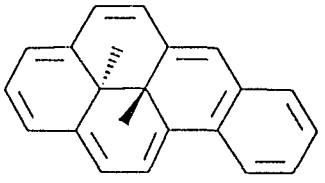 **92**	98.15	2.59
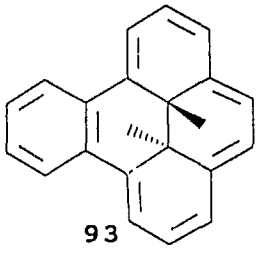 **93**	99.31	2.82
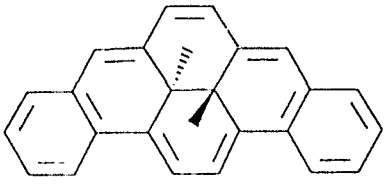 **95**	167.6	0.95

Table 15: Calculated δCH_3 for selected fused DMDHPs

Compound	$\Delta\delta$	δ	δ_{expt}	$\delta_{from\ (4)}$
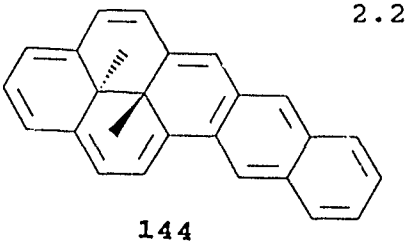 **144**	2.24	-1.27	-0.44	-1.28
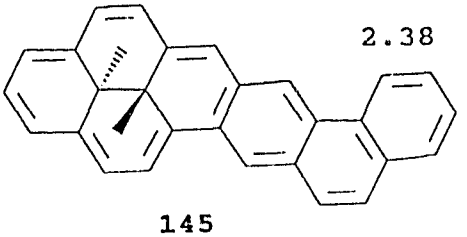 **145**	2.38	-1.41	-0.88	-1.43
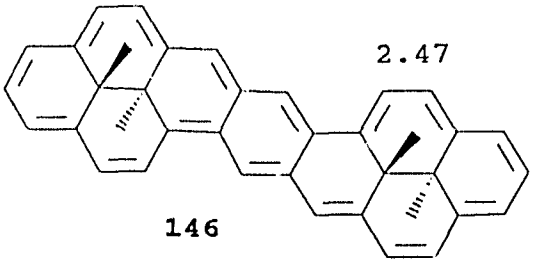 **146**	2.47	-1.50	-1.60	-1.52
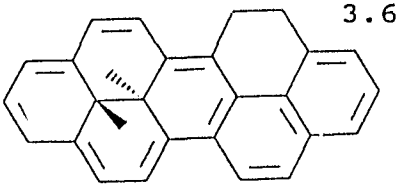 **96**	3.67	-2.70	-2.78	-2.75
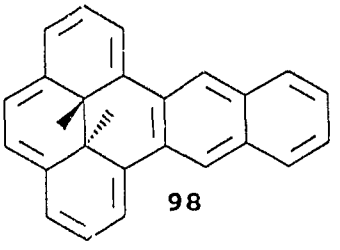 **98**	2.21	-1.24	-0.74	-1.25

Table 15 continued,

4.43	-3.46	-4.19, -4.28	-3.51

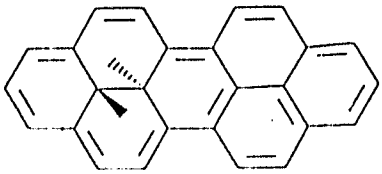

97

3.95	-2.98	-3.20	-2.99

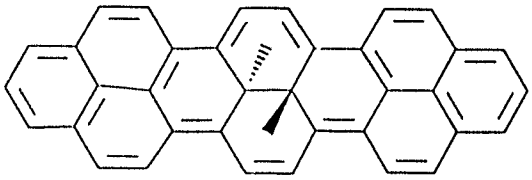

147

2.61	-1.64	-1.35, -1.41	-1.70

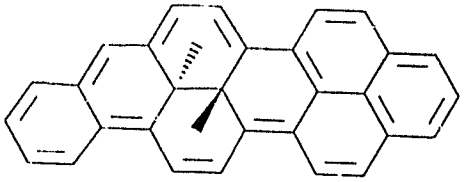

148

As can be seen from Table 15, there are essentially no differences in the chemical shifts obtained from either equation. Some improvement in the prediction, especially for the compounds **145** and **148** is achieved. It should be noted that the calculated chemical shift value

for **97** was erroneously reported as -3.97 ppm using equation (4). The calculated chemical shift should be -3.51 ppm.[92] Using the new equation 10, the calculated value is -3.46 ppm. A slight correction is also introduced for compound **148**. The correct value should be -1.70 instead of -1.73 ppm. The calculated value using the new equation is -1.64 ppm.

Using the new equation, we also calculated the internal chemical shifts for the anions **101a** and **101b**. Table 16 lists the predicted chemical shift values using the π-SCF output for all ⊥3 bonds of the macroring. Table 17 lists the values calculated using the bond orders obtained from experimental ^{1}H NMR data and the corresponding bond orders from the π-SCF output.

Table 16: Calculated δCH_3 for anion **101** from π-SCF output

Parameter	**101a**	**101b**
ΔP	968	853
m	13	13
Δr	74.4	65.6
δCH_3 from (10)	-2.46	-2.69
δCH_3 from (4'	-2.54	-2.77
Expt.	-3.17	-2.85

Table 17: Calculated δCH_3 for **101** using experimental data

Parameter	**101a**		**101b**	
	NMR	π-SCF	NMR	π-SCF
$\triangle P$	254	274	350	221
m	4	4	4	4
$\triangle r$	63.5	68.5	87.5	55.3
δCH_3 from (10)	-2.75	-2.62	-2.11	-2.96
δCH_3 from (4)	-2.87	-2.74	-2.21	-3.09
Expt.	-3.17		-2.85	

As can be seen from the two tables, no substantial changes in the predictions are apparent. The prediction for **101b**, using the bond orders obtained from NMR parameters is not improved. Since the predicted values from equation 10 are generally slightly lower, the predicted chemical shift for **101b** is actually worse than that from equation 4. Hence, the new equation does not contribute to solving the problem involving a predicted lower chemical shift for the anion **101b**. Thus this abnormal value can not be explained here based on either of the two equations. The electrostatic interactions between the counter cation and the anion in solution is apparently the primary factor contributing to the error. In the π-SCF calculations, these interactions are not

introduced in the calculation, hence, based on primarily ring current effects, the more reasonable the predicted chemical shift values are.

3.1.5 A 6 π-14 π-System

The total count of electrons in the anion **101** is 18π-electrons, hence its aromaticity as demonstrated by the low field ^{1}H NMR signals of the peripheral protons and the high field signal of the internal methyl protons. The anion is a 17-carbon system and is isoelectronic with the 17-annulenyl anion **60**, whose internal protons resonate at a very high field (-7.97 ppm). The external protons of **60** resonate at δ 9.52-8.21 ppm.

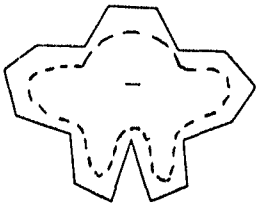

60

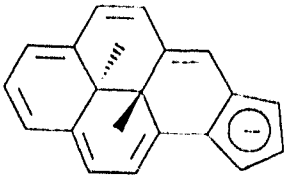

101

The anion, **101**, obeys the Mitchell equation (4 as well as 10) which is designed to calculate the internal chemical shifts of annuleno-fused dmdhp, based on bond fixation. It is then evident that the anion does indeed behave as a fused annulene.

In the anion **101a**, the π-SCF output indicates the presence of only 40% of the negative charge in the macroring. In **101b**, there is only 18% of the charge in

the same ring. The negative charge is thus localized in the 5-membered ring. The resistance of the 5-membered ring to lose the electron density to the larger ring indicates its preference to stay delocalized and hence render bond fixation to the macroring. It behaves as a 6 π-electron aromatic annulene fused to the dihydropyrene moiety. That some of the electron density is spread through conjugation into the macroring leads to the overall stability of the anion.

An additional proof to the argument comes from the π-SCF bond order calculations. The joint bond between benzene and dmdhp in **92** has an order of 0.538. The same bond in **101** has an order of 0.542, remarkably close to that of **92**. In **95**, the same bond has an order of 0.508. Hence, the bond behaves as a joint bond for two fused aromatics: cyclopentadienide anion and dmdhp.

3.1.6 Comparisons With Benz[a]DMDHP, 92

3.1.6.1 Effective Bond Fixing Ability

The anion **101** and the benzo-fused dmdhp **92** are isoelectronic aromatic species with 18π-electrons in each. Compound **92** has its internal methyl protons resonating at δ -1.62 ppm. The rest of its ^{1}H NMR data is listed in Figure 8. For all purposes, the chemical shift value of -2.85 ppm will be used as the internal

methyl chemical shift for the anion **101**. We have decided to use this value because it is an experimental one and is very close to the effective shift which we determined previously as -2.77 ppm.

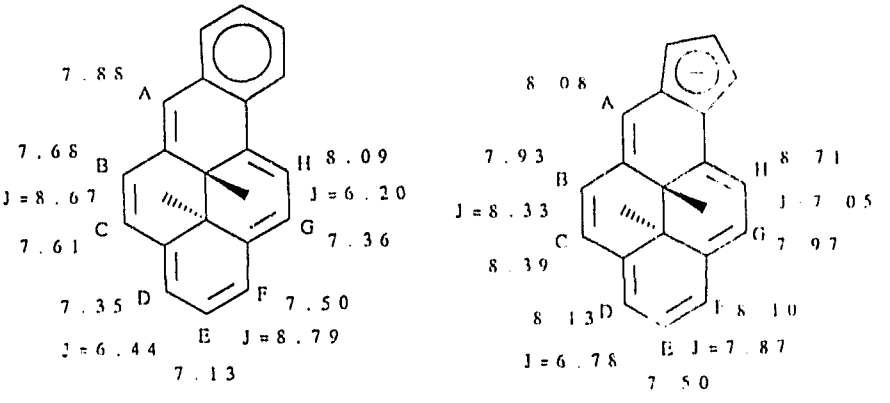

92 **101a**

Figure 8: Comparison of experimental chemical shift data for **101** and **92**.

The chemical shifts listed in the figure are those corrected for the negative charge. Compared to those of **92**, the chemical shifts of the external protons on the macroring are all at lower field. The low field shift differences range from 0.78 ppm for proton C to 0.20 ppm for proton A. These numbers indicate that the 14-annulene is a greater ring current in **101** than in **92**, resulting in more deshielded external protons. Evidently, benzene introduces more bond fixation into the 14-annulene than does cyclopentadienyl anion.

This same conclusion can be drawn from a comparison between the internal methyl protons chemical shifts as well. It was discussed earlier that the value of the shift is a first indicator of the extent of bond fixation in the system. This is so because of the dependence of the chemical shielding value $\Delta\delta$ on the bond alternation average, Δr. Over the 4 bonds BC, DE, EF, and HG, the value for Δr derived from NMR parameters for the anion **101** is 61.6×10^{-3}. In the case of **92**, Δr is 80.8×10^{-3} over the same 4 bonds. The larger Δr value for **92** indicates that benzene does indeed introduce more bond fixation into the 14 π-system than does the 5-membered ring anion.

To quantitatively relate the bond fixation introduced by the two aromatic systems, we can use the EBFA parameter we have introduced earlier. Using equation 7a, the value is calculated as 0.44. From equation 7b the EBFA value is 0.54. The average of the two, equation 7c, is calculated as 0.49. From equation 6, the same parameter is calculated as 0.53. Since we had a problem using the coupling constants for the anion **101b**, and since we are also looking for the use of a maximum number of bonds for our calculations, it is more appropriate to use the latter value for comparison. We thus can conclude that cyclopentadienyl anion when fused to dimethyldihydropyrene has a 53% effective bond fixing ability of a benzene ring fused to the same system.

3.1.6.2 Effective Resonance Energy

Since the resonance energy and ring current are directly related in aromatic annulenes, one would expect a relation to exist between the chemical shielding and resonance energy. Mitchell and others[137] have recently correlated resonance energies of fused aromatics to dmdhp to that of the internal methyl chemical shifts. The effective resonance energy parameter, RE^*, in terms of that of a benzene ring fused to dmdhp, correlates linearly, for RE^* values up to about twice that of benzene, with the chemical shift parameter $\triangle$.

$$\triangle = 2.50\ RE^* + 0.08 \quad \text{----------(11)}$$

where $\triangle = (4.25 + \delta CH_3)$ ppm, and RE^* is the resonance energy of the fused aromatic minus a residual aromatic resonance energy term, in the case of condensed aromatics, in terms of benzene units.

The internal methyl chemical shift of the anion **101** is -2.85 ppm. The calculated effective resonance energy of cyclopentadienyl anion is then 0.53 benzene unit. Since this value is an experimental one, we will term it the effective experimental resonance energy of cyclopentadienyl anion. Thus, in terms of benzene resonance energy units, Cp when fused to dmdhp has an effective experimental resonance energy of 0.53. Taking into

consideration the RE of benzene as 150 kJ/mol (36 kcal/mol)[128], this value corresponds to 80 kJ/mol.

The calculated value above is only about half of that based on calculated resonance energy of cyclopentadienyl anion mentioned earlier in the introductory part of this chapter. The apparent discrepancy can be described in terms of the anion's stability and reactivity. The calculated values take into consideration a model and the resonance energy values calculated are those of the difference between the energy of the anion and the model. These calculations, however, do not take into consideration the reactivity, and hence stability of the aromatic anion. In our approach we have a common reference for both benzene and cyclopentadienyl. Thus our experimental values reflect experimentally determined parameters, namely NMR chemical shifts determined at ambient temperature. The omission of separate references makes it possible for us to directly relate the effective resonance energies of the two aromatic moieties.

3.1.7 Anisotropic Effects of Cp on Proton E

It was shown earlier that the negative charge has a shielding effect of about 0.40 ppm on the chemical shift of the internal methyl protons. The effect of the aromatic anisotropy was also shown to be minimal on the

same protons. To confirm the validity of our neglect of the aromatic anisotropy, we can use equation (5) to recalculate the chemical shift of proton E and compare it with the experimental one.

$$\delta_{RCM} = -2.60\ \delta_{RCH} - 0.029 \quad \text{----------(5)}$$

The chemical shift of the internal methyls is taken as δ -2.85 ppm. This yields a chemical shift value for the external proton E at δ 7.61 ppm. The experimental value is 7.50 ppm. The two values are in very good agreement. The agreement between the experimental and the calculated value leads us to conclude that, after taking into account the effect of the negative charge on both the internal and external protons, the aromatic species has a negligible anisotropic effect on the shift of the internal methyl protons. Moreover, since equation (5) was derived for fused dmdhp, the agreement above lends extra support to the evidence discussed earlier regarding the behavior of the anion **101** as a fused cp-dmdhp.

3.1.8 Summary

In the preceding section, we have discussed the properties of the anion **101**. It was concluded that the charged species is a cyclopentadienyl-fused dimethyl-dihydropyrene and acts as such. After taking into

consideration the negative charge effects, the chemical shift of the internal methyl protons is assigned as -2.85 ppm. Compared to compound **92**, a benzo-fused analogue, it was determined that cyclopentadienyl anion when fused to dmdhp has 53% effective bond fixing ability when compared to a benzene fused to the same 14-annulene. Using a similar approach of comparison, the effective experimental resonance energy of cyclopentadienyl anion was calculated as 80 kJ/mol.

3.2 DIHYDROPYRENE METAL COMPLEXES

3.2.1 Introduction

Arene metal complexes are an important class of molecules structurally as well as theoretically. Structurally, they are a composite of an organic fragment, an aromatic species, and a second inorganic fragment such as a metal or a metal carbonyl. Therefore they are an invaluable bridge between molecular orbital theories of both organic and inorganic chemistry. More importantly, at least at present, these molecules have become indispensable tools to study the ring current effects and chemical shift origins in aromatic compounds. Indeed, metal complexes of benzene, co densed aromatic hydrocarbons and heterocycles have been extensively studied.[132a,138] More recently arene metal complexes of

cyclophanes have been actively investigated, partly because of their structural properties, but also because of the interest in their NMR spectra. Their study has provided a great deal of information regarding the anisotropy effects of the metals and hence on the origin of the upfield chemical shift experienced by the aromatic fragment upon complexation.[139]

As seen from Table 18, complexation of benzene to chromium tricarbonyl leads to an upfield shift of the protons equal to 1.9 ppm. In the case of complexation of another aromatic moiety such as cyclopentadienyl anion, the upfield shift is even greater. In cyclopentadienyl-manganese tricarbonyl, **152**, the upfield shift, after charge correction, is 3.0 ppm. In ferrocene, it is 3.5 ppm. In charged complexes such as **155** and **156**, the magnitude of the upfield chemical shift is smaller due to the deshielding effect of the positive charge.

Table 18: Proton chemical shifts of selected aromatics and complexes

Compound	Chemical shift (ppm)	Ref.
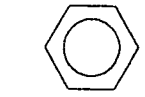	7.27	30
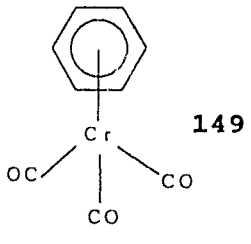 **149**	5.37	140

Table 18 continued,

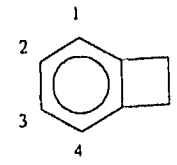 **150**	7.09 (1,4), 6.92 (2,3), 2.92	141
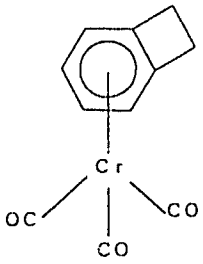 **151**	4.58 (1,4), 4.17 (2,3), 2.25 (exo), 2.54 (endo)	141
 **15**	5.52 (7.66)	57
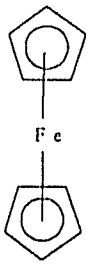 **131**	4.11	142
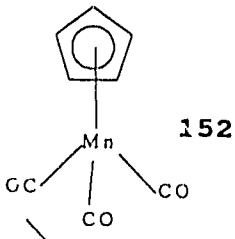 **152**	4.65	142
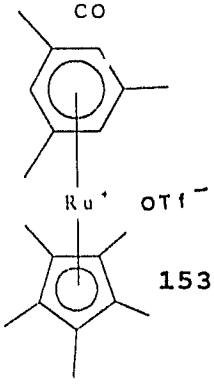 **153**	1.90 (cp*), 5.56 (3H), 2.18 (9H)	143

Table 18 continued,

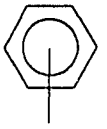	4.12	144
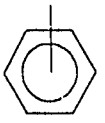 154		
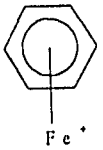	5.23 (cp), 6.44 (6H)	145
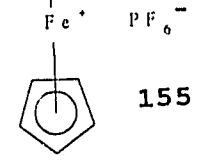 155		
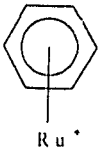	5.45 (cp), 6.20 (6H)	145
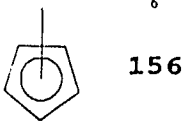 156		

To investigate the origin of the upfield chemical shift, arene chromium tricarbonyl complexes have been widely used as models, partly because of their stability, but mostly due to their accessibility. Such shifts have been interpreted as a combination of effects including quenching of the ring current, withdrawal of electron density from the ring by the $Cr(CO)_3$, the magnetic anisotropy of the chromium-ligand bond and partial rehybridization of the ring carbon atoms.[138,139]

In benzene tricarbonyl chromium, the upfield chemical shift of 1.9 ppm can be interpreted in terms of a small reduction in the ring current due to complexation. This is supported by studies of cyclophanes such as **157** and **159**. In cyclophane **157**, the protons of the complexed ring experience an upfield shift of 1.82

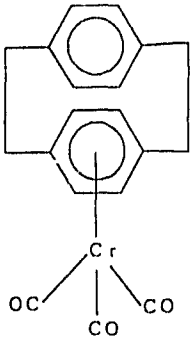

157

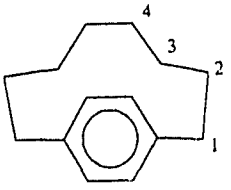

158

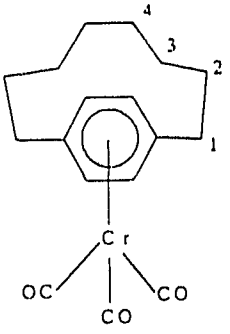

159

ppm (in the free ligand, the chemical shift of the aromatic proton is 6.46 ppm). The protons of the uncomplexed ring in **157** experience a downfield shift of 0.31 ppm. This downfield shift is explained in terms of reduction of the ring current of the complexed ring.[146] The most shielded proton in **159** (H_4) experiences a reduction in shielding by 0.5 ppm on going from the ligand **158** to the complex. In the same molecule, the aromatic protons experience a 1.73 ppm upfield shift. These observations can similarily be explained in terms of ring current reduction on complexation to the $Cr(CO)_3$ fragment.[146,147]

3.2.2 Separation Of Ring Current Reduction From Anisotropy Effects

The attempts to assess the magnitude of ring current reduction in arene metal complexes are always hindered by the inability to determine the anisotropy effect of the metal fragment. Recently, McGlinchy[148] has been able to calculate the anisotropy effect of chromium tricarbonyl on distant protons. Using the McConnell equation[149], which relates the chemical shift increment, σ, and the molar diamagnetic anisotropy, X, through a geometric term (equation 12a), he calculated the anisotropy effect of the fragment, in terms of a supercarbonyl as 2124×10^{-36} m^3/molecule. The model compounds for the calculations were a pair of (estradiol)$Cr(CO)_3$ geometrical isomers. Using the value above, the McConnell equation can be rewritten as equation (12b).

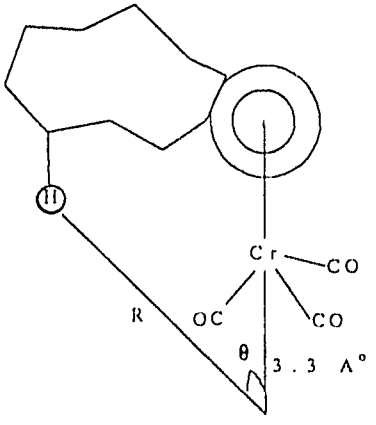

$$\sigma = X/N \{(1-3\cos^2 \theta)/3R^3\} \quad \text{-----(12a)}$$

$$\sigma = 55.34 \{(3\cos^2\theta - 1)/R^3\} \quad \text{-----(12b)}$$

The supercarbonyl notation here refers to a resolution of the three carbonyls into one along the C_3-axis, with the center of anisotropy being almost exactly midway between chromium and oxygen. This corresponds to a distance of 3.3 A^o from the chromium atom.

Using the above approach, Mitchell et al[99] were able to successfully explain the chemical shift difference between the two internal methyl protons of the complex **160**, made very recently as a consequence of an improved synthesis of the ligand **92**.

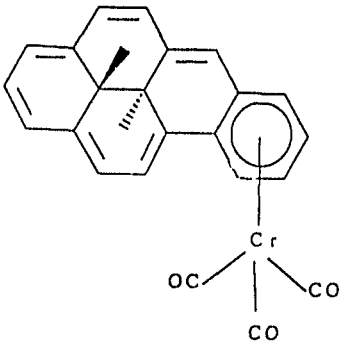

160

Using this approach we may be able to explain some discrepancies in the literature, of which the complex **162** is a well recognized example. A comparison of the chemical shifts of H_a and H_b in both the free ligand, **161**, and the complex **162**, shows virtually no change in the chemical shifts of these protons. Keller claimed that this observation makes it necessary to rule out the disruption of the aromatic ring current of the arene ligand as the origin of the upfield shift of the aromatic

protons in such systems.[150] However, using the McGlinchy approach, we are able to calculate the shielding effects due to $Cr(CO)_3$ as 0.14 ppm for proton a and 0.26 ppm for proton b. The parameters were determined from the molecular mechanics output.

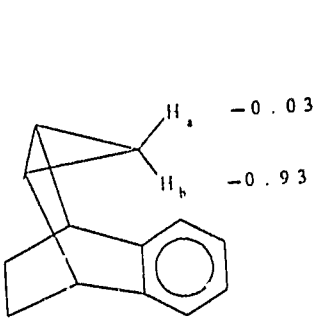

161

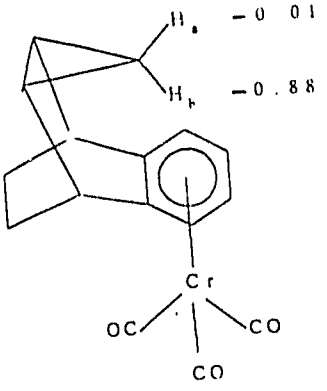

162

θ_a=15.0°

θ_b=8.12°

R_a=8.99 A°

R_b=7.41 A°

The corrected chemical shifts are therefore +0.13 ppm for proton a and -0.62 ppm for proton b. Since the author neglects the anisotropy effect of the $Cr(CO)_3$ group on the chemical shift in his explanation, it seems to us that his conclusion is invalid. The reduction in the chemical shift shielding in the complex indicates that there is indeed a reduction in the ring current due to complexation of the arene to the tricarbonyl chromium group.

In a similar fashion as for chromium tricarbonyl, McGlinchy was also able to estimate the anisotropy effect of ferrocene. The anisotropy center of the complex was placed at the iron atom. It therefore is feasible for us to use the same approach to estimate the anisotropy effect of a variety of metal fragments. We can do so by

generating pairs of isomers of the same compound in which, provided no geometrical changes are taking place, a set of protons of identical chemical shifts are placed syn or anti to the metal fragment. In using dimethyldihydropyrene as our model compound, we eliminate the need to use two isomers, since the two internal methyl groups are disposed in two opposite sides of the metal fragment.

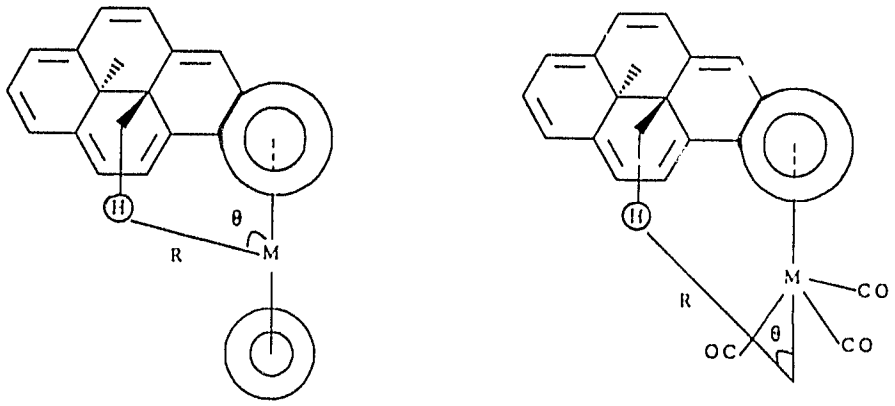

Figure 9: A model for calculation of anisotropy effects of a metal fragment.

Our model is as shown in Figure 9 above. By determining the experimental chemical shifts of the two internal methyls and the geometrical parameters from either X-ray data or PCMODEL/MMX calculations, we should be able to calculate the anisotropy effects of any metal fragment. We can do so provided that no geometrical changes take place in going from the ligand to the complex.

3.2.3 Large Annulene Metal Complexes

Small annulene metal complexes such as **163**[151] and the complexes **149**, **157**, and **159** dicussed above have been well documented. Large annulene metal complexes , however, are rare in the literature. The first reported metal complexed bridged annulene, **164**, appeared in the literature in 1966. It was reported by Vogel[152], who subsequently reported the synthesis of **165**[153] and then **166**[154] in 1982. No further development in this area has occurred, perhaps in part because of the limited accessibility and stability of large annulenes.

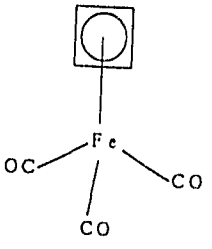

163

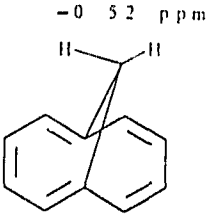

26

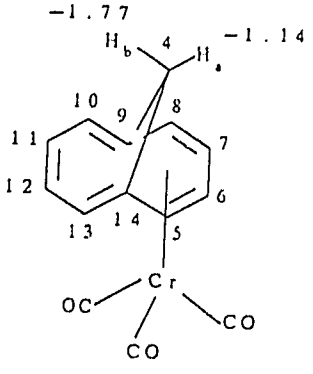

164

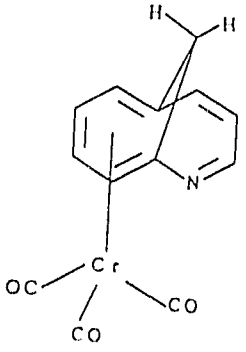

165

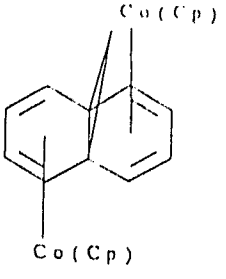

166

In the proton NMR spectrum of **164**, the bridge methylene protons appear at δ -1.77 and -1.14 ppm. considerably upfield from the ligand **26**. The internal bridge hydrogens in **165** are also shifted upfield from 0.67 and -0.36 ppm in the uncomplexed annulene to δ 0.15 and -1.02 ppm in the complexed species. This upfield shift is unexpected based on a ring current reduction hypothesis. Since there is no geometry changes in going from the free ligand to the complex **164**, as verified from their X-ray data[155], the change in the chemical shift of the methylene bridge must be primarily due to delocalization and anisotropy effects.

To estimate the anisotropoy effects, we used the McGlinchy equation, 12b. The geometric parameters were obtained from the published X-ray data for the complex coupled with the MMX output. Table 19 contains selected values for the parameters from X-ray[155] and the corresponding value determined by querrying the MMX output structure. The calculated parameters are:

$$\theta_a = 4.68^{\circ}, \qquad R_a = 7.09\ A^{\circ}$$
$$\theta_b = 18.81^{\circ}, \qquad R_a = 7.33\ A^{\circ}$$

These values correspond to a calculated shielding of 0.31 ppm for proton a and 0.24 ppm for proton b. Thus, the corrected chemical shift for the two protons are -0.83 and -1.53 ppm, respectively. The corrected values

Table 19: A comparison of parameters for complex **164**

Parameter	MMX	X-Ray
5-14	1.45A^{o}	1.45A^{o}
5-6	1.37	1.41
6-7	1.44	1.42
7-8	1.38	1.39
8-9	1.44	1.42
9-14	2.17	2.14
9-4	1.48	1.47
4-14	1.49	1.49
5-14-13	125.4^{o}	125.0^{o}
8-9-10	124.8	127.6
4-9-8	116.8	115.5
4-14-5	115.9	116.9
9-4-14	94.0	92.4

are still more upfield than those of the ligand, indicating that the shift is indeed due to a change in the delocalization pattern. Perhaps complexation to $Cr(CO)_3$ results in the making of two homobenzene rings, with the ring complexed to chromium having a smaller ring current as indicated by the lower shielding of H_a in comparison with H_b. This conclusion is supported by the fact that the distance between carbons 9 and 14 becomes

smaller on complexation by about 0.12 A^{o}. The presence of other electron withdrawing groups in the parent ligand, brings these two carbons even closer.[156]

3.2.4 Dimethyldihydropyrene Metal Complexes

When we started the project, no dmdhp metal complexes were known. Metal complexes of annelated dmdhps have been of interest for sometime now because of the excellent bond fixing indicator properties of the 14-annulene. Due to the large distance between the internal methyl groups and the metal fragment, the effect through space on these methyls should be small. Nevertheless, their chemical shift values can be used, employing the McGlinchy approach, to evaluate the anisotropy effects of the metal fragment. Any substantial chemical shift change of the methyl protons will, however, reflect a delocalization change in the macroring as discussed in chapter one.

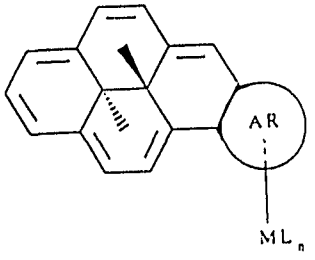

167

Given our success in synthesizing the anion **101**, we thus decided to generate complexes of the type **167**, where

the ML_n fragment is either a metal cyclopentadienyl or a metal tricarbonyl. This will hopefully allow us to make definitive statements on anisotropy effects due to complexation to these fragments as well as on bond delocalization present in both the complexing ring and the macroring.

3.2.5 Properties of Ruthenium-DMDHP Complex, 139a

The complex **139a** is a ruthenocenyl-fused dimethyl-dihydropyrene. Its physical properties were mentioned in chapter two. The internal methyl protons of the complex resonate at δ -0.548 and -0.691 ppm. Its proton NMR spectrum is on the next page, along with the simulated spectrum for the aromatic protons. The chemical shift values are listed in Table 20. The external protons of the macroring resonate in the range δ 6.95-6.57 ppm. Compared to the anion **101**, where the corresponding protons resonate between δ 8.35 and 6.83 ppm, these protons are shifted considerably upfield. The chemical shifts of the ruthenocenyl protons are comparable to those in the indenyl analogue **168**.[125c]

The difference in the shielding of the internal methyl groups is only 0.14 ppm. The small difference indicates that the anisotropy of the ruthenocene moiety is indeed negligible at this distance. In the case of the other isomer, **139b**, the difference is noticeably

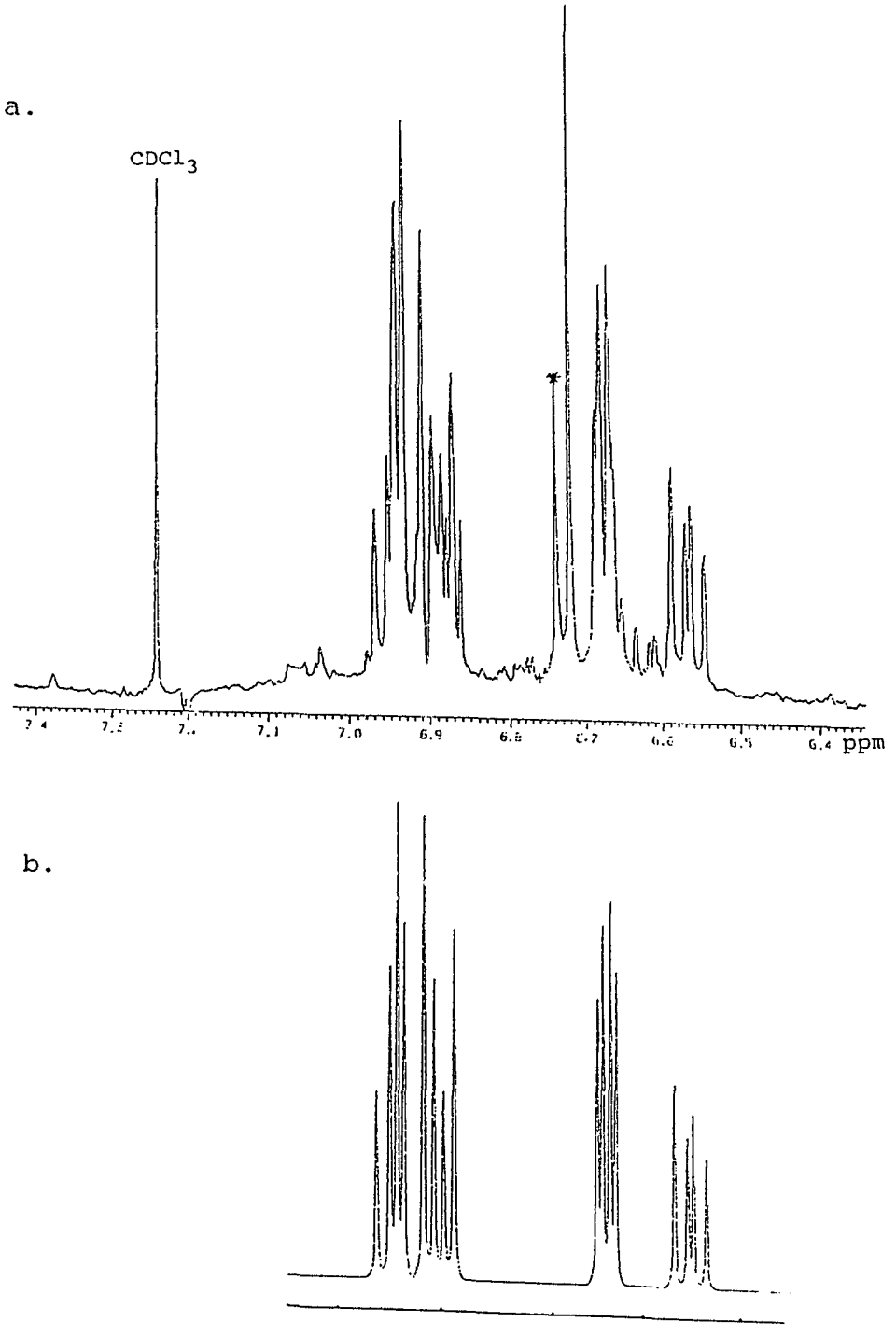

Figure 10: Proton NMR spectra (aromatic region) for **139a**. a. Experimental (360 MHz), b. Simulated. Starred signal is due to isomer **139b**. Refer to text for assignment.

Table 20: Proton NMR data for complex **139a**

Proton	δ ppm
A	6.72
B	6.95
C	6.90
D	6.68
E	6.57
F	6.88
G	6.67
H	6.94
J	4.99
K	4.39
L	4.70
Int. CH_3	-0.543
	-0.691
Ext. CH_3	1.68

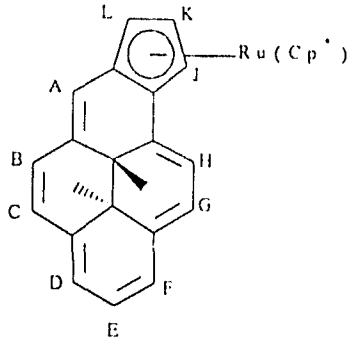

139a

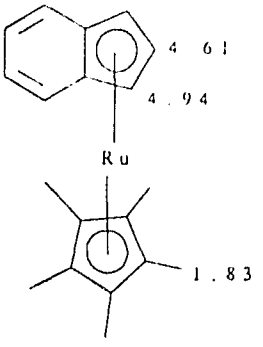

168

larger. It is calculated as 0.35 ppm. This is due to geometrical differences between the two complexes. In the case of isomer **139b**, the closest methyl is syn to the pentamethylcyclopentadienyl ruthenium fragment, introducing strain in the molecule. This is verified by

the MMX structure output, where the macroring is actually bent. Thus the larger difference in **139b** is due to geometrical changes and not necessarily the anisotropy effect of the aromatic ruthenocene alone. This is also true for the tricarbonyl manganese complex discussed below. Only complexes **139a** and **141a** will thus be used for our calculations.

3.2.6 Properties Of Manganese Complex 141a

The complex **141a** is a tricarbonyl manganese cyclopentadienyl-fused dimethyldihydropyrene. Its internal methyls resonate at δ -0.728 and -0.784 ppm. Table 21 lists its proton NMR data. Figure 11 has the proton spectrum and the simulated spectrum for the aromatic region of the complex.

The resonances of the external protons in the macroring are all located in the range δ 7.16-6.83 ppm. Compared with these of the anion **101**, the resonances are all upfield indicating the presence of a lesser ring current in the macroring in **141a**. The difference in the chemical shifts of the internal methyl protons in the complex is only 0.056 ppm, indicating that the magnitude of these chemical shifts is mainly dependent on ring current changes due to complexation.

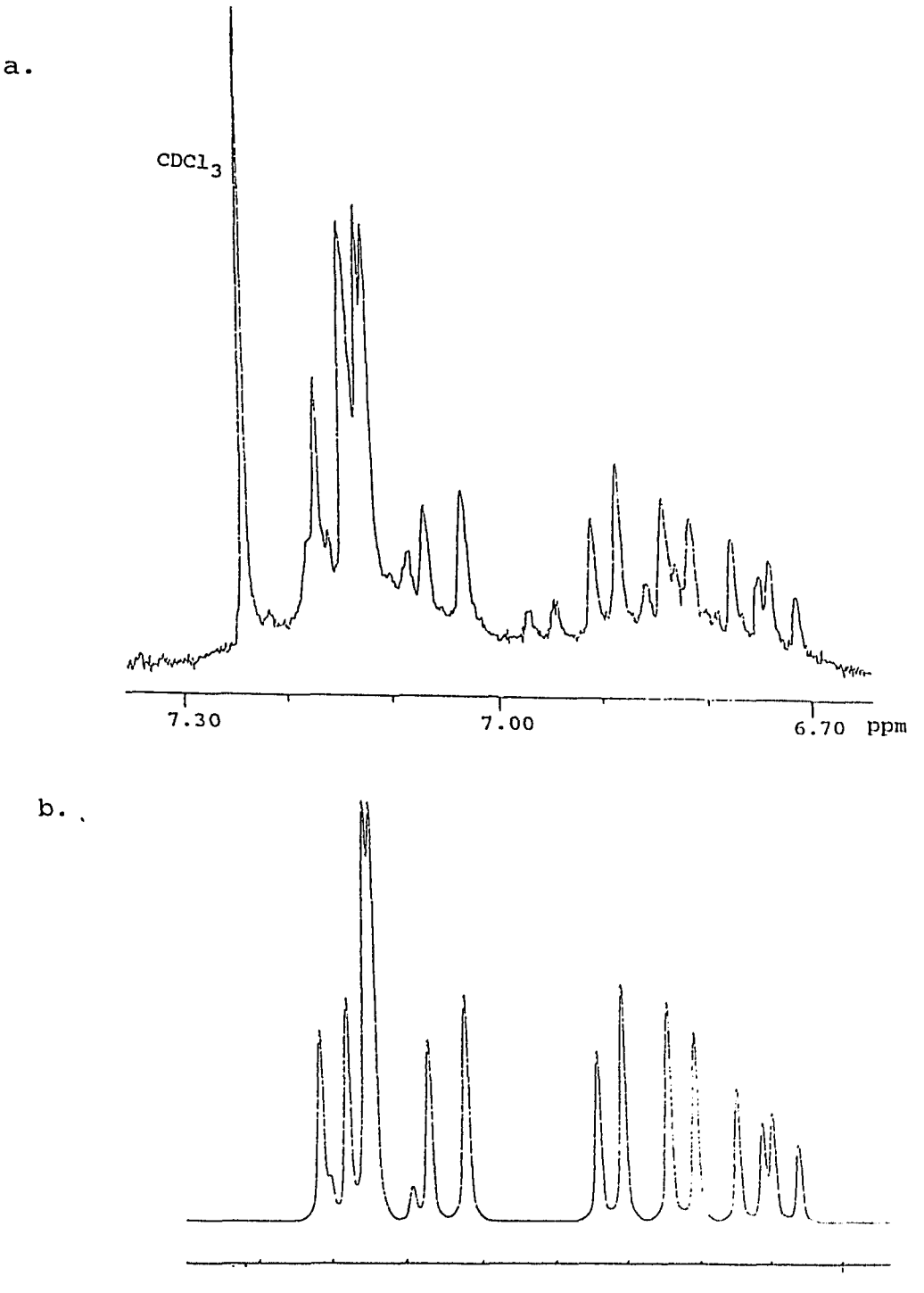

Figure 11: Proton NMR spectra (aromatic region) for **141a** a. Experimental (250 MHz). b. Simulated. Refer to text for assignment.

Table 21: Proton chemical shifts for complex **141a**

Proton	δ (ppm)
A	7.15
B	7.13
C	7.11
D	6.89
E	6.74
F	7.05
G	6.83
H	7.16
J	5.54
K	5.08
L	5.09
CH_3	-0.728
	-0.784

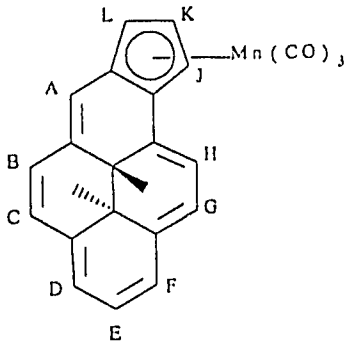

141a

3.2.7 Chemical Shift-Coupling Constant Correlation

Since the anisotropy effect of the metallic fragments are negligible, each of the two complexes **139a** and **141a** can be considered as a fused annulene. In other words, just as benzene bond fixes the 14 π-annulene in **92**, ruthenocene and cyclopentadienyl tricarbonyl

manganese should have a bond fixing ability equivalent to an annulene, and should be treated as such. To find the extent of bond fixation due to these equivalent annulenes, and to test whether this is true, we can employ the equation we derived earlier, equation (10), to calculate the chemical shift of the internal methyls. Table 22 has the coupling constants derived from the simulated spectra for both complexes. The bond orders were calculated using equation (3).

Table 22: Predicted internal chemical shifts for complexes **139a** And **141a**

	Complex **139a**		Complex **141a**	
Bond	J(Hz)	Bond Order	J(Hz)	Bond Order
BC	9.09	825	8.76	791
DE	6.08	513	6.25	530
EF	8.85	800	8.74	789
GH	6.41	547	6.32	537
ΔP	557		505	
Δr	139		126	
δCH_3*	-0.73		-1.07	
δCH_3**	-0.67		-1.03	
δCH_3expt	-0.548, -0.691		-0.728, -0.784	

* From equation (10), ** from equation (4)

The calculated chemical shifts of the internal methyl protons of the two complexes are in very good agreement with the experimental values. The shifts calculated using the original Mitchell equation are slightly better, but the differences are minimal.

The agreement between the calculated and experimental values leads us to unequivocally conclude that both of the complexes essentially act as a bond fixing annulene, with little effect on the internal methyl chemical shifts due to through space interaction.

Using equation (5), we can calculate the chemical shifts of the internal methyls as -0.35 ppm for the complex **139a** and -0.61 for the manganese complex **141a**. The calculated values are in fair agreement with the experimental ones. The difference between the experimental value and the calculated one here for the ruthenium complex is 0.27 ppm. The corresponding value for the manganese complex is noticeably smaller (0.15 ppm). This indicates that the anisotropy effect of the ruthenocene is larger than that of the tricarbonyl manganese.

The ring current chemical shift is defined in equation (5) as (0.97 - δCH_3) in ppm. So, in the absence of anisotropy effects, the value calculated from the equation should be equal to 1.59 for complex **139a**. If we consider the difference value of 0.27 ppm as being due to the anisotropy effect, then the ratio (0.27/1.59) should

give us an estimate of the magnitude of that effect. The ratio is calculated as 0.17. Thus, the anisotropy effect of ruthenocene on the internal methyl chemical shift is about 17% of the total effect. In the case of the manganese complex **141a**, the ring current chemical shift is calculated as 1.73 ppm. The anisotropy effect is then only 9% of the total effect.

3.2.8 Comparison of the Complexes 139a and 141a With Benzene

In both complexes, the internal methyl protons are less shielded than in the benzo-fused dmdhp **92**. As we have done in the case of the anion **101**, we can calculate the relative effective bond fixing ability of the complexes in terms of equivalent annulenes. Table 23 below lists the results of the calculations using equation (6). Also included in the table are the results for the complex **160**.

We have concluded previously that the chemical shift of the internal methyls is mainly dependent on the changes in the ring current. Therefore, looking at the results of the calculations in the table, we can conclude that ruthenocene is about 1.38 times more bond-fixing than benzene when fused to dimethyldihydropyrene. Similarily, cyclopentadienyl tricarbonyl manganese is about 1.33 times better than benzene in the effective

Table 23: Comparison of Effective Bond Fixing Ability (EBFA) and Experimental Resonance Energy (ERE) for Ruthenocene, Benzene-$Cr(CO)_3$, Cp-$Mn(CO)_3$, and Benzene

Compound	δCH_3 (ppm)	EBFA	ERE
Benzene	-1.62	1.00	1.00
Ruthenocene	-0.62	1.38	1.42
CP-$Mn(CO)_3$	-0.76	1.33	1.36
Benzene-$Cr(CO)_3$	-0.93	1.26	1.30

bond fixing ability. By the same argument, benzene tricarbonyl chromium is 1.26 times more bond-fixing than benzene itself.

From equation (11) we can calculate the effective experimental resonance energy, ERE, for the aromatic complexes. The results of the calculations are included in Table 23 above. Not surprisingly, the same order as for bond fixation is followed, with ruthenocene having 1.4 times the effective resonance energy of benzene when fused to dmdhp. Taking into consideration the resonance energy for benzene as 150 kJ/mol, the effective experimental resonance energy of ruthenocene is calculated as 213 $kJmol^{-1}$. It is equal to 204 $kJmol^{-1}$ for Cp-$Mn(CO)_3$. For benzene tricarbonyl chromium, it is calculated as 195 $kJmol^{-1}$.

3.2.9 Diamagnetic Anisotropy Of CyclopentadienylRuthenium and TricarbonylManganese

As discussed earlier, the McGlinchy approach enables us to calculate the diamagnetic anisotropy, X, of ruthenocene and Cp-$Mn(CO)_3$. We will first calculate the X value for the metallocene and compare its magnitude with the values in the literature. Following this, we will calculate X for $Mn(CO)_3$. To our knowledge, no such value exists in the literature for this fragment.

In the ruthenocene case, the center of anisotropy is located at the metal center. Since attempts to make suitable crystals for X-ray analysis were not successful, we decided to use the output geometry from the PCMODEL/MMX structure. The parameters obtained from the output such as the metal to carbon distances agree very well with published crystallographic data for complexes such as the analogous indenyl complex **168**.[125c] The distance R was taken as the average distance between the ruthenium atom and the three protons on each methyl. Similarily, the angle θ was taken as the average angle at the metal center as in Figure 9. The values of R_1 and R_2 were calculated as 4.810 A^o and 5.409 A^o with the corresponding θ_1 and θ_2 values being 80.57^o and 29.35^o. The difference between the chemical shift values for the two methyl protons, 0.143 ppm, is taken as the difference in the shielding increments ($\sigma_1 - \sigma_2$). The calculated X

value using the above parameters is -330×10^{-36} m^3 per molecule. This value is in excellent agreement with that determined by Richie and others (-321±36).[157] It is also in good agreement with the value determined by Mulay from the crystal structure data for ruthenocene (-400).[158]

The results of the calculations provide us with confidence to use the molecular mechanics structure output when determining the parameters required for calculations of complexes analogous to **139a.** We will, thus, later use the same approach to calculate X using the MMX structure output for complex **141a.**

The diamagnetic anisotropy we have just calculated can be used to evaluate the anisotropy effect on the chemical shifts of the external protons on the macroring. The parameters and calculated effects are listed in Figure 12 below.

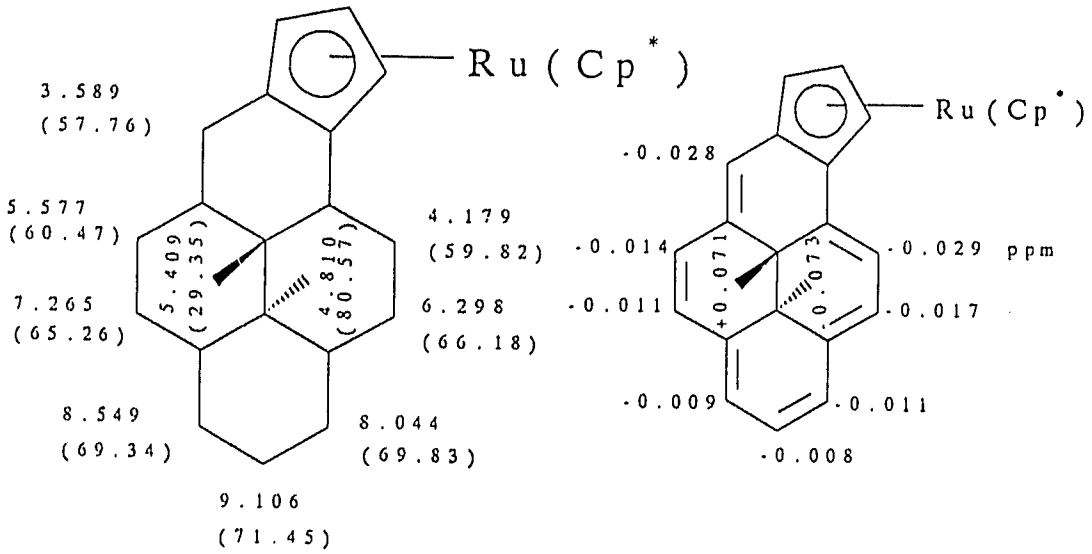

Figure 12: MMX parameters and anisotropy effects (ppm) of ruthenocene in complex **139a.** (angles are in brackets)

It can be concluded from the data in the figure that the anisotropy effect of ruthenocene on these protons is indeed negligible. Thus, the upfield chemical shifts of the macroring protons are essentially due to ring current reduction in going from **32** to the fused ruthenocene **139a**.

The mapping of the shielding and deshielding regions associated with the ruthenocene molecule, judging from the diamagnetic anisotropy values of the protons of the 14-annulene, is identical with that proposed for ferrocene by Turbitt and Watts[159] based on the magnetic susceptibility measurements of Mulay and Fox.[160]. Thus a general map for the diamagnetic anisotropy of metallocenes may be drawn as shown in the figure below. In the case of **139a**, the only protons located in the shielding region are those of the internal methyl anti to the ruthenocene.

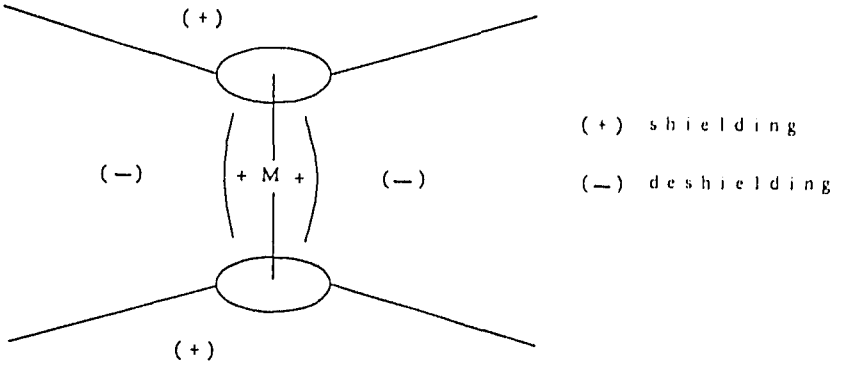

Figure 13: A general map for the diamagnetic anisotropy of metallocenes.

To test the model, we employed the complex **169** as an example, to rationalize the chemical shifts of the syn and anti protons. According to the model, both protons should experience a deshielding due to the presence of the aromatic ruthenocene. This is indeed the case as seen from their proton NMR values of δ 1.60 and 1.33 ppm.[161] In the parent bicyclo[2.2.1]heptane, the two protons resonate at δ 1.21 ppm.[132b] Evidently, due to ruthenocene, the syn proton experiences a deshielding of 0.39 ppm, whereas the anti proton experiences a deshielding of 0.12 ppm.

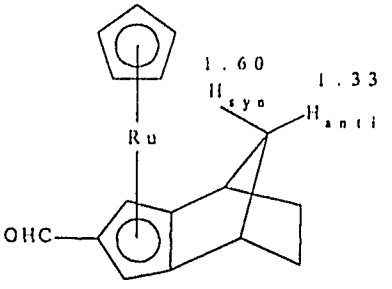

169

R_{syn} = 2.76 A°

θ_{syn} = 82.72°

R_{anti} = 4.33 A°

θ_{anti} = 69.82°

Just as we did with other complexes previously, we constructed a molecular mechanics structure whose parameters, fortunately, agreed with those published from the X-ray crystal structure for the complex **169**.[161] Using the X value of -330×10^{-36}, the calculated parameters correspond to a deshielding value of 0.40 ppm for the syn proton and 0.07 ppm for the anti proton.

These values are in ramarkably good agreement with the literature spectrum.

In the case of complex **141a**, calculation of the diamagnetic anisotropy, X, due to the tricarbonyl manganese is complicated by the difficulties in locating the center of anisotropy. Since the difference in the the chemical shifts of the internal methyls of the chromium complex **160** can be explained in terms of a supercarbonyl, we think the analogous supercarbonyl model for the complex **141a** should represent an accurate picture for the center of the anisotropy.

When the center of anisotropy is placed at the metal atom, the value of X is determined as -160×10^{-36} m^3 per molecule. The distance parameters used are R_1 equal to 4.513 A^o and R_2 equal to 5.722 A^o. The corresponding angles are 97.85 and 44.10 degrees. Using the calculated X value, we estimated the anisotropy effect on the macroring protons. The parameters used for these protons and the calculated anisotropy effects are in Figure 14a.

In Figure 14b, we have placed the center of anisotropy midway along the carbon-oxygen bond. The distance R is taken as the distance from this point to the proton and θ is the angle made by R with the Mn-C-O axis, taking into consideration contributions from all three carbonyls to each proton. The geometric term used is the average of the sum of these contributions on the three methyl protons. This picture corresponds to

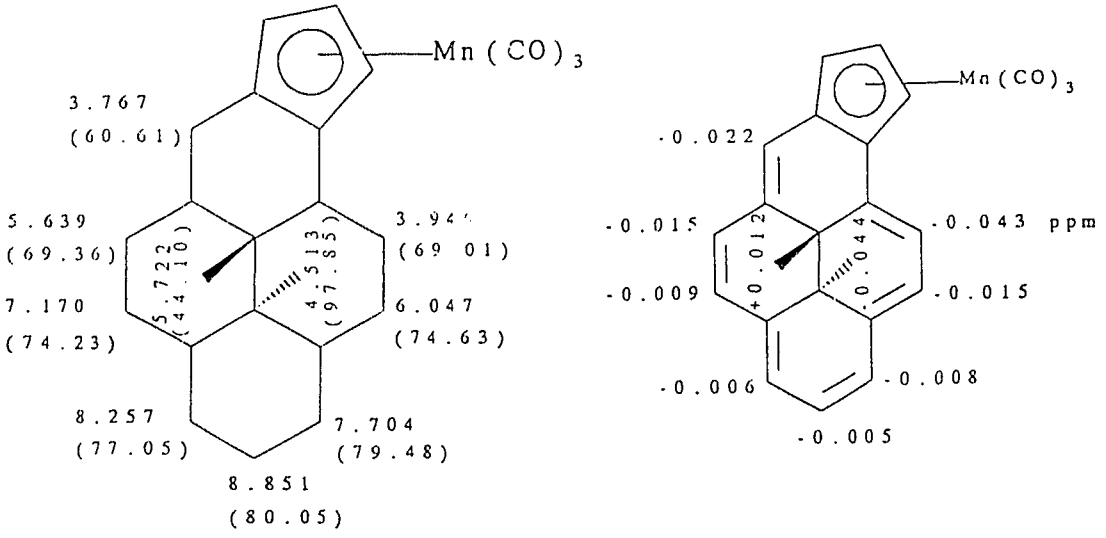

Figure 14a: MMX parameters and anisotropy of $Mn(CO)_3$ in complex **141a.** Center of anisotropy is at Mn atom.

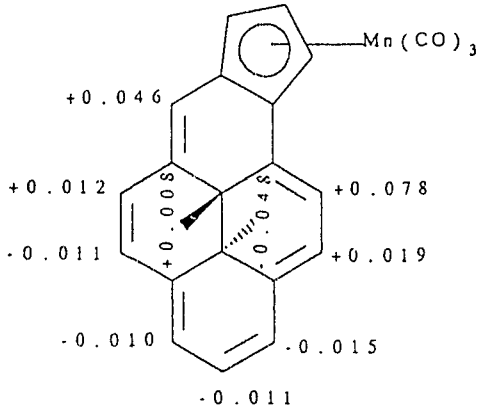

Figure 14b: Anisotropy effects of $Mn(CO)_3$. Center of anisotropy is at half distance between C-O.

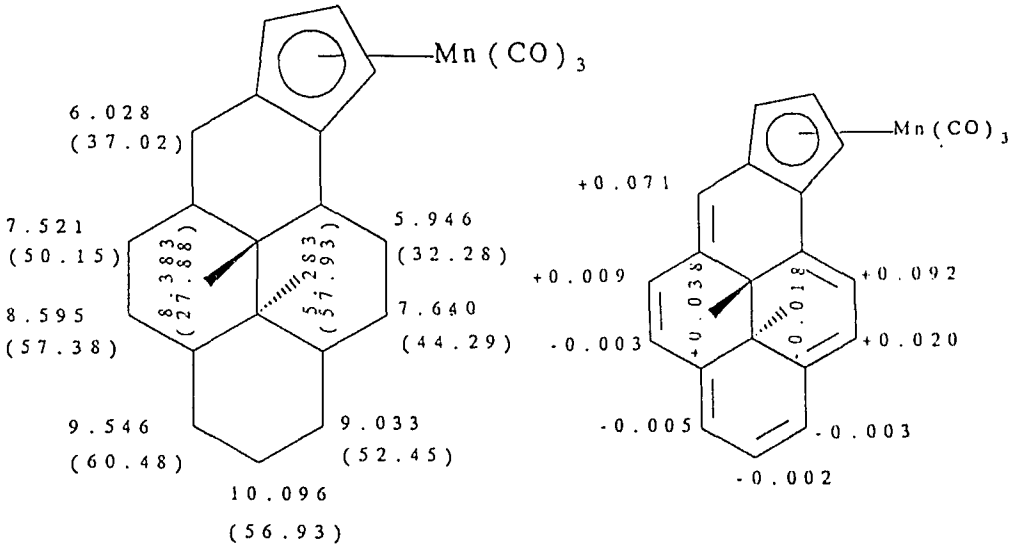

Figure 14c: MMX parameters and anisotropy of $Mn(CO)_3$. Supercarbonyl center. (angles are in brackets)

a description of rotating carbonyls. The diamagnetic anisotropy calculated from the model here is -194×10^{-36} m^3/molecule. The calculated anisotropy shifts using the above value are listed in Figure 14b.

In Figure 14c above, we have treated the three carbonyls in $Mn(CO)_3$ as a supercarbonyl. The center of anisotropy is located at 3.2 A^O down from the manganese atom. The parameter R_1 is calculated as 5.288 A^O and R_2 is calculated as 8.383 A^O, with corresponding angles of 57.93 and 27.88 degrees. The value for the diamagnetic anisotropy is then determined as -635×10^{-36} m^3 per molecule. Using this value and parameters determined

from the MMX structure output, we calculated the anisotropy effects on the macroring protons. The results of the calculations are listed in Figure 14c.

It should be noted here that the model in Figure 14b is probably the most realistic of all three. However, it is very cumbersome and the calculations are very time consuming. Since the calculated anisotropy effects from the model are very comparable to those determined from the supercarbonyl model, we will concentrate on the latter. As stated earlier, we think this model represents a true picture of the shielding map of the manganese tricarbonyl moiety.

A literature search for a suitable example to test the accuracy of the calculated anisotropy value for $Mn(CO)_3$ did not yield many useful results. We found only one report in the literature which discusses the magnetic non-equivalence of methylene protons in disubstituted cyclopentadienyl manganese tricarbonyl.[162] Proton NMR data for a number of disubstituted complexes, recorded at -60^{o}, suggested that, in the presence of bulky groups, the methylene protons become magnetically non-equivalent. No crystal structures of any of the examples in the report are available in literature.

An interesting case is that of the complex **170**, whose proton NMR spectrum at room temperature shows two doublets for the two methyl protons with a chemical shift difference of about 0.017 ppm.[162]

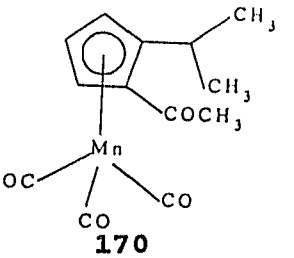

170

No crystal structure data is available for the complex. Hence we decided to use the output from the molecular mechanics structure in order to evaluate the parameters required for the calculations. The most stable structure for the complex was one in which the two methyls are located in two opposite sides of the 5-membered ring plane. The calculated chemical shift difference using the supercarbonyl model is approximately 0.01 ppm. It should be noted here that the two methyls are magnetically non-equivalent. The remaining difference in the chemical shift (0.007 ppm) is thus equal to the chemical shift difference in the absence of the anisotropy of the metal fragment.

The calculated anisotropy effects on the peripheral protons of the macroring are minimal, the highest shielding being only 0.092 ppm for proton H in complex **141a**. In the case of **139a**, the highest deshielding is 0.029 for the same proton. The effects on the internal methyl protons are also negligible, with the highest value being only 0.073 ppm in the case of complex **139a**. Hence, our conclusion regarding the primary source of the chemical shift changes is verified here. The decreased shielding of the internal methyl protons in going from

dimethyldihydropyrene, **32**, to the cyclopentadienyl-fused complexes **139a** and **141a**, is indeed essentially due to the ring current reduction in the 14 π-annulene. The upfield chemical shift experienced by the peripheral protons of the macroring are also essentially due to the same current reduction effect, introduced due to bond fixation caused by the fusion of **32** to the aromatic ruthenocene and cyclopentadienyl tricarbonyl manganese complexes.

3.2.10 Bond Fixation Versus Reduction in Ring Current

The upfield shift in the peripheral protons of an aromatic compound resulting from complexation to metals is, as discussed earlier, attributed to the reduction in the ring current. Hence, in examples such as **149**, **157** and **159**, the reduction in the ring current is invoked, successfully, to explain the experimental chemical shifts. In its crystal structure, benzene tricarbonyl chromium has benzene bonds alternating between 1.423 and 1.406 A^{o}.[163] In non-complexed aromatics, bond alternation leads to ring current reduction. Thus, as a simple argument suggests, bond alternation exibited by benzene in the above complex *a priori* causes a smaller ring current. This of course agrees with the NMR spectroscopic data.

A closer look at the Proton NMR data of the complex **171** reveals the opposite. In naphthalene, the coupling

constant J_{12} is 8.3 Hz and J_{23} is 6.9 Hz. Upon complexation, J_{12} becomes 8.5 Hz and J_{23} is now 6.0 Hz. Since the bond order is directly related to the coupling constant (cf. equation 3),the uncomplexed ring in **171** is undoubtedly more bond fixed than in the free ligand. This in turn leads us to conclude that complexed benzene is more bond fixing than free benzene. This conclusion, of course, appears to contradict the ring current reduction hypothesis. In the dimethyldihydropyrene tricarbonyl chromium complex **160**, the same conclusion was also drawn.[99]

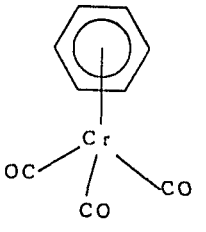

149

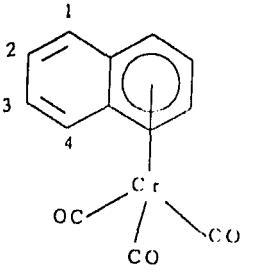

171

In the case of μ^5-indenyl complexes, unfortunately, not enough information on the coupling constants between the benzene protons are available. However, hydrogenation with hydrogen in the presence of catalysts has been investigated for a series of indenyl complexes such as cyclopentadienyl (indenyl) iron, diindenyl ruthenium, and a dimer of dicarbonyl indenyl iron.[103a] In all of the above indenyl complexes, the six-membered ring of the ligand is easily hydrogenated, indicating that the

cyclopentadienyl fragment possesses a larger bond fixing ability than benzene itself. Evidently, this experimental evidence contradicts that obtained from NMR chemical shift data since ring current reduction in the cyclopentadienyl ring upon complexation should lead to a lesser degree of bond fixing ability.

Using the internal methyl chemical shift as a measure of bond fixation, we previously concluded that in the two complexes **139a** and **141a** the cyclopentadienyl fragment is more bond fixing than benzene itself. The same conclusion can be drawn from the coupling constant differences, obtained experimentally, for the peripheral protons of the bonds BC, HG, DE, and EF (cf equations 7a and 7b). Moreover, the chemical shifts of all eight peripheral protons of the 14-membered ring in the two complexes are shifted upfield when compared to the corresponding protons in the benz-fused annulene **92**. The upfield shifts indicate a lesser ring current in the macroring, again leading to the same conclusion drawn above.

Apparently, in complexed aromatics, two distinct effects are operating: a reduced ring current and an increased bond fixing ability. This can only be explained in terms of metal-ligand interaction. A metal fragment such as Cp-M or $M(CO)_3$ is electron withdrawing. Upon complexation to an aromatic compound, it reduces the electron density of the aromatic, thus reducing its ring

current. The most stable structure of the complex, however, is a structure where the metal atom is equidistant from the carbon atoms of the ligand. In fused aromatics, this apparently occurs at the expense of the uncomplexed ring, leading to its being more bond fixed than in the uncomplexed π-ligand.

In the complexes **168** and **172-174** below, there seems to be a general feature in the magnitude of the difference between the longest and shortest bond in each ring.

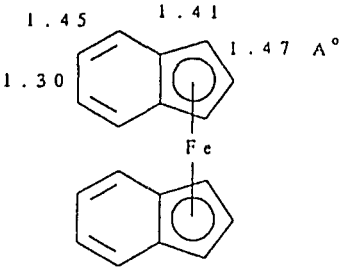

172[164]

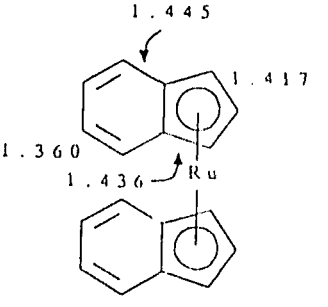

173[165]

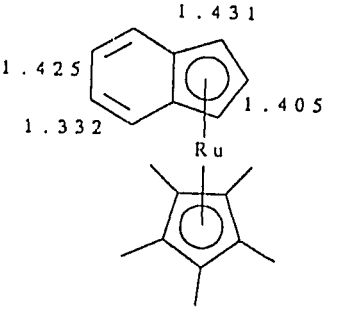

168[125c]

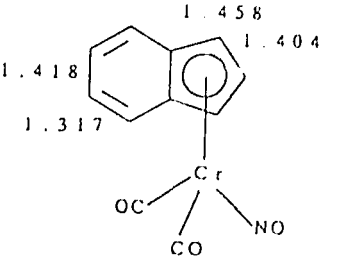

174[166]

Excluding the fusion bond, the above difference is at least twice as large in the complexed ring as in the

uncomplexed ring. This finding indicates the tendency in these complexes to bond fix the uncomplexed ring while minimising bond fixation in the complexed ring.

3.2.11 Summary

In the preceding section, we have discussed the proton NMR properties of the two novel complexes, **139a** and **141a**. It was concluded that the anisotropy effect of the metal fragments is negligible on the internal methyl protons and thus the chemical shifts are mainly dependent on the ring current of the 14 π-annulene. The diamagnetic anisotropy for ruthenocene was calculated as -330×10^{-36} m^3 per molecule. For the tricarbonyl manganese fragment, the diamagnetic anisotropy was calculated as -635×10^{-36} m^3 per molecule, using a supercarbonyl model. It was found that both ruthenocene and cyclopentadienyl tricarbonyl manganese have a larger effective bond fixing ability than benzene when fused to dimethyldihydropyrene. It was also found that in benzene resonance energy units, ruthenocene has an effective experimental resonance energy of 1.42. Similarily, cyclopentadienyl tricarbonyl manganese has an effective experimental resonance energy of 1.36 in the same benzene units.

CHAPTER FOUR

THE CRYSTAL STRUCTURE OF TRANS-10b,10c-DIMETHYLDIHYDROPYRENE

trans-10b,10c-Dimethyldihydropyrene, **32**, is an aromatic compound as judged by its proton NMR spectrum. As we have seen earlier, the molecule has proved invaluable in the study of ring current reduction effects caused by bond fixation introduced by annelation.

An important criterion for aromaticity of a molecule is its bond lengths. The absence of bond alternation in conjugated systems is indicative of their aromaticity. Consequently, molecules such as the tricyclic [10]annulene **175**[167], the 1,6-methanoannulene **26**[168], the didehydro[14]annulene **39**[169], and the ethano-bridged [14]annulene **30**[38], all are classified as aromatic, whereas the *anti*-bismethano[14]annulene **176**[170], is not. In the latter, the carbon-carbon bonds of the annulene ring are twisted. The torsional angle of the C_6-C_7 bond, Figure 15, reaches a value of 84^{o}. As a consequence, the π-orbital overlap at the C_6-C_7 bond is minimal, thus the loss of aromaticity. This is manifested in the pronounced alternation of single and double bonds.

The planarity and the absence of bond alternation in **32** is implied by comparison to its close analogues **25**[27] and **177**[171], whose crystal structures were determined in 1965 and 1967, respectively. The crystal structure for another analogue, **178**, which has one of the methyls

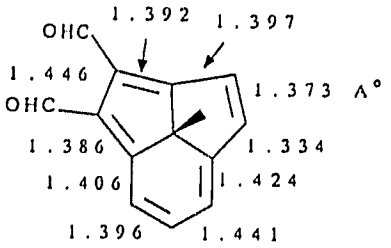

175

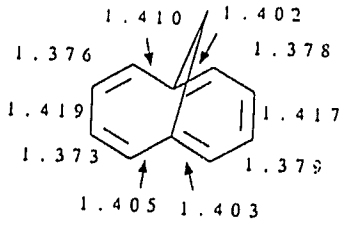

26

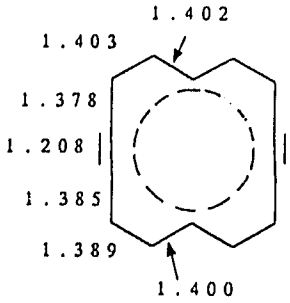

39

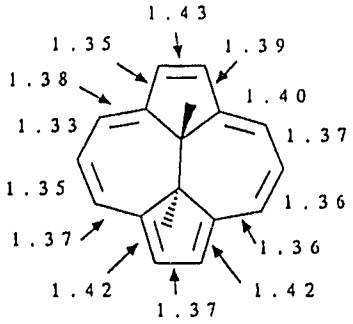

30

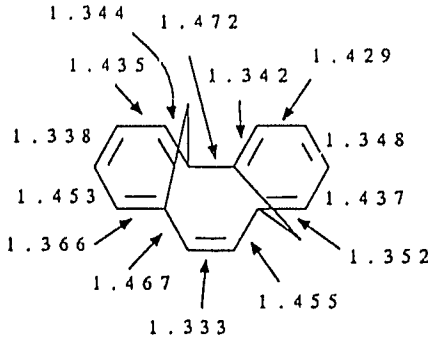

176

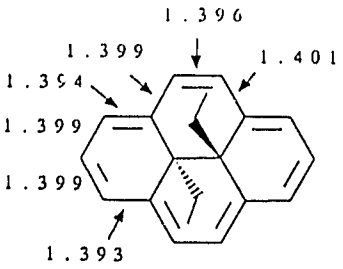

177

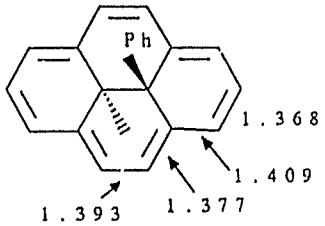

178

Figure 15: Bond lengths for selected annulenes.

replaced with a phenyl group, is also known.[79] The absence of a crystal structure for **32** from the chemical literature creates a void in the pool of information available on such a fundamental molecule. The lack of such a structure is due to the difficulty in generating suitable crystals for X-ray analysis. Indeed, successive recrystalization from aqueous alcoholic solvents failed to generate any suitable crystals. Recrystalization from methanol or ethanol or hydrocarbon solvents also failed to produce the desired crystals. After many trials, a mixture of petroleum ether and methanol proved to be the "magic solution". The crystal structure for **32** was then determined at room temperature (20 ^{o}C).

The compound crystalizes as two distinct molecules. In the following discussion, only one of these will be considered since the parameters for the two are essentially the same. The rest of the crystal structure data on the second molecule, along with other data on the first can be found in Appendix 1. Selected crystal data are collected in Table 24. Figure 16b has the ORTEP drawing of the second molecule. A first glance at the ORTEP diagram confirms that the internal methyl groups in **32** are indeed in the centre of the π-cavity.

Table 24: Crystal Structure data for **32**:

---

trans-10b,10c-dimethyldihydropyrene $C_{18}C_{16}$

triclinic, centrosymmetric mol. wt. 232.1

space group $P\bar{1}$ Z = 2

a = 7.495(3) A^{o} α = 101.10(3)^{o}

b = 7.593(4) β = 80.92(3)

c = 12.859(4) γ = 115.41(3)

$D_{meas.}$ = 1.208 $D_{calc.}$ = 1.192 $g.cm^{-3}$

crystal dimensions: 0.10x0.78x0.40 mm

No. of reflections in the final data set = 1225

refinement method: least squares

final R value: 0.076

Selected Data:

Bond Lengths:

C_{22}-C_{23}	1.396(9)	C_{21}-C_{34}	1.390(7)
C_{23}-C_{24}	1.393(7)	C_{24}-C_{35}	1.509(6)
C_{24}-C_{25}	1.393(8)	C_{34}-C_{35}	1.521(6)
C_{33}-C_{34}	1.379(7)	C_{35}-C_{36}	1.562(6)
C_{21}-C_{22}	1.354(9)	C_{35}-C_{37}	1.545(8)

Angles:

C_{22}-C_{23}-C_{24}	120.1(7)	C_{35}-C_{24}-C_{25}	116.5(5)
C_{23}-C_{24}-C_{25}	124.6(6)	C_{35}-C_{34}-C_{21}	117.4(6)
C_{21}-C_{22}-C_{23}	123.2(6)	C_{35}-C_{34}-C_{33}	116.8(5)
C_{22}-C_{21}-C_{34}	121.7(6)	C_{24}-C_{35}-C_{34}	114.2(4)
C_{21}-C_{34}-C_{33}	125.3(6)	C_{36}-C_{35}-C_{34}	105.5(4)

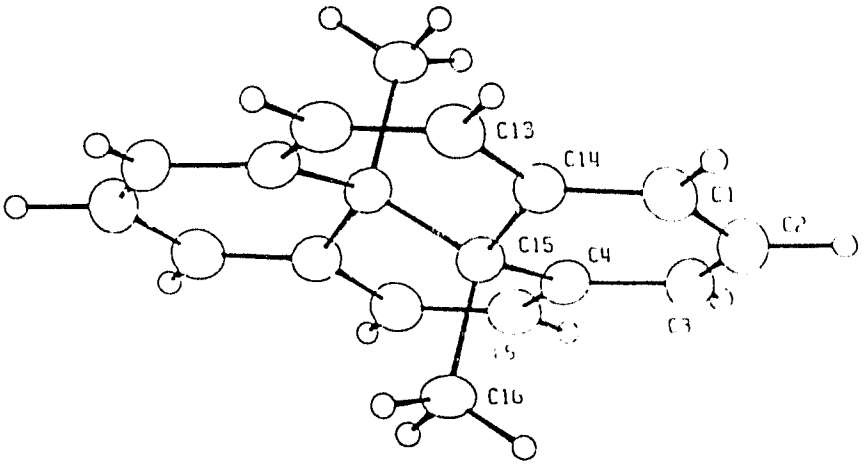

Figure 16a: ORTEP drawing of **32** (first molecule)

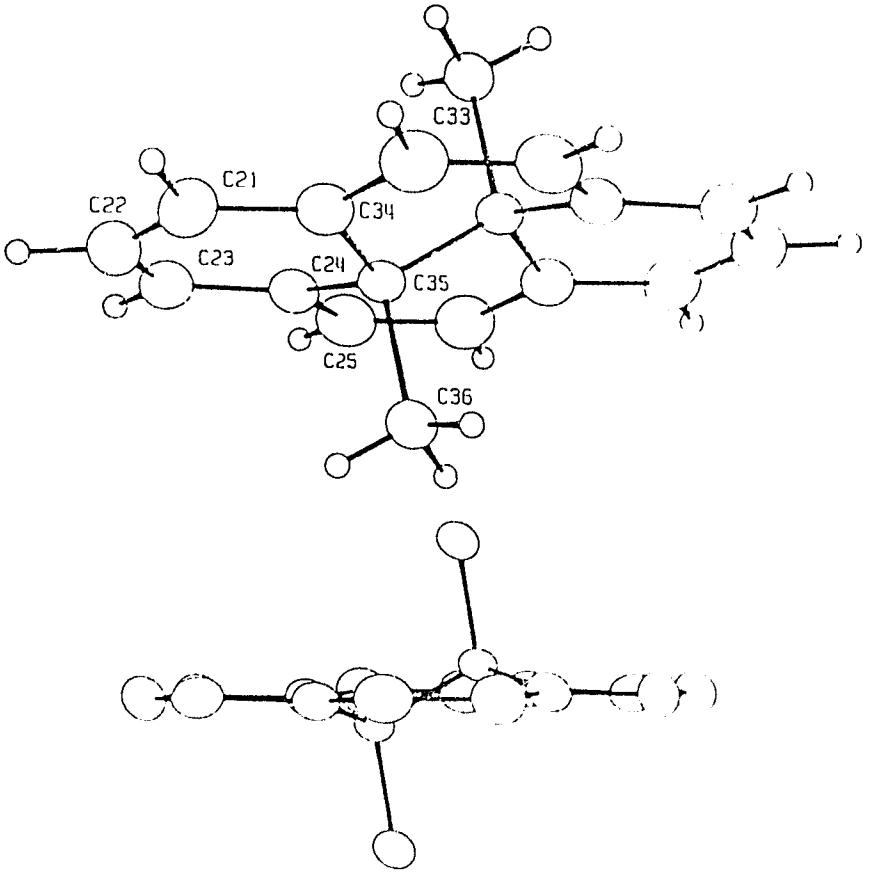

Figure 16b: ORTEP drawing for **32** (second molecule)

Except for a slight flattening at the bridge carbons (C_{24}, C_{34}), the angles of the 14 π-perimeter approach the ideal angle of 120°. The largest torsional angle around the perimeter (C_{21}-C_{22}-C_{23}-C_{24}) is only 4.04°. We can therefore conclude that the 14 π-periphery of the molecule is virtually planar.

Bond alternation is absent in the periphery of the molecule, with bond lengths ranging from 1.396-1.377 A°. These bond lengths are very comparable with those of the analogous derivatives **25**, **177**, and **178**. The only deviation in **32** is the C_{21}-C_{22} bond length which has a value of 1.354 A°. The corresponding value in **178** is 1.368 A°. This deviation may, however, not be genuine. Shorter bond lengths are present in other aromatic systems. In the aromatic molecules **30** and **175**, the shortest bond in only 1.33 A°. We can therefore confirm that *trans*-10b,10c-dimethyldihydropyrene, **32**, judging by its bond lengths and virtual planarity, is an aromatic compound.

CHAPTER FIVE

CONCLUSIONS AND FUTURE WORK

The synthesis of *trans*-11b,11c-dimethyl-11b,11c-dihydro-7H-cyclopent[a]pyrene, **109**, from *trans*-10b,10c-dimethyl-10b,10c-dihydropyrene, **32**, was achieved in six steps in an overall yield of 29%. Deprotonation of **109** gave the first annuleno-fused cyclopentadienide, *trans*-11b,11c-dimethyl-11b,11c-dihydrocyclopent[*a*]pyrene, ion(1-), **101**. Experimental and theoretical proton NMR results for the anion in the presence and absence of the counter cation were analysed. The cyclopentadienyl anion, when fused to **32**, has 53% of the effective bond-fixing ability of benzene fused to the same system. In terms of benzene resonance energy units, cyclopentadienyl anion has an effective experimental resonance energy of 0.53. The synthesis of biscyclopentadienyl-fused dimethyldihydropyrene utilizing the same procedures for making **101** should be investigated. The properties of these dianions can then be compared with the already known *syn* and *anti* dibenzo-fused derivatives **94** and **95**. In this direction, during the course of this work, the saturated bisester-2,7-dmdhp was synthesized in a fair yield from the saturated monoester **122**.

Metal complexation of the cyclopent[a]dihydropyrene, **101**, was investigated, and gave the first two cyclopent-fused large annulene metal complexes, [6a,7,8,9,9a-μ^5]-

trans-11b,11c-dimethyl-11b,11c-dihydrocyclopent[a]pyrene-pentamethylcyclopentadienylruthenium(II), **139**, and [6a,7,8,9,9a-μ^5]*trans*-11b,11c-dimethyl-11b,11c-dihydro-cyclopent[a]pyrene-tricarbonylmanganese(I), **141**. Experimental and theoretical ^{1}H NMR results for the two complexes were analysed. Ruthenocene, when fused to **32**, was found to be 1.38 times more bond-fixing than benzene itself. Similarily, cyclopentadienylmanganesetricarbonyl is 1.33 times more bond-fixing than benzene. In terms of benzene resonance energy units, the two complexes have effective experimental resonance energies of 1.42 and 1.36, respectively.

The diamagnetic susceptibility, X, of a cyclopenta-dienylruthenium moiety, with the center of anisotropy located at the metal atom, was calculated as -330×10^{-36} m^3 per molecule. The same parameter for a manganese tricarbonyl moiety, with the center of anisotropy being located at 3.2 A^o down from the manganese atom, was calculated as -635×10^{-36} m^3 per molecule.

To complete a series of studies, more metal complexes of the type **167** should be made and their bond fixing ability investigated. These complexes, where applicable, might serve as models to calculate the diamagnetic susceptibilities of metal-ligand moieties. Studies of metal complexes of the bis-anion should prove interesting since bis-complexed annulenes are rare in literature.

An X-ray structure determination of **32** was finally achieved some 25 years after its first synthesis. The structural data confirm the planarity and lack of bond alternation in the bridged annulene, indicating that it is aromatic.

CHAPTER SIX

EXPERIMENTAL SECTION

6.1 Instrumentation

Melting points are uncorrected and were determined on a Reichert 7905 melting point apparatus integrated to an Omega Engineering Model 199 Chromel-alumel thermocouple. Infrared spectra, calibrated with polystyrene, were recorded on a Perkin-Elmer 283 spectrometer. Ultraviolet spectra were recorded on a perkin-Elmer Lambda-4B spectrophotometer using cyclohexane (unless otherwise specified) as a solvent. Proton NMR spectra of solutions in chloroform-d (unless otherwise specified) were recorded on a Perkin-Elmer R-32 (90 MHz) using tetramethylsilane as internal standard, a Bruker WM 250 (250 MHz) spectrometer or a Bruker AMX 360 (360 MHz) spectrometer using the solvent deuterium signal as the lock signal at room temperature. Carbon-13 NMR spectra were recorded on a Bruker WM 250 (62.9 MHz) using solutions in chloroform-d and the solvent peak (77.0 ppm) for calibration. Mass spectra were recorded on a Finnigan 3300 gas chromatography-mass spectroscopy system using methane as a carrier gas for chemical ionization. Exact mass determinations were done on a Perkin-Elmer Hitachi RMU-6E spectrometer with 70 ev electron impact ionization using perfluorokerosene as the standard.

Elemental analyses were performed by Canadian Microanalytical Services Ltd., Vancouver, British Columbia. X-ray structure determination for **32** was performed by Dr. G. W. Bushnell and Kathy Beveridge on a Picker 4 circle diffractometer automated with a PDP 11/10 computer.

6.2 Experimental Procedure

2-formyl-*trans*-10b,10c-dimethyl-10b,10c-dihydropyrene,120

Titanium tetrachloride (1.43 mL, 12.9 mmol) was added dropwise under nitrogen to a solution of DMDHP[40,105] (2.00 g, 8.62 mmol) in 60 mL dry methylenechloride at 0°C. To the green-reddish solution was added α,α-dichloromethyl methyl ether (1.01 mL, 11.2 mmol) dropwise and the resulting blue-green solution was stirred at room temperature for 1.5 hours, after which it was slowly added to 250 mL of ice-cooled water. The organic layer was separated and the aqueous layer washed with 3 portions of methylenechloride (50 mL each). The combined organic extracts were dried and evaporated to yield a dark-red solid gum, which was chromatographed over silica gel with CH_2Cl_2-petroleum ether (1:25) as eluant. The first fraction eluted yielded dark green crystals (470 mg, 20%) after slow evaporation of solvents. This fraction was identified as 4-formyl-*trans*-10b,10c-dimethyl-10b,10c-dimethyldihydropyrene,

120, mp. 109°C (literature 107-108); ^{1}H NMR (90 MHz, $CDCl_3$) δ: 11.16 (s, 1H, CHO), 9.82 (d, 1H, H-3), 8.62 (m, 7H, H-1,2,5,6,8,9,10), 8.16 (t, 1H, H-7), -4.00 (s, 3H, int. methyl), -4.07 (s, 3H, int. methyl).

The second fraction gave a dark-red gummy solid (1.63 gm, 75%), which was recrystallized from methanol to give **119** as thin plates, mp. 129-130°C (literature 129-131°C); ^{1}H NMR (90 MHz, $CDCl_3$) δ: 10.50 (s, 1H, CHO), 9.08 (s, 2H, H-1,3), 8.73/8.64 (ABq, $J_{4,5} = J_{9,10} = 7.75$, 4H, H-4,5,9,10), 8.54 (d, J = 7.82, 2H, H-6,8), 8.19 (t, J = 7.82, 1H, H-7), -3.91(s, 6H, int. methyls).

Ethyl *trans*-3-(2-*trans*-10b,10c-dimethyl-10b,10c-dihydropyrenyl)propenoate, 121

Triethylphosphonoacetate (1.32 mL, 6.64 mmol) was added to a suspension of sodium hydride (162 mg, 6.76 mmol) in 35 mL dry THF at 0°C under nitrogen. After hydrogen gas evolution had subsided, 2-formyl-dimethyl-dihydropyrene, **119** (1.90 g, 6.15 mmol) dissolved in 80 mL dry THF was added dropwise. The reaction mixture was allowed to warm to room temperature and was subsequently refluxed for an hour. Saturated ammonium chloride solution (50 mL) and dichloromethane (100 mL) were then added to the cooled mixture. The organic layer was separated, dried over sodium sulfate and evaporated to give a marroon solid residue, which was chromatographed

over silica gel with dichloromethane-petroleum ether (1:20) as eluant to give pure **121** (2.0 g, 98%). Recrystallization from ether-pentane gave dark red crystals of **121**, mp. 146-147°C; ^{1}H NMR (250 MHz, $CDCl_3$) δ: 8.68 (s, 1H, H-1,3), 8.59/8.50 (ABq, $J_{4,5} = J_{9,10} =$ 7.90, H-4,5,9,10), 8.46 (d, $J_{6,7} = 7.78$, 2H, H-6,8), 8.30 (d, $J_{2',3'} = 15.8$, 1H, H-3), 8.03 (t, $J_{6,7} = 7.78$, 1H, H-7), 6.91 (d, $J_{2',3'} = 15.8$, 1H, H-2), 4.35 (q, J = 7.13, 2H, $-OCH_2$), 1.41 (t, J = 7.13, 3H, $-CH_2-CH_3$), -3.85 (s, 3H, int. Methyl), -3.87 (s, 3H, int. methyl); ^{13}C NMR (62.9 MHz, $CDCl_3$) δ: 167.3 (carbonyl C), 146.2, 140.0 (C-3a,5a,8a,10a), 136.4, 128.2, 124.8, 124.2, 123.5, 122.0 (C-1,2,2',3,4,5,6,7,8,9,10), 117.9 (C-2'), 60.4 ($CH_3-CH_2-CO_2-$), 31.1, 30.3 (C-10b,10c), 15.1, 14.8 (int. methyl C), 14.4 ($CH_3-CH_2-CO_2-$); ms. peaks (EI) at m/e (relative intensity): 330 (45), 315 (70), 300 (8), 242 (31), 241 (100), 227 (34), 226 (46), 113 (37); ms. peaks (CI) at m/e (relative intensity): 331 (100), 315 (43), 225 (40), 75 (61); IR (KBr, major bands, cm^{-1}): 3120, 3015, 2965, 2910, 1698, 1613, 1270, 1174, 1150, 1032, 852, 816, 655; UV (cyclohexane) wavelength max. nm ($\log\varepsilon_{max}$): 669 (2.30), 619 (sh,2.37), 604 (2.49), 518 (4.32), 495 (sh,4.16), 399 (4.51), 375 (4.33), 346 (4.90), 332 (sh,4.63); anal.: calcd for $C_{23}H_{24}O_2$: C 83.60, H 6.71; found C 83.43, H 6.78.

Ethyl 3-(2-*trans*-10b,10c-dimethyl-10b,10c-dihydropyrenyl)propionate

To the unsaturated ester **121** (2.03 g, 6.15 mmol) in ethylacetate (100 mL) was added palladium (on activated charcoal, 10%) in catalytic amount. The reaction mixture was stirred under hydrogen for approximately 2.5 hours (at which time one equivalent of H_2 was consumed). The mixture was then vacuum filtered, washed with dichloromethane and the solvent evaporated to give a gummy dark-green solid. The product was chromatographed over silica gel with pentane to give a dark-green gummy solid (1.75 g, 86%). All attempts to crystallize the product failed. ^{1}H NMR (250 MHz, $CDCl_3$) δ: 8.45 (s, 2H, H-1,3), 8.61/8.56 (ABq, $J_{4,5} = J_{9,10} = 7.79$, 4H, H-4,5,9,10), 8.55 (d, $J_{6,8} = 7.65$, 2H, H-6,8), 8.04 (t, $J_{6,7} = 7.65$, 1H, H-7), 4.13 (q, J = 7.15, 2H, $-OCH_2$), 3.66 (t, $J_{2',3'} = 7.71$, 2H, $Ar-CH_2-CH_2-$), 2.99 (t, $J_{2',3'} = 7.71$, 2H, $Ar-CH_2-CH_2-$), 1.17 (t, J = 7.15, 3H, CH_3-CH_2O), -4.16 (s, 3H, int. methyl), -4.16 (s, 3H, int. methyl); ^{13}C NMR (62.9 MHz, $CDCl_3$) δ: 172.6 (carbonyl C), 136.9, 136.0 (C-3a,5a,8a,10a), 135.6, 123.6, 123.4, 123.1, 122.3 (C-1,2,3,4,5,6,7,8,9,10), 60.2 (CH_2O-), 36.6 ($Ar-CH_2-CH_2$), 32.9 ($Ar-CH_2-CH_2$), 29.7, 29.5 (C-10b,10c), 14.1 ($CH_3-CH_2-CO_2-$), 14.1, 13.7 (int. CH_3); ms. peaks (EI) at m/e (relative intensity): 332 (79), 317 (8), 302 (5), 271 (68), 229 (100); ms. peaks (CI) at m/e (relative

intensity): 333 (53), 332 (81), 271 (100), 229 (46); IR (KBr, major bands cm^{-1}): 3020, 2955, 2905, 2850, 1730, 1368, 1334, 1176, 1153, 1035, 863, 810, 655; UV (cyclohexane) wavelength max. nm ($log\epsilon_{max}$): 642 (2.23), 625 (2.04), 606 (sh, 2.11), 594 (1.95), 529 (1.93), 470 (3.85), 455 (3.83), 377 (4.61), 355 (4.22), 338 (4.98); exact mass: calcd. 332.17761, found 332.16772.

3-(2-*trans*-10b,10c-dimethyl-10b,10c-dihydropyrenyl)-propionic acid

The saturated ester **122** (2.00 g, 6.02 mmol) was refluxed in 75 mL 1N aq. sodium hydroxide for 15 hours. The solution was then cooled to room temperature, treated with concentrated hydrochloric acid and the vacuum filtered. The dry solid was chromatographed over silica gel with diethylether as eluant to give 90% of dark green microcrystals. Recrystallization from cyclohexane-petroleum ether gave dark green short needles, mp.: 165°C; ^{1}H NMR (250 MHz, $CDCl_3$) δ: 10.98 (broad, -COOH), 8.59/8.53 (ABq, $J_{4,5} = J_{9,10} = 7.75$, 4H, H-4,5,9,10), 8.55 (d, $J_{6,8} = 7.69$, 2H, H-6,8), 8.44 (s, 2H, H-1,3), 8.05 (t, $J_{6,7} = 7.69$, 1H, H-7), 3.66 (t, $J_{2',3'} = 7.86$, 2H, Ar-CH_2-CH_2-), 3.06 (t, $J_{2',3'} = 7.86$, 2H, Ar-CH_2-CH_2-), -4.19 (s, 3H, int. methyl), -4.20 (s, 3H, int. methyl); ^{13}C NMR (62.9 MHz, $CDCl_3$) δ: 179.1 (carbonyl C), 137.1, 136.3 (C-3a,5a,8a,10a), 135.2, 123.9, 123.6,

123.4, 122.6 (C-1,2,3,4,5,6,7,8,9,10), 36.4 (Ar-CH_2-CH_2), 32.9 (Ar-CH_2-CH_2), 29.9,29.7 (10b,10c), 14.2, 13.9 (int. methyl C); ms. peaks (EI) at m/e (relative intensity): 304 (20), 289 (3), 274 (3), 271 (26), 229 (100), 216 (20), 215 (30), 114 (21); ms. peaks (CI) at m/e (relative intensity) 305 (100), 304 (58), 287 (27), 245 (20); IR (KBr, major bands, cm^{-1}): 3540-3350, 3015, 2960, 2905, 1683, 1440, 1368, 1327, 1253, 865, 811, 658, 605; UV (cycloxexane) wavelength max. nm ($log\epsilon_{max}$): 642 (2.48), 629 (2.25), 607 (sh,1.95), 529 (2.08), 470 (3.67), 455 (3.51), 377 (4.29), 351 (4.12), 338 (4.73); anal. calcd for $C_{21}H_{20}O_2$: C 82.68, H 6.57; found C 82.34, H 6.38.

Attempted synthesis of 125 using the saturated ester 122

The saturated ester **122** (150 mg, 0.45 mmol) was stirred in liqiud HF (5 mL) for approximately one hour, after which hydrogen fluoride was evaporated by bubbling nitrogen into the flask. The remaining solid was taken up in 10 mL dichloromethane and then washed with 15 mL of water. The organic extract was dried, and solvent evaporated, giving a black tar. No traces traces of the intended product **125** could be detected; instead extensive decomposition of the ester has resulted.

Attempted synthesis of 125 using the acid 123 and PPA

The acid **123** (100 mg, 0.33 mmol) was added to approximately 10 g of polyphosphoric acid (PPA) and the resulting gel was mechanically stirred for 30 minutes, after which the resulting dark-reddish mixture was added to iced water (25 mL), followed by diethylether (20 mL). The organic extract was dried, and solvent evaporated, giving a black-reddish solid. The solid could not be characterized by available instrumentation (NMR, IR, MS.). No ketone could be detected and no starting material could be recovered.

Attempted synthesis of 125 using the acid 123 and HF

The acid **123** (100 mg, 0.33 mmol) was stirred in 5 mL hydrogen fluoride for 2 hours, after which condensed HF was evaporated by bubbling nitrogen into the flask. The remaining dark-green solid was taken up into 15 mL dichloromethane and washed with 15 mL of water. The organic extract was dried and solvent evaporated to give a dark green solid. Paper chromatography and proton NMR spectrum of the product revealed that the only species present in the product was the starting material **123** (about 50% recovery). Further treatment as above for longer than 3.5 hours led to full decomposition.

Attempted synthesis of 124 using the acid 123 and $AlCl_3$/NaCl

A mixture of sodium chloride (1 g) and aluminium chloride (2 g) were heated to 150°C in a flask equipped with a mechanical stirrer. The acid **123** (100 mg) was then added and the mixture stirred for 2 minutes, after which dichloromethane (15 mL) was added. The organic extract was dried and solvent evaporated to give a dark green solid. The IR spectrum of the solid showed, along with the carboxyl stretch peak at 1683 cm^{-1}, a peak at 1802 cm^{-1}, which was determined as that due to the carbonyl stretch in **124**. Heating a similar mixture at the same temperature as above, but for longer times, resulted in the loss of the green color, giving a black solid that could not be characterized.

***trans*-11b,11c-Dimethyl-7,8,11b,11c-tetrahydro-9-oxo-9H-cyclopenta[a]pyrene, 125**

To the acid **123** (200 mg, 0.66 mmol), dissolved in dry dichloromethane (15 mL), was added excess oxalyl-chloride (3 eqiuvalent). The solution was stirred at room temperature for 6 hours, after which the solvent was evaporated and the solid residue dried under vacuum for about one hour to get rid of excess chlorinating reagent. An infrared spectrum of the dark-green solid (KBr disc)

showed a sharp peak at 1802 cm^{-1}. The peak at 1683 cm^{-1}, due to the starting material was absent.

The dark-green solid residue was taken up in 100 mL of dry dichloromethane and 1.2 equivalent of BF_3.etherate were added to the mixture. The solution was then allowed to stirr for approximately 9 hours, after which aqueous potassium carbonate was added and the organic layer dried, and concentrated to give a dark green solid which was chromatographed over silica gel with dichloromethane as eluant to give dark-green crystals of **125** (120 mg, 63%). A second fraction eluted was the starting material **123** (approx. 8% recovery). Recrystallization of **125** from cyclohexane gave dark-green plates, mp. 210-211°C; ^1H NMR (250 MHz, $CDCl_3$)δ: 9.66/8.51(ABq, $J_{10,11}$ = 7.25, 2H, H-10,11), 8.61/8.49 ($J_{4,5}$ = 8.13, 2H, H-5,4), 8.50 (d, $J_{1,2}$ = 7.68, 1H, H-1), 8.47 (d, $J_{2,3}$ = 7.68, 1H, H-3), 8.45 (s, 1H, H-6), 7.95 (t, $J_{1,2} = J_{2,3}$ = 7.68, 1H, H-2), 3.73 (m, 2H, H-7), 3.05 (m, 2H, H-8), -3.72 (s, 3H, int. methyl), -3.73 (s, 3H, int. methyl); ^{13}C NMR (62.9 MHz, $CDCl_3$) δ: 208.9 (carbonyl C), 153.6 (C-6a), 142.2 (C-9a), 136.9, 136.8, 130.0, 126.0 (C-3a,5a,9b,11a), 128.1, 126.9, 126.2, 123.7, 123.3, 120.3, 119.9 (C-1,2,3,4,5,6, 10,11), 37.3 (C-8), 30.3, 30.9 (C-11b,11c), 27.5 (C-7), 14.8, 14.4 (int. methyl C); ms. peaks (EI) at m/e (relative intensity): 286 (26), 271 (43), 256 (9), 229 (100); ms. peaks (CI) at m/e (relative intensity): 287 (54), 286 (12), 93 (100); IR (KBr, major bands, cm^{-1}):

3020, 2950, 2905, 1670, 1580, 1540, 1450, 1404, 1335, 1298, 1270, 1236, 1157, 1128, 1070, 963, 875, 844, 828, 654, 498; UV (cyclohexane) wavelength max. nm ($\log\epsilon_{max}$): 679 (2.74), 665 (sh, 2.33), 619 (1.97), 611 (2.03), 594 (1.87), 558 (1.87), 471 (2.86), 442 (sh, 3.07), 429 (sh, 3.11), 367 (4.30), 322 (sh, 3.10); anal. calcd. for $C_{21}H_{18}O$: C 87.99, H 6.33; found C 87.71, H 6.43.

trans-11b,11c-Dimethyl-11b,11c-dihydro-7H-cyclopenta[a]-pyrene, 109

Ketone **125** (100 mg, 0.35 mmol) was stirred at room temperature with lithium aluminium hydride (1.3 equivalent) in dry THF (20 mL) for 1.5 hours, after which iced water was added to destroy excess reagent. Hydrochloric acid (20%, 10 mL) was then added, followed by CH_2Cl_2 (30 mL) and the reaction mixture was stirred for an additional hour. The organic layer was then extracted, dried and evaporated to yield a dark green solid which was chromatographed using pentane as eluant to yield 77 mg of small dark-green plates (81%). Recrystallization from cold methanol gave thin dark-green plates, mp. 114-116^{o}C; ^{1}H NMR (250 MHz, $CDCl_3$) δ: 8.84/8.63 (ABq, $J_{10,11}$ = 7.76, 2H, H-10,11), 8.74 (s, 1H, H-6), 8.61/8.58 (ABq, $J_{4,5}$ = 7.68, 2H, H-5,4), 8.56 (d, $J_{1,2} = J_{2,3}$ = 7.72, 2H, H-1,3), 8.05 (t, $J_{1,2}$ = 7.72, 1H, H-2), 7.98 (d, $J_{8,9}$ = 5.66, 1H, H-9), 6.97 (dt, $J_{8,9}$ =

5.66, $J_{7,8}$ = 2.10, 1H, H-8), 3.99 (m, 2H, H-7), -4.15 (s, 3H, int. methyl), -4.16 (s, 3H, int. methyl); ^{13}C NMR (62.9 MHz, $CDCl_3$) δ: 139.6, 138.3, 136.6, 136.3, 136.0, 128.6 (C-3a,5a,6a,9a,9b,11a), 135.2 (C-9), 130.9, 123.1, 122.9(2), 122.6(2), 122.2, 119.7, 118.9 (C-1,2,3,4,5, 6,8,10,11), 40.7 (C-7), 30.4, 30.3 (C-11b,11c), 14.4, 13.8 (int. methyl C); ms. peaks (CI) at m/e (relative intensity): 271 (100), 270 (66), 255 (17); IR (KBr, major bands, cm^{-1}): 3005, 2960, 2905, 1625, 1362, 1258, 1070, 870, 820; UV (cyclohexane) wavelength max. nm ($log\epsilon_{max}$): 658 (1.95), 644 (2.06), 632 (sh, 1.92), 616 (1.83), 597 (1.79), 471 (3.49), 456 (sh, 3.45), 390 (4.13), 356 (4.57), 348 (sh, 4.40); anal. calcd. for $C_{21}H_{18}$: C 93.19, H 6.72; found C 92.77, H 7.00.

Isomerization of 109; Synthesis of *trans*-11b,11c-dimethyl-11b,11c-dihydro-9H-cyclopenta[a]pyrene, 108

To 50 mg of **109** in dry THF (under argon) was added 1.1 equivalent of KH and the mixture was stirred for 15 minutes, after which 1 mL of wet THF was added. Attempts to seperate the two isomers were not successful. A proton NMR spectrum of a solution of the mixture in $CDCl_3$, using the integrated internal methyl peaks for calibration, indicated that the isomers **108** and **109** were present in a 3:2 ratio. ^1H NMR of **108** (250 MHz, $CDCl_3$) δ: 8.78-8.40 (m, 8H, H-1,2,3,4,5,6,10,11), 7.42 (d, $J_{7,8}$

= 5.65, 1H, H-7), 6.94 (dt, $J_{7,8}$ = 5.65, $J_{8,9}$ = 2.10, 1H, H8), 4.23 (m, 2H, H-9), -4.09 (s, 6H, int. methyls).

trans-11b,11c-dimethyl-11b,11c-dihydrocyclopent[a]pyrene, ion(1-), 101

To a solution of **109** (25 mg) in dry deaerated THF-d_8 (0.4 mL) in a glove bag was added 1.1 equivalent KH. The intense red solution was then filtered into an nmr tube which was previously flushed with argon. ^{1}H NMR for **101b** (250 MHz, THF-d_8) δ: 8.25 (s, 1H, H-6), 7.79/7.61 (ABq, $J_{10,11}$ = 7.14, 2H, H-10,11), 7.70/7.57 (ABq, $J_{4,5}$ = 8.70, 2H, H-5,4), 7.55 (d, $J_{1,2}$ = 8.40, 1H, H-1), 7.39 (d, $J_{2,3}$ = 6.62, 1H, H-3), 7.30 (m, 1H, H-9), 6.97 (t, $J_{8,9}$ = $J_{7,8}$ = 3.31, 1H, H-8), 6.90 (dd, $J_{1,2}$ = 8.40, $J_{2,3}$ = 6.62, 1H, H-3), 6.67 (m, 1H, H-7), -2.83 (s, 3H, int. methyl), -2.88 (s, 3H, int. methyl); ^{1}H NMR for **101a** (250 MHz, THF-d_8) δ: 8.35 (s, 1H, H-6), 7.92/7.70 (ABq, $J_{10,11}$ = 7.05, 2H, H-10,11), 7.71/7.59 (ABq, $J_{4,5}$ = 8.33, 2H, H-5,4), 7.58 (d, $J_{1,2}$ = 7.87, 1H, H-1), 7.43 (m, 1H, H-9), 7.41 (d, $J_{2,3}$ = 6.78, 1H, H-3), 7.10 (t, $J_{7,8}$ = $J_{8,9}$ = 3.20, 1H, H-8), 6.83 (unresolved dd, J = 7.33, 1H, H-2), 6.76 (m, 1H, H-7), -3.14 (s, 3H, int. methyl), -3.19 (s, 3H, int. methyl); ^{13}C NMR for **101b** (62.9 MHz, THF-d_8) δ: 137.1 (C-6), 136.5, 136.0,131.6, 130.6 (C-3a,5a,9b,11a), 123.4, 123.3, 123.8(2), 124.3, 124.6, 124.5 (C-1,2,3,4,5,10,11), 119.8, 120.6 (C-6a,9a), 118.1, 119.3,

123.1 (C-7,8,9), 31.5, 30.6 (C-11b,11c), 15.5, 14.3 (int. methyl C); UV for **101b** (THF-d_8), wavelength max. ($\log\epsilon_{max}$); 654 (3.46), 645 (3.54), 593 (3.39), 477 (4.43), 454 (4.45), 391 (4.74), 357 (4.98), 250 (4.10).

Attempted synthesis of [6a,7,8,9,9a-μ^5]-*trans*-11b,11c-dimethyl-11b,11c-dihydrocyclopent[a]pyrene-cyclopentadienyliron(II), 129a

To a solution of **109** (100 mg, 0.37 mmol) in dry THF (4 mL) at -78°C was added 1.05 equivalent of MeLi, after which the solution was warmed to room temperature and stirred for an hour. The dark red solution was then transferred to a flask containing a suspension of ferrous chloride (1 equivalent) followed by addition of one equivalent CpLi, generated as above, and the reaction mixture stirred for 30 minutes. After cold evaporation of the solvent, the solid residue was taken up in dry deaerated cyclohexane and the organic extract was then concentrated to give an orange solid (70% based on CpLi) whose proton NMR is identical to that of ferrocene (90 MHz, $CDCl_3$: δ 4.05, singlet). No traces of the starting material could be detected. Repetition of the reaction at +50 to -60°C range also gave the same negative results. Repetition of the reactions using pentamethylcyclopentadienyllithium also failed to give **129b**.

In a diversion from the above method, a solution of the anion **101** was added to $FeCl_2$ and stirred for 0.5 hour followed by the additon of CpLi and the mixture stirred for 0.5 hour. After work-up, the only product detected was ferrocene. Replacement of the reagent with $FeCl_2$-THF adduct gave the same negative results as above. The yield of ferrocene in this case was about 80% based on CpLi. Repetition of the reactions at the above mentioned temperature range also failed to give **129a.**

Attempted synthesis of the bis-complex 130

A solution of **109** (100 mg, 0.37 mmol) in dry deaerated THF (5 mL) at -78°C was treated with 1.1 equivalent of MeLi, after which the solution warmed to room temperature and stirred for an hour. Ferrous chloride, or ferrous chloride-THF adduct (0.18 mmol) was then added and the reaction mixture stirred for 30 minutes. The solvent was then evaporated under vacuum and the solid residue taken up in cyclohexane. No organometallic complexes could be detected upon further work-up.

Attempted synthesis of [6a,7,8,9,9a-μ^5]-trans-11b,11c-dimethyl-11b,11c-dihydrocyclopent[a]pyrene-pentamethyl-cyclopentadienyliron(II), 129b, using $Cp^*Fe(acac)$

To ferrous diacetyldiacetonate (49 mg, 0.19 mmol) in dry THF (5 mL) at -78°C was added Cp^*Li (0.19 mmol), prepared from pentamethylcyclopentadiene and methyllithium, after which the resulting red orange solution was warmed to room temperature, and one equivalent of the anion **101** in THF (3 mL) was added. The mixture was then stirred for one hour, after which the solvent was evaporated under vacuum, and cyclohexane added. No traces of **129b** could be detected in the organic extract. Replacement of pentamethylcyclopentadiene with **109** failed to give any dihydropyrene-iron complexes. The starting material could not be recovered at the end of the reaction.

Attempted synthesis of [6a,7,8,9,9a-μ^5]-*trans*-11b,11c-dimethyl-11b,11c-dihydrocyclopent[a]pyrene-thalium(I), 134

To a solution of potassium hydroxide (21 mg, 0.37 mmol) and thalium sulfate (95 mg, 0.19 mmol) at 90°C was added **109** (100 mg, 0.37 mmol). The reaction mixture was vigorously shaken, using a mechanical stirrer, for one hour, after which the mixture was allowed to cool, and the water extract pipetted out. The solid residue was then dried under vacuum. A proton NMR spectrum for a solution of the residue did not indicate the presence of **134**. Extensive decomposition of the organic substrate

had resulted. Repetition of the reaction at 25-85°C range also failed to give the target **134.**

Synthesis of ferrocene by photolysis

To a solution of cyclopentadiene (100 mg, 1.5 mmol) in dry DMF (6 mL) was added KH (1 equivalent) and the mixture stirred for about 15 minutes, after which the complex **135** (450 mg, 1.2 mmol) was added. The reaction mixture was then photolyzed for 4 hours (reflector, 150W flood lamp). Petroleum ether was added in 3 portions (20 mL each), and the organic extracts collected and concentrated to give orange crystals of ferrocene (170 mg, 80%). ^{1}H NMR (90 MHz, $CDCl_3$) δ: 4.06, singlet.

Synthesis of indenyl-ferrocene by photolysis

To indene (130 mg, 1.1 mmol) in dry DMF (6 mL) was added KH (1 equivalent) and the mixture stirred for 30 minutes, after which the complex **135** (370 mg, 1.0 mmol) was added, and the reaction photolysed for 3 hours. Extraction with petroleum ether (4 portions, 30 mL each) and evaporation of the solvent gave a red-violet solid, which was chromatographed over basic alumina with petroleum ether as eluant. Two fractions were collected; the first one was ferrocene (10 mg), followed by indenyl-

ferrocene (163 mg, 69%) whose proton NMR spectrum was identical with an authentic sample.

Attempted synthesis of fluorenyl-ferrocene by photolysis

An identical procedure to the one described above was carried out using 100 mg of fluorene (0.60 mmol) and 200 mg (0.54 mmol) of the cation complex. The only organometallic product detected after work-up was ferrocene.

Attempted synthesis of 129a by photolysis

To the diene **109** (80 mg, 0.30 mmol) in dry DMF (5 mL) was added KH (1 equivalent) and the mixture stirred for 30 minutes. To the resulting intense red solution was added the cation complex (100 mg, 0.27 mmol) and the mixture photolysed for 50 minutes. Cyclohexane was then added (3 portions, 20 mL each) and the collected extracts concentrated to give ferrocene as the only product. The starting diene **109** could not be recovered.

[6a,7,8,9,9a-μ^5]-*trans*-11b,11c-dimethyl-11b,11c-dihydrocyclopent[a]pyrene-pentamethylcyclopentadienyl-ruthenium(II), 139a

The anion **101** was generated by the treatment of a solution of **109** (50 mg, 0.19 mmol) in dry deaerated THF (2.0 mL) with MeLi (1 equivalent) at -78°C, after which the solution was warmed to room temperature, and stirred for a further 15 minutes. The reagent **140** (58 mg, 0.19 mmol) was then added and the reaction mixture stirred at room temperature for 30 minutes, after which it was heated to 40°C for an extra 15 minutes. The solvent was then evaporated from the cooledd mixture and the solid residue taken up in cyclohexane and chromatographed over basic alumina. Concentration of the eluate gave 65 mg (70%) of **139** as a mixture of isomers **139a** and **139b** in 3.7:1 ratio. An anlytically pure sample was obtained by recrystallization from ethanol. Sublimation at 235°C (0.1 mmHg); ^{1}H NMR (360 MHz, $CDCl_3$) δ: 6.95/6.90 (ABq, $J_{4,5}$ = 9.09, 2H, H-5,4), 6.94/6.67 (ABq, $J_{10,11}$ = 6.41, 2H, H-10,11), 6.72 (s, 1H, H-6), 6.88 (d, $J_{1,2}$ = 8.85, 1H, H-1), 6.68 (d, $J_{2,3}$ = 6.08, 1H, H-3), 6.57 (dd, $J_{1,2}$ = 8.85, $J_{2,3}$ = 6.08, 1H, H-2), 4.99 (d, $J_{8,9}$ = 2.45, 1H, H-9), 4.70 (d, $J_{7,8}$ = 2.45, 1H, H-7), 4.39 (t, $J_{7,8}$ = 2.45, 1H, H-8), 1.68 (s, 15H, ext. methyl), -0.548 (s, 3H, int. methyl), -0.691 (s, 3H, int. methyl); ^{13}C NMR (62.9 MHz, $CDCl_3$) δ: 139.2, 137.3, 135.8, 135.4 (C-3a,5a,9b,11a), 126.6, 126.0, 123.9, 122.0, 121.4, 121.1, 120.5, 113.7 (C-1,2,3,4,5,6, 10,11), 85.2 (Cp^*) 85.0, 83.9 (C-6a,9a), 74.3, 71.6, 69.3 (C-7,8,9), 39.7, 38.3 (C-11b,11c), 20.1, 18.9 (int. methyl C), 11.5 (ext.

methyl C); ms. peaks (CI) at m/e (relative intensity): 508 (39), 507 (85), 506 (100), 505 (62), 504 (42), 490 (5), 475 (5), 391 (10), 285 (26), 270 (17), 255 (20), 240 (10), 183 (91), 129 (13), 113 (13), 105 (9); IR (KBr, major bands, cm^{-1}): 3050, 2895, 2860, 1447, 1363, 1308, 1267, 1172, 1028, 936, 698; UV (cyclohexane), wavelength max. ($log\epsilon_{max}$): 564 (sh, 2.48), 538 (sh, 2.65), 502 (sh, 2.77), 358 (4.74), 249 (4.56); Anal. calcd. for $C_{31}H_{32}Ru$: C 73.61, H 6.38; found C 73.36, H 6.08.

[6a,7,8,9,9a-μ^5]-*trans*-11b,11c-Dimethyl-11b,11c-dihydrocyclopent[a]pyrene-tricarbonylmanganese(I), 141a

The anion **101** was generated by the treatment of a solution of **109** (60 mg, 0.23 mmol) in dry deaerated THF (2.0 mL) with MeLi (1 equivalent) at -78°C, after which the solution was warmed to room temperature and stirred for a further 15 minutes. Manganese pentacarbonyl bromide (62 mg, 1 equivalent) was then added, and the reaction mixture stirred at room temperature for 10 minutes, after which it was heated to 40°C for an extra 20 minutes. The solvent was then evaporated from the cooled reaction mixture and the solid residue taken up in cyclohexane and chromatographed over basic alumina. Concentration of the eluate gave 57 mg (61%) of **141** as a dark-brown mixture of isomers **141a** and **141b** in 2.5:1 ratio. An analytically pure sample was obtained by

recrystallization from dichloromethane/pentane. mp. 217-219 (decom.), ^{1}H NMR (250 MHz, $CDCl_3$) δ: 7.16/6.83 (ABq, $J_{10,11}$ = 6.32, 2H, H-10,11), 7.15 (s, 1H, H-6), 7.13/7.11 (ABq, $J_{4,5}$ = 8.76, 2H, H-5,4), 7.05 (d, $J_{1,2}$ = 8.74, 1H, H-1), 6.89 (d, $J_{2,3}$ = 6.25, 1H, H-3), 6.74 (dd, $J_{1,2}$ = 8.74, $J_{2,3}$ = 6.25, 1H, H-2), 5.54 (br. s, 1H, H-9), 5.09 (m, 1H, H-7), 5.08 (m, 1H, H-8), -0.728 (s, 3H, int. Methyl), -0.784 (s, 3H, int. methyl); ^{13}C NMR (62.9 MHz, $CDCl_3$) δ: 226 (carbonyl, v. weak), 140.7, 139.4, 138.4, 135.8 (C-3a,5a,9a,11a), 127.3, 126.6, 126.0, 124.3, 124.1, 120.8, 118.4, 116.5 (C-1,2,3,4,5,6,10,11), 85.1, 77.8 (C-6a,9a), 76.2, 74.5, 74.0 (C-7,8,9), 37.9, 37.1 (C-11b,11c), 20.4, 18.9 (int. methyl C); ms. peaks (CI) at m/e (relative intensity): 409 (100), 285 (62), 253 (18), 225 (19), 200 (93), 83 (18); ms. peaks (EI) at m/e (relative intensity): 408 (10), 324 (10), 309 (24), 270 (12), 239 (100); IR (KBr, major bands, cm^{-1}): 2995, 2980, 2880, 2028, 1935, 1472, 1460, 1385, 1273, 1105, 1079, 817, 749, 710, 678, 635, 615; UV (cyclohexane), wavelength max. ($log\epsilon_{max}$); 646 (2.26), 473 (3.15), 381 (sh, 4.25), 346 (4.48), 231 (2.54); Anal. calcd. for $C_{24}H_{17}MnO_3$: C 70.58, H 4.20; found C 70.16, H 4.24.

REFERENCES

1. Faraday, M. *Phil. Trans. Roy. Soc.* **1825**, *115*, 440.

2. Mitscherlich, E. *Ann. Phys.* **1833**, *106*, 231.

3. LIoyd, D. *Non-benzenoid conjugated carbocyclic compounds*; Elsevier: New York, *1984*; Chapter 1.

4. Bamberger, E. *Liebigs Ann. Chem.* **1893**, *273*, 373.

5. Armit, J. W.; Robinson, R. *J. Chem. Soc.* **1925**, *127*, 1604-1618.

6. Huckel, E. *Z. Phys.*, **1931**, *70*, 204-286.

7. a. Sondheimer, F.; Wolovsky, R. *J. Am. Chem. Soc.* **1962**, *84*, 260-269. b. Sondheimer, F.; Wolovsky, R.; Amiel, Y. *J. Am. Chem. Soc.* **1962**, *84*, 274-284.

8. Vogel, E. *Pure Appl. Chem.* **1990**, *62*, 557-564.

9. Kovac, B.; Mohraz, M.; Heilbronner, E.; Boekelheide, V.; Hopf, H. *J. Am. Chem. Soc.* **1980**, *102*, 4314-4324.

10. Vogel, E. *Isr. J. Chem.* **1980**, *20*, 215-224.

11. Destro, R.; Pilati, T.; Simonetta, M. *Acta Crystallogr.* **1977**, *B33*, 940-942.

12. Platt, J. R. *J. Chem. Phys.* **1954**, *22*, 1448-1455.

13. Volpin, M. E. *Russ. Chem. Rev.* **1960**, *29*, 129-138.

14. a. Randic, M. *Chem. Phys. Lett.* **1976**, *38*, 68-70. b. Randic, M. *J. Am. Chem. Soc.* **1977**, *99*, 444-450.

c. Randic, M. *Tetrahedron* **1977**, *33*, 1905-1920.

15. Merling, G. *Ber. Dtsch. Chem. Ges.* **1891**, *24*, 3108.

16. Doering, W. Von E.; Knox, L.H. *J. Am. Chem. Soc.* **1954**, *76*, 3203-3206.

17. Thiele, J. *Ber.* **1900**, *33*, 660.

18. a. Rabinovitz, M.; Willner, I. *Pure Appl. Chem.* **1980**, *52*, 1575-1585. b. Mullen, K.; Huber, W.; Meul,T.; Nakagawa, M.; Iyoda, M. *J. Am. Chem. Soc.* **1982**, *104*, 5403-5411. c. Rabinovitz, M. *Acc. Chem. Res.* **1983**, *16*, 298-304. d. Prakash, G.; Rawdah, T.; Olah, G. *Angew. Chem, Int. Ed. Engl.* **1983**, *22*, 390-401. e. Mullen, K.; Meul, T.; Schade, P.; Schmickler, H.; Vogel, E. *J. Am. Chem. Soc.* **1987**, *109*, 4992-5003. f. Klabunde, K.; Mullen, K.; Vogler, H. *Tetrahedron* **1987**, *43*, 1183-1196. g. Rabinovitz, M. Cohen, Y. *Tetrahedron*, **1988**, *44*, 6957-6994.

19. Garratt, P.J. *Aromaticity*; John Wiley & Sons: New York, *1986*; pp 292-296.

20. a. Ref. 19; p 54. b. Badger, G. M. *Aromatic Character and Aromaticity*; Cambridge: London; *1969*, p 58.

21. a. Dewar, M. J. S.; Gleicher, G. J. *J. Am. Chem. Soc.* **1965**, *87*, 685-692. b. Dewar, M. J. S.; de LIano, C. *J. Am. Chem. Soc.* **1969**, *91*, 789-795. c. Dewar, M. J. S.; Harget, A. J.; Trinajstic, N.; Worley, S. D. *Tetrahedron*, **1970**, *26*, 4505-4516.

22. a. Hess, B. A.; Schaad, L. J. *J. Am. Chem. Soc.* **1971**, *93*, 305-310. b. Hess, B. A.; Schaad, L. J.; Agaranat, I. *J. Am. Chem. Soc.* **1978**, *100*, 5268-5271.

23. a. Herndon, W. C. *J. Am. Chem. Soc.* **1973**, *95*, 2404-2406. b. Swinborne-Sheldrake; Herndon, W. C.; Gutman, I. *Tetrahedron Lett.* **1975**, 755-758. c. Herndon, W. C. *J. Chem. Soc., Chem. Commun.* **1977**, 817-818.

24. a. Aihara, J. *Bull. Chem. Soc. Jpn.* **1975**, *48*, 517-520. b. Aihara, J. *J. Am. Chem. Soc.* **1976**, *98*, 2750-2758, 6840-6844. c. Aihara, J. *Chem. Phys. Lett.* **1980**, *73*, 404-406.

25. Gutman, I.; Milun, M.; Trinajstic, N. *J. Am. Chem. Soc.* **1977**, *99*, 1692-1704.

26. Childs, R. F.; Mahendran, M.; Zweep, S.; Shaw, G.; Chadda, S.; Burke, N.; George, B.; Faggiani, R.; Lock, C. *Pure Appl. Chem.* **1986**, *58*, 111-128.

27. Hanson, A. W. *Acta. Crystallogr.* **1965**, *18*, 599-604.

28. Bregman, J.; Hirshfeld, F. L.; Rabinovitz, D.; Schmidt, G. M. J. *Acta. Crystallogr.* **1965**, *19*, 227-234.

29. Haddon, R. C. *Tetrahedron*, **1972**, *28*, 3635-3655.

30. Haigh, C. W.; Mallion, R. B. *Mol. Phys.* **1970**, *18*, 737-750.

31. Crasselli, J. G.; *Atlas of Spectral data and Physical Constants for Organic Compounds*: CRC press, *1973*; p B460.

32. a. Masamune, S.; Seidner, R. T. *J. Chem. Soc, Chem. Commun.* **1969**, 542-544. b. Masamune, S.; Hojo, K.; Bigam, G.; Rabinstein, D. L. *J. Am. Chem. Soc.* **1971**, *93*, 4966-4968.

33. a. Vogel, E.; Roth, H. D. *Angew. Chem., Int. Ed. Engl.* **1964**, *3*, 228-229. b. Vogel, E.; Boll, W. A. *Angew. Chem., Int. Ed. Engl.* **1964**, *3*, 642.

34. Vogel, E.; Konigshofen, H.; Mullen, K.; Oth, J. F. M. *Angew. Chem., Int. Ed. Engl.* **1974**, *13*, 281-283.

35. Hafner, K.; Kuhn, V. *Angew. Chem., Int. Ed. Engl.* **1986**, *25*, 632-633.

36. Oth, J. F. M. *Pure Appl. Chem.* **1971**, *25*, 573-622.

37. Mullen, K. *Helv. Chim. Acta.* **1978**, *61*, 2307-2317.

38. Huber, W.; Lex, J.; Meul, T.; Mullen, K. *Angew. Chem., Int. Ed. Engl.* **1981**, *20*, 391-393.

39. Mitchell, R. H.; Boekelheide, V. *J. Chem. Soc., Chem Commun.* **1970**, 1555-1557.

40. Boekelheide, V.; Philips, J. B. *Proc. Natl. Acad. Sci. U.S.A.* **1964**, *51*, 550-552.

41. a. Vogel, E.; Kurschener, U.; Schmickler, H.; Lex, J.; Wennerstrom, O.; Tanner, D.; Norinder, U. *Tetrahedron Lett.* **1985**, 3087-3090. b. Tanner, D.; Wennerstrom, O.; Vogel E. *Tetrahedron Lett.* **1982**, 1221-1224.

42. Gilles, J. M.; Oth, J. F. M.; Sondheimer, F.; Woo, E. P. *J. Chem. Soc. (B)* **1971**, 2177-2186.

43. Otsubo, T.; Gray, R.; Boekelheide, V. *J. Am. Chem. Soc.* **1978**, *100*, 2449-2456.

44. Yamamoto, K.; Kuroda, S.; Nozawa, Y.; Fujita, S.;

Osjima, J. *J. Chem. Soc., Chem. Commun.* **1987**, 199-200.

45. McQuikin, R. M.; Metcalf, B. W.; Sondheimer, F. *J. Chem. Soc., Chem. Commun.* **1971**, 338-339.

46. Yamamoto, K.; Shibutani, M.; Kuroda, S.; Ejiri, E.; Ojima, J. *Tetrahedron Lett.* **1986**, 975-976.

47. Sondheimer, F. *Acc. Chem. Res.* **1972**, *5*, 81-91.

48. Nakagawa, M. *Pure Appl. Chem.* **1975**, *44*, 885-924.

49. Sondheimer, F.; Gaoni, Y. *J. Am. Chem. Soc.* **1960**, *82*, 5765-5766.

50. Nakagawa, M. *Angew. Chem., Int. Ed. Engl.* **1979**, *18*, 202-214.

51. Dauben, H. J.; Wilson, J. D.; Laity, J. L. *J. Am. Chem. Soc.* **1968**, *90*, 811-813. *ibid*, **1969**, *91*, 1991-1998.

52. a. Aihara, H. *J. Am. Chem. Soc.* **1979**, *101*, 5913-5916. b. Aihara, H. *Pure Appl. Chem.* **1982**, *54*, 1115-1128.

53. Katritzky, A. R.; Barczynski, P.; Musumarra, G.; Pisano, D.; Szafram, M. *J. Am. Chem. Soc.* **1989**, *111*, 7-15.

54. Zhou Z.; Parr, R. G. *J. Am. Chem. Soc.* **1989**, *111*, 7371-7379.

55. Boekelheide, V.; Philips, J. B.; *J. Am. Chem. Soc.* **1967**, *89*, 1695-1704.

56. Mitchell, R. H.; Klopfenstein, C.; Boekelheide, V. *J. Am. Chem. Soc.* **1969**, *91*, 4931-4932.

57. a. Spiesecke, H.; Schneider, W. *J. Chem. Phys.* **1961**, *35*, 731-738. b. Spiesecke, H.; Schneider, W. *Tetrahedron Let.* **1961**, 468-472.

58. Schaefer, T.; Schneider, W. *Can. J. Chem.* **1963**, *41*, 966-982.

59. a. Huber, W.; Mullen, K.; Wennerstrom, O. *Angew. Chem., Int. Ed. Engl.* **1980**, *19*, 624-625. b. Huber, W.; Mullen, K. *J. Chem. Soc., Chem. Commun.* **1980**, 698-700.

60. Breslow, R.; Groves, J. *J. Am. Chem. Soc.* **1970**, *92*, 984-988.

61. Olah, G. A.; Staral, J. *J. Am. Chem. Soc.* **1976**, *98*, 6290-6304.

62. Minsky, A.; Klein, J.; Rabinovitz, M. *J. Am. Chem. Soc.* **1981**, *103*, 4586-4587.

63. Oth, J. F. M.; Mullen, K.; Konigshoften, H.; Mann, M.; Sakata, Y.; Vogel, E. *Angew. Chem., Int. Ed. Engl.* **1974**, *13*, 284-285.

64. Oth, J. F. M.; Smith, D.; Prange, U.; Schroder, G. *Angew. Chem., Int. Ed. Engl.* **1973**, *12*, 327-328.

65. Grimme, W.; Hoffmann, H.; Vogel, E. *Angew. Chem., Int. Ed. Engl.* **1965**, *4*, 354-355.

66. Simonetta, M. *Pure Appl. Chem.* **1980**, *52*, 1597-1610.

67. Mullen, K.; Meul, T.; Vogel E.; Kurschner, U.; Shmickler, H.; Wennerstrom, O. *Tetrahedron Lett.* **1985**, 3091-3094.

68. Grimme, W.; Kanfhold, M.; Dettmeier, U.; Vogel, E. *Angew. Chem., Int. Ed. Engl.* **1966**, *5*, 604-605.

69. Shroder, G.; Plinke, G.; Smith, D.; Oth, J. F. M. *Angew. Chem., Int. Ed. Engl.* **1973**, *12*, 325-326.

70. Schmalz, D.; Gunther, H. *Angew. Chem., Int. Ed. Engl.* **1988**, *27*, 1692-1693.

71. Kuwajima, S.; Soos, Z. G. *J. Am. Chem. Soc.* **1986**, *108*, 1707-1708.

72. a. Kuwajima, S.; Soos, Z. G. *J. Am. Chem. Soc.* **1987**, *109*, 107-113. b. Oth, J. F. M., Baumann, H.; Gilles, J. M., Schroder, G. *J. Am. Chem. Soc.* **1972**, *94*, 3498-3512.

73. Sondheimer, F.; Jackman, L. M.; Amiel, Y.; Ben-Efraim, D. A.; Gaoni, Y.; Wolovsky, R.; Bothnerby, A. *J. Am. Chem. Soc.* **1962**, *84*, 4307-4312.

74. Mitchell, R. H.; Lai, Y. H.; Williams, R. V. *J. Org. Chem.* **1979**, *44*, 4733-4735.

75. a. Philips, J. B.; Molyneux, R. J.; Sturm, E.; Boekelheide, V. *J. Am. Chem. Soc.* **1967**, *89*, 1704-1709. b. Boekelheide, V.; Sturm, E. *J. Am. Chem. Soc.* **1969**, *91*, 902-908.

76. Mitchell, R. H.; Chaudhary, M.; Dingle, T. M.; Williams, R. V. *J. Am. Chem. Soc.* **1984**, *106*, 7776-7779.

77. Mitchell, R. H.; Calder, I.; Huisman, H.; Boekelheide, V. *Tetrahedron Lett.* **1975**, 1109-1111.

78. Tashiro, M.; Yamato, T.; *J. Am. Chem. Soc.* **1982**, *104*, 3701-3707.

79. Mitchell, R. H. *Adv. Theor. Interesting Mol.* **1989**, *1*, 135-199.

80. Mitchell, R. H. *Isr. J. Chem.* **1980**, *20*, 294-299.

81. Cresp, T. M.; Sondheimer, F. *J. Am. Chem. Soc.* **1975**, *97*, 4412-4413.

82. Cresp, T. M.; Sondheimer, F. *J. Am. Chem. Soc.* **1977**, *99*, 194-204.

83. Meissner, W. E.; Gensler, A.; Staab, H. A. *Angew. Chem., Int. Ed. Engl.* **1976**, *15*, 365-366.

84. Weaver, R. T.; Sondheimer, F. *Angew. Chem., Int. Ed. Engl.* **1974**, *13*, 141-142.

85. Mitchell, R. H.; Carruthers, R. J. *Tetrahedron Lett.* **1975**, 4331-4334.

86. Bergmann, E. D.; Pelchowicz, Z. *J. Am. Chem. Soc.* **1953**, *75*, 4281-4286.

87. Griffin, C. E.; Martin, K. R.; Douglas, B. E. *J. Org. Chem.* **1962**, *27*, 1627-1631.

88. Trahanovsky, W. S.; Fischer, D. R. *J. Am. Chem. Soc.* **1990**, *112*, 4971-4972.

89. a. Oda, M.; Oikawa, H. *Tetrahedron Lett.* **1980**, 107-

110. b. Kabuto, C.; Oda, M. *Tetrahedron Lett.* **1980**, 103-106.

90. a. Cremer, D.; Gunther, H. *Justus Liebigs, Ann. Chem.* **1972**, *763*, 87-108. b. Gunther, H.; Shyoukh, A.; Cremer, D.; Risch, K. *Justus Liebigs, Ann. Chem.* **1978**, *769*, 150-164. c. Gunther, H.; Gunther, M.; Mondeshka, D.; Schmickler, H. *Chem. Ber.* **1979**, *112*, 71-83.

91. Gunther, H.; Shyoukh, A.; Cremer, D.; Frisch K. H. *Tetrahedron Lett.* **1974**, 781-783.

92. Mitchell, R. H.; Williams, R. V.; Mahadevan, R.; Lai, Y. H.; Dingle, T. W. *J. Am. Chem. Soc.* **1982**, *104*, 2571-2578.

93. Mitchell, R. H.; Carruthers, R. J.; Mazuch, L.; Dingle, T. W. *J. Am. Chem. Soc.* **1982**, *104*, 2544-2551.

94. Mitchell, R. H.; Carruthers, R. J.; Mazuch, L. *J. Am. Chem. Soc.* **1978**, *100*, 1007-1008.

95. Haddon, R. C. *J. Am. Chem. Soc.* **1979**, *101*, 1722-1728.

96. Mitchell, R. H.; Mahadevan, R. *Tetrahedron Lett.* **1981**, 5131-5134.

97. Venugopalan, S. *M.Sc. Thesis*, **1989**, University of Victoria.

98. Lai, Y. L. *J. Am. Chem. Soc.* **1985**, *107*, 6678-6683.

99. Mitchell. R. H.; Zhou, P.; Venugopalan, S.; Dingle, T. W. *J. Am. Chem. Soc.* **1990**, *112*, 7812-7813.

100. Haddon, R. C. *Tetrahedron*, **1972**, *28*, 3613-3633.

101. Woodward, R. B.; Rosenblum, M.; Whiting, M. C. *J. Am. Chem. Soc.* **1952**, *74*, 3458-3459.

102. Ref. 19, pp 130-133.

103. a. Lobanova, I. A.; Zdanovich, V. I. *Russ. Chem. Rev.* **1988**, *57*, 967-980, and references therein. b. Kelly, R. T.; Meghani, P. *J. Org. Chem.* **1990**, *55*, 3684-3688.

104. Jemmis, E. D.; Schleyer, P. VonR. *J. Am. Chem. Soc.* **1982**, *104*, 4781-4788.

105. a. Mitchell. R. H.; Boekelheide, V. *Tetrahedron Lett.* **1970**, 1197-1202. b. Mitchell, R. H.; Boekelheide, V. *J. Am. Chem. Soc.* **1974**, *96*, 1547-1557.

106. Gerson, F.; Heilbronner, E.; Boekelheide, V. *Helv. Chim. Acta.* **1964**, *47*, 1123-1137.

107. Lee, H.; Harevey, , R. G. *J. Org. Chem.* **1982**, *47*, 4364-4367.

108. Metz, G. *Synthesis* **1972**, 612-614.

109. Hopf, H.; Raulfs, F. W. *Isr. J. Chem.* **1985**, *25*, 210-216.

110. a. Gutsche, C. D. *J. Am. Chem. Soc.* **1951**, *73*, 786-792. b. Lednicer, D.; Hauser, C. R. *J. Am. Chem. Soc.* **1958**, *80*, 6364-6367.

111. Normant, J. F.; Foulon, J. P.; Deshayes, H. *Compt. Rend.* **1969**, *269C*, 1325-1328.

112. Wade, L. G.; Acker, K. J.; Earl, R. A.; Osteryoung, R. A. *J. Org. Chem.* **1979**, *44*, 3724-3725.

113. a. Fischer, E. O.; Deus, D. Z. *Naturforsh*, **1953**, *8b*, 694-696. b. Pauson, P. L.; Wilkinson, G. *J. Am. Chem. Soc.* **1954**, *76*, 2024-2026. c. King, R. B.; Bisnette, M. B. *Inorg. Chem.* **1964**, *3*, 796-800.

114. Levanda, C.; Beckgaard, K.; Cowan, D. O.; Mueller-Westerhoff, U. T.; Eilbracht, P.; Candela, G. A.; Collins, R. L. *J. Am. Chem. Soc.* **1976**, *98*, 3181-3187.

115. Bunel, E. E.; Valle, L.; Manriquez, J. M. *Organometallics*, **1985**, *4*, 1680-1682.

116. Buckingham, D. A.; Gorges, R. C; Henry, J. T. *Aust. J. Chem.* **1967**, *20*, 281-296.

117. a. Meister, H. *Angew. Chem.* **1957**, *69*, 533-534. b. Nesmyanov, A. N.; Materilova, R. B.; Branina, E. M.; Kochetkova, N. S. *Izv. Akad. Nauk. SSSR, Ser. Khim.* **1969**, 1323-1326.

118. Chandra, K.; Sharma, R. K.; Garg, A. K.; Garg, B. S. *Chem. Ind.* **1980**, 537.

119. Gill, T. P.; Mann, K. R. *Inorg. Chem.* **1980**, *19*, 3007-3010.

120. Laganis, E. D.; Finke, R. G.; Boekelheide, V. *Pro. Natl. Acad. Sci. U. S. A.* **1981**, *78*, 2657-2658.

121. Johnson, J. W.; Treichel, P. M. *J. Am. Chem. Soc.* **1977**, *99*, 1427-1436.

122. Ustynyuk, N. A.; Pomazanova, N. A.; Novikova, L. N.; Kravtsov, D. N.; Ustynyuk, Y. A. *Izv. Akad. Nauk. SSSR, Ser. Khim.* **1986**, 1688.

123. Webster, O. W. *J. Am. Chem. Soc.* **1966**, *88*, 4055-4060.

124. Bamfield, P.; Cookson, R. C.; Crabtree, A.; Henstock, J.; Judec, J.; Johnson, A. W.; Whitear, B. *Chem. Ind.* **1964**, 1313-1314.

125. a. Oshima, N.; Suzuki, H.; Moroka, Y. *Chem. Lett.* **1984**, 1161-1164. b. Tilley, T. D.; Grubbs, R. H.; Bercaw, J. E. *Organometallics* **1984**, *3*, 274-278. c. Gassman, P. G.; Winter, G. H. *J. Am. Chem. Soc.* **1988**, *110*, 6130-6135.

126. a. Abel, E. W.; Wilkinson, G. *J. Chem. Soc.* **1959**, 1501-1505. b. Lynch, T. J.; Helvenston, M. C. *Organometallics* **1989**, *8*, 1959-1963.

127. Hieber, V. W.; Schropp, W. Z. *Naturforshg.* **1959**, *14b*, 460-461.

128. Yates, K. *Huckel Molecular Orbital Theory;* Academic: New York, *1978;* Chapter III.

129. Stamm, S.; Jackel, H. *J. Am. Chem. Soc.* **1989**, *111*, 6544-6550.

130. Nambu, M.; Siegel, J. S. *J. Am. Chem. Soc.* **1988**, *110*, 3675-3676.

131. Bartlett, P. D.; Wu, C. *J. Am. Chem. Soc.* **1983**, *105*, 100-104.

132. a. Elschenbroich, C.; Schneider, J. *Organometallics* **1986**, *5*, 2091-2096. b. Tori, K.; Anono, K.; Hata, Y.; Muneyuki, R.; Tsuji, T.; Tanida, H. *Tetrahedron Lett.* **1966**, 9-17.

133. Available from Serena Software, Box 3076, Bloomington, In. 47402-3076.

134. Memory, J. D. *J. Magn. Reson.* **1977**, *27*, 241-244.

135. Dailey, B. P.; Gawer, A.; Neikam, W. C. *Discuss. Faraday Soc.* **1962**, *34*, 18-24.

136. Rhine, W. E.; Stucky, G. D. *J. Am. Chem. Soc.* **1975**, *97*, 737-743.

137. Mitchell, R. H.; Venugopalan, S.; Zhou, P.; Dingle, T. W. *Tetrahedron Lett.* **1990**, 5281-5284.

138. a. Bauer, R. A.; Fischer, E. O.; Kreiter, C. G. *J. Org. Chem.* **1970**, *24*, 737-751. b. Elschenbroich, C.; Mockel, R.; Massa, W.; Birkham, M.; Zenneck, U. *Chem. Ber.* **1982**, *115*, 334-345. c. Mutterties, E. L.; Blecke, J. R.; Wucherer, E. J. *Chem. Rev.* **1982**, *82*, 499-525.

139. a. Mitchell, R. H.; Vinod, T. K.; Bodwell, G.; Bushnell, G. W. *J. Org. Chem.* **1989**, *54*, 5871-5879. b. Mori, N.; Kakamori, M. *Magn. Reson. Chem.* **1986**, *24*, 151-155. c. Koray, A. R.; Zahn, T.; Ziegler, M. L. *J. Organomet. Chem.* **1985**, *291*, 53-60. d. Swann, R. T.; Boekelheide, V. *J. Organomet. Chem.* **1982**, *231*, 143-149.

140. Bailey, M. F.; Dahl, L. F. *Inorg. Chem.* **1965**, *4*, 1314-1319.

141. Elschenbroich, C.; Koch, J.; Schneider, J.; Spangenberg, B. *J. Organomet. Chem.* **1986**, *317*, 41-54.

142. Lauterbur, P. C.; King, R. B. *J. Am. Chem. Soc.* **1965**, *87*, 3266-3267.

143. Fagan, P. J.; Ward, M. D.; Calabrese, J. C. *J. Am. Chem. Soc.* **1989**, *111*, 1698-1719.

144. Graves, V.; Lagowski, J. J. *J. Organomet. Chem.* **1976**, *120*, 397-405.

145. Nesmeyanov, A. N.; Vokenau, N. A.; Shulpina, L. S. *J. Organomet. Chem.* **1979**, *182*, C36-38.

146. Ohno, H.; Horita, H.; Otsubo, T.; Sakata, Y.; Misumi, S. *Tetrahedron Lett.* **1977**, 265-268.

147. Kaneda, T.; Otsubo, T.; Horita, H.; Misumi, S. *Bull. Chem. Soc. Jpn.* **1980**, *53*, 1015-1018.

148. McGlinchy, M. J.; Burns, R. C.; Hofer, R.; Top, S.; Jaouen, G. *Organometallics* **1986**, *5*, 104-109.

149. McConnell, H. M. *J. Chem. Phys.* **1957**, *27*, 226-229.

150. Keller, L. S. *Tetrahedron Lett.* **1978**, 2361-2362.

151. Emerson, G. F.; Watts, L.; Pettit, R. *J. Am. Chem. Soc.* **1965**, *87*, 131-133.

152. Fischer, E. O.; Ruhle, H.; Vogel, E.; Grimme, E. *Angew. Chem., Int. Ed. Engl.* **1966**, *5*, 518-519.

153. Hilken, G.; Kinkel, T.; Schwanbom, M.; Lex, J.; Schmickler, H.; Vogel, E. *Angew. Chem., Int. Ed. Engl.* **1982**, *21*, 784-785.

154. Mues, P.; Benn, R.; Kruger, C.; Tsay, Y. H.; Vogel, E.; Wilke, G. *Angew. Chem., Int. Ed. Engl.* **1982**, *21*, 868.

155. Baikie, P. E.; Mills, O. S. *J. Chem. Soc. (A)* **1969**, 328-333.

156. Frydman, L.; Frydman, B.; Kustanovich, I.; Vega, S.; Vogel, E.; Yannoni, C. *J. Am. Chem. Soc.* **1990**, *112*, 6472-6476.

157. Richie, G. L.; Cooper, M. K.; Calvert, R. L.; Dennis, G. R.; Philips, L.; Vrbancich, J. *J. Am. Chem. Soc.* **1983**, *105*, 5215-5219.

158. Mulay, L. N.; Mulay, I. L. *Anal. Chem.* **1966**, *38*, 501R-513R.

159. Turbitt, T. D.; Watts, W. E. *Tetrahedron* **1972**, *28*, 1227-1235.

160. Mulay, L. N.; Fox, M. E. *J. Chem. Phys.* **1963**, *38*, 760-764.

161. Paquette, L. A.; Schirch, P. F.; Hathaway, S. J.; Hsu, L. H.; Gallucci, J. C. *Organometallics* **1986**, *5*, 490-499.

162. Egger, H.; Nikiforov, A. *Monatsh. Chem.* **1969**, *100*, 242-253.

163. Rees, B.; Coppens, P. *Acta. Crystallogr.* **1973**, *B29*, 2516-2528.

164. Trotter, J. *Acta. Crystallogr.* **1958**, *11*, 355-360.

165. Webb, N. C.; Marsh, R. E. *Acta. Crystallogr.* **1967**, *22*, 382-387.

166. Shakir, R.; Atwood, J. L. *Acta. Crystallogr.* **1981**, *B37*, 1656-1659.

167. McCague, R.; Moody, C. J.; Rees, C. W.; Williams, D. J. *J. Chem. Soc., Perkin Trans. 1* **1984**, 909-914.

168. Bianchi, R.; Pilati, T.; Simonetta, M. *Acta Crystallogr.* **1980**, *B36*, 3146-3148.

169. Bailey, N. A.; Mason, R. *Proc. Roy. Soc.* **1966**, *A290*, 94-114.

170. Vogel, E.; Schieb, T.; Schulz, W. H.; Schmidt, K.; Schmickler, H.; Lex, J. *Angew. Chem., Int. Ed. Engl.* **1986**, *25*, 723-725.

171. Hanson, A. W. *Acta. Crystallogr.* **1967**, *23*, 476-481.

APPENDIX

Supplementary crystal structure data for **32**

TABLE 1.

Fractional atomic coordinates and temperature parameters.

Atom	x/a	y/b	z/c	Ueq
C(1)	-1232(10)	-3043(9)	1522(4)	72(3)
C(2)	684(10)	-2457(9)	1819(5)	79(4)
C(3)	2286(9)	-941(9)	1441(4)	68(3)
C(4)	2142(7)	55(8)	674(4)	61(3)
C(5)	3669(8)	1645(8)	274(4)	68(3)
C(13)	-3425(8)	-2622(8)	481(4)	67(3)
C(14)	-1547(8)	-2167(7)	785(4)	62(3)
C(15)	228(7)	-799(7)	136(4)	56(2)
C(16)	544(10)	-2161(10)	-907(5)	65(3)
C(21)	3360(9)	5221(13)	3253(5)	80(4)
C(22)	4243(9)	7212(13)	3353(5)	85(4)
C(23)	3517(8)	8424(11)	4075(5)	79(3)
C(24)	1875(7)	7603(8)	4784(4)	60(2)
C(25)	1006(10)	8675(10)	5516(5)	74(3)
C(33)	650(9)	2221(10)	3819(5)	75(3)
C(34)	1697(7)	4236(9)	3907(4)	63(3)
C(35)	1138(6)	5450(7)	4881(3)	49(2)
C(36)	2202(9)	5342(11)	5803(5)	64(3)
H(1)	-231(8)	-405(7)	185(4)	8(2)'
H(2)	92(8)	-307(8)	243(5)	10(2)'
H(3)	367(7)	-8(6)	167(3)	6(1)'
H(5)	497(7)	212(7)	59(4)	7(1)'
H(13)	-448(7)	-360(7)	79(4)	7(1)'
H(161)	78(7)	-331(8)	-75(4)	8(2)'
H(162)	151(8)	-138(8)	-134(4)	8(2)'
H(163)	-44(9)	-271(9)	-140(5)	11(2)'
H(21)	367(6)	434(7)	266(4)	7(1)'
H(22)	545(11)	792(10)	292(6)	16(3)'
H(23)	412(9)	993(9)	412(5)	11(2)'
H(25)	156(6)	995(7)	556(3)	5(1)'
H(33)	88(8)	137(9)	329(5)	9(2)'
H(361)	178(6)	394(7)	587(3)	6(1)'
H(362)	194(6)	615(6)	650(4)	6(1)'
H(363)	350(7)	607(6)	569(3)	6(1)'

Estimated standard deviations are given in parentheses.

Coordinates $x10^{n}$ where n = 5,4,4,4 for P,O,N,C.

Temperature parameters $x10^{n}$ where n = 4,3,3,3 for P,O,N,C.

U_{eq} = the equivalent isotropic temperature parameter.

$$U_{eq} = 1/3 \sum_i \sum_j U_{ij} a_i^* a_j^* (a_i . a_j)$$

Primed values indicate that U_{iso} is given

$$T = \exp-(8\pi^2 U_{iso} \sin^2\theta/\lambda^2)$$

TABLE 2.

Interatomic distances (A).

Atoms		Distance
C(2)	-C(1)	1.403(8)
C(14)	-C(1)	1.358(7)
C(3)	-C(2)	1.360(8)
C(4)	-C(3)	1.396(7)
C(5)	-C(4)	1.378(6)
C(15)	-C(4)	1.516(7)
C(14)	-C(13)	1.399(7)
C(15)	-C(14)	1.530(6)
C(16)	-C(15)	1.582(7)
C(15)	-C(15)	1.506(9)
C(22)	-C(21)	1.354(9)
C(34)	-C(21)	1.390(7)
C(23)	-C(22)	1.396(9)
C(24)	-C(23)	1.393(7)
C(25)	-C(24)	1.393(8)
C(35)	-C(24)	1.509(6)
C(34)	-C(33)	1.379(7)
C(35)	-C(34)	1.521(6)
C(36)	-C(35)	1.562(6)
C(35)	-C(35)	1.545(8)

Estimated standard deviations are given in parentheses.

TABLE 3.

Bond angles (d).

Atoms			Angle	Atoms			Angle
C(14)	-C(1)	-C(2)	120.5(6)	C(34)	-C(21)	-C(22)	121.7(6)
C(3)	-C(2)	-C(1)	122.7(6)	C(23)	-C(22)	-C(21)	123.2(6)
C(4)	-C(3)	-C(2)	121.7(5)	C(24)	-C(23)	-C(22)	120.1(7)
C(5)	-C(4)	-C(3)	125.5(5)	C(25)	-C(24)	-C(23)	124.6(6)
C(15)	-C(4)	-C(3)	118.0(5)	C(35)	-C(24)	-C(23)	118.4(5)
C(15)	-C(4)	-C(5)	116.1(5)	C(35)	-C(24)	-C(25)	116.5(5)
C(13)	-C(14)	-C(1)	123.6(5)	C(33)	-C(34)	-C(21)	125.3(6)
C(15)	-C(14)	-C(1)	119.4(5)	C(35)	-C(34)	-C(21)	117.4(6)
C(15)	-C(14)	-C(13)	116.5(5)	C(35)	-C(34)	-C(33)	116.8(5)
C(14)	-C(15)	-C(4)	113.3(4)	C(34)	-C(35)	-C(24)	114.2(4)
C(16)	-C(15)	-C(4)	105.9(4)	C(36)	-C(35)	-C(24)	106.5(4)
C(16)	-C(15)	-C(14)	105.2(4)	C(36)	-C(35)	-C(34)	105.5(4)

TABLE 4.

Selected intermolecular distances (A).

Atoms	Distance	Sym	Tx	Ty	Tz
C(15) ...C(1)	3.691	-1	0	0	0
C(22) ...C(2)	3.674	1	0	1	0
C(23) ...C(2)	3.653	1	0	1	0
C(5) ...C(3)	3.628	-1	1	0	0
C(13) ...C(4)	2.446	-1	0	0	0
C(14) ...C(4)	2.885	-1	0	0	0
C(15) ...C(4)	2.496	-1	0	0	0
C(16) ...C(4)	3.015	-1	0	0	0
C(13) ...C(5)	1.406	-1	0	0	0
C(14) ...C(5)	2.444	-1	0	0	0
C(15) ...C(5)	2.823	-1	0	0	0
C(16) ...C(5)	3.305	-1	0	0	0
C(13) ...C(13)	3.468	-1	-1	-1	0
C(15) ...C(13)	2.823	-1	0	0	0
C(16) ...C(13)	3.321	-1	0	0	0
C(15) ...C(14)	2.489	-1	0	0	0
C(16) ...C(14)	3.018	-1	0	0	0
C(16) ...C(15)	2.539	-1	0	0	0
C(23) ...C(23)	3.353	-1	1	2	1
C(33) ...C(24)	2.424	-1	0	1	1
C(34) ...C(24)	2.868	-1	0	1	1
C(35) ...C(24)	2.499	-1	0	1	1
C(36) ...C(24)	3.020	-1	0	1	1
C(25) ...C(25)	3.515	-1	0	2	1
C(33) ...C(25)	1.377	-1	0	1	1
C(34) ...C(25)	2.419	-1	0	1	1
C(35) ...C(25)	2.824	-1	0	1	1
C(36) ...C(25)	3.311	-1	0	1	1
C(35) ...C(33)	2.812	-1	0	1	1
C(36) ...C(33)	3.309	-1	0	1	1
C(35) ...C(34)	2.500	-1	0	1	1
C(36) ...C(34)	3.032	-1	0	1	1
C(36) ...C(35)	2.569	-1	0	1	1

The symmetry positions are for the second atom.
They are defined:

A negative symmetry position denotes inversion.
The translations (T) are applied finally.

TABLE S1.

Hydrogen atom fractional atomic coordinates and isotropic temperature parameters.

Atom	x/a	y/b	z/c	Uiso
H(1)	-231(8)	-405(7)	185(4)	8(2)
H(2)	92(8)	-307(8)	243(5)	10(2)
H(3)	367(7)	-8(6)	167(3)	6(1)
H(5)	497(7)	212(7)	59(4)	7(1)
H(13)	-448(7)	-360(7)	79(4)	7(1)
H(161)	78(7)	-331(8)	-75(4)	8(2)
H(162)	151(8)	-138(8)	-134(4)	8(2)
H(163)	-44(9)	-271(9)	-140(5)	11(2)
H(21)	367(6)	434(7)	266(4)	7(1)
H(22)	545(11)	792(10)	292(6)	16(3)
H(23)	412(9)	993(9)	412(5)	11(2)
H(25)	156(6)	995(7)	556(3)	5(1)
H(33)	88(8)	137(9)	329(5)	9(2)
H(361)	178(6)	394(7)	587(3)	6(1)
H(362)	194(6)	615(6)	650(4)	6(1)
H(363)	350(7)	607(6)	569(3)	6(1)

Estimated standard deviations are given in parentheses.

Coordinates $x10^{n}$, temperature parameters $x10^{n}$.

$T = \exp-(8\pi^2 U_{iso} \sin^2\theta/\lambda^2)$

TABLE S2.

Anisotropic temperature parameters (&2).

Atom	U11	U22	U33	U23	U13	U12
C(1)	78(4)	78(4)	66(4)	19(3)	8(3)	38(4)
C(2)	99(5)	94(5)	65(4)	17(3)	-4(3)	57(4)
C(3)	64(4)	91(4)	63(3)	13(3)	-6(3)	44(4)
C(4)	54(3)	71(4)	64(3)	4(3)	-4(2)	34(3)
C(5)	60(4)	73(4)	70(4)	5(3)	2(3)	31(3)
C(13)	51(3)	73(4)	68(3)	12(3)	3(3)	20(3)
C(14)	66(3)	62(3)	63(3)	10(3)	1(3)	33(3)
C(15)	51(3)	63(3)	61(3)	14(2)	4(2)	29(3)
C(16)	74(4)	68(4)	59(3)	-4(3)	2(3)	42(3)
C(21)	65(4)	125(6)	62(4)	17(4)	5(3)	51(4)
C(22)	55(4)	124(7)	72(4)	30(4)	-5(3)	26(4)
C(23)	69(4)	89(5)	76(4)	31(4)	-22(3)	16(4)
C(24)	54(3)	64(4)	63(3)	15(3)	-17(2)	18(3)
C(25)	87(4)	51(4)	90(4)	7(3)	27(4)	27(4)
C(33)	84(4)	81(5)	77(4)	-1(4)	-11(3)	52(4)
C(34)	55(3)	81(4)	63(3)	11(3)	-9(2)	37(3)
C(35)	44(2)	60(3)	49(3)	9(2)	-11(2)	24(2)
C(36)	47(3)	85(5)	66(4)	19(3)	-9(3)	27(3)

Estimated standard deviations are given in parentheses.

U values $x10^{n}$ where n=4,3,3 for S,C,N.

$T = \exp-2\pi^2(U_{11}h^2a^{*2} + \ldots + 2U_{23}klb^*c^* + \ldots)$

TABLE S2.

Interatomic distances for the hydrogen atoms (A).

Atoms	Distance	Atoms	Distance
H(1) -C(1)	0.948(48)	H(21) -C(21)	0.981(46)
H(2) -C(2)	1.059(60)	H(22) -C(22)	0.981(72)
H(3) -C(3)	1.017(44)	H(23) -C(23)	1.029(59)
H(5) -C(5)	1.004(48)	H(25) -C(25)	0.870(42)
H(13) -C(13)	0.917(45)	H(33) -C(33)	0.896(59)
H(161)-C(16)	1.017(55)	H(361)-C(36)	0.993(46)
H(162)-C(16)	0.902(51)	H(362)-C(36)	1.023(46)
H(163)-C(16)	0.948(69)	H(363)-C(36)	0.893(45)

Estimated standard deviations are given in parentheses.

U values $\times 10^{n}$ where n=4,3,3 for S,C,N.

$T = \exp -2\pi^2(U_{11}h^2a^{*2} + \ldots + 2U_{23}klb^*c^* + \ldots)$

TABLE 3S.

Bond angles involving H atoms (d).

Atoms	Angle	Atoms	Angle
H(1) -C(1) -C(2)	119.0(30)	H(21) -C(21) -C(22)	124.5(26)
H(1) -C(1) -C(14)	120.5(31)	H(21) -C(21) -C(34)	113.0(27)
H(2) -C(2) -C(1)	120.8(30)	H(22) -C(22) -C(21)	122.5(44)
H(2) -C(2) -C(3)	116.1(30)	H(22) -C(22) -C(23)	114.3(44)
H(3) -C(3) -C(2)	135.0(24)	H(23) -C(23) -C(22)	123.7(33)
H(3) -C(3) -C(4)	102.3(24)	H(23) -C(23) -C(24)	116.3(33)
H(5) -C(5) -C(4)	115.4(27)	H(25) -C(25) -C(24)	118.0(28)
H(13) -C(13) -C(14)	116.7(30)	H(33) -C(33) -C(34)	123.8(36)
H(161)-C(16) -C(15)	112.9(27)	H(361)-C(36) -C(35)	108.6(27)
H(162)-C(16) -C(15)	107.7(36)	H(362)-C(36) -C(35)	111.5(24)
H(162)-C(16) -H(161)	114.6(44)	H(362)-C(36) -H(361)	112.6(35)
H(163)-C(16) -C(15)	118.7(37)	H(363)-C(36) -C(35)	108.1(29)
H(163)-C(16) -H(161)	106.0(47)	H(363)-C(36) -H(361)	117.8(40)
H(163)-C(16) -H(162)	96.0(47)	H(363)-C(36) -H(362)	98.0(37)

Estimated standard deviations are given in parentheses.

TORSION ANGLES ON DMD

A	B	C	ALPHA	BETA	GAMMA
7.4950	7.5930	12.8590	101.1000	80.9200	115.4100

LABEL	X	Y	Z
C1	-0.123230	-0.304260	0.152170
C1	0.000960	0.000900	0.000430
C2	0.068450	-0.245730	0.181910
C2	0.000990	0.000940	0.000460
C3	0.228600	-0.094060	0.144090
C3	0.000870	0.000910	0.000400
C4	0.214240	0.005540	0.067360
C4	0.000710	0.000760	0.000390
C5	0.366950	0.164490	0.027410
C5	0.000850	0.000820	0.000430
C13	-0.342510	-0.262200	0.048070
C13	0.000800	0.000850	0.000430
C14	-0.154720	-0.216650	0.078480
C14	0.000770	0.000740	0.000390
C15	0.022750	0.079890	0.013630
C15	0.000650	0.000670	0.000360
C16	0.054430	-0.216150	-0.090670
C16	0.000990	0.000980	0.000470
C5'	-0.366950	-0.164490	-0.027410
C5'	0.000850	0.000820	0.000430
C13'	0.342510	0.262200	-0.048070
C13'	0.000800	0.000850	0.000430
C15'	-0.022750	0.079890	-0.013630
C15'	0.000650	0.000670	0.000360
H1	-0.230740	-0.404850	0.184990
H1	0.007570	0.007140	0.003860
H2	0.092390	-0.307050	0.242910
H2	0.007990	0.008100	0.004620
H3	0.367150	-0.007780	0.167200
H3	0.006770	0.006340	0.003370
H5	0.496540	0.211910	0.059130
H5	0.007260	0.006640	0.003620
H13	-0.447730	-0.359570	0.079040
H13	0.007130	0.006880	0.003610
H161	0.077590	-0.330860	-0.075240
H161	0.006970	0.007600	0.003650
H162	0.150950	-0.138280	-0.133810
H162	0.008150	0.007770	0.004210
H163	-0.043530	-0.270790	-0.140020
H163	0.009290	0.009110	0.005130

TORSION ANGLES

C5'	C15	C14	C1	178.9176	0.5615
H13	C13	C14	C1	1.9064	2.7239
C13	C14	C1	H1	1.7567	2.5101
C13	C14	C1	C2	177.4476	0.5717
C14	C1	C2	C3	3.6998	0.9749
H1	C1	C2	H2	175.9677	3.7980
C1	C2	C3	H3	175.5159	3.6305
C1	C2	C3	C4	161.7257	4.0857
H2	C2	C3	C4	4.2478	0.9816
C2	C3	C4	C5	176.8484	3.6413
H3	C3	C4	C5	177.6841	0.6046
C3	C4	C5	C15	9.6901	0.8618
C3	C4	C5	C15	179.5884	2.3608
H5	C4	C5	C5	7.7845	2.8187
C3	C4	C5	C13'	178.3683	0.5769
C3	C4	C15	C15'	146.9246	0.4942
H161	C16	C15	C14	22.0635	0.7110
H162	C16	C15	C15'	176.6479	2.6581
H163	C16	C15	C15'	55.8641	4.6750
H161	C16	C15	C5	51.6062	4.5237
H162	C16	C15	C4	82.5662	2.6850
H163	C16	C15	C4	64.9224	4.6793
H161	C16	C15	C4	172.3927	4.5079
H162	C16	C15	C14	57.7200	2.7041
H163	C16	C15	C14	174.7913	4.6587
C4	C15	C14	C13	67.3210	4.5380
C4	C15	C14	C1	164.7599	0.4939
C1	C14	C15	C15'	22.8926	0.6973
C13	C14	C15	C15'	148.3879	0.4868
C5'	C13	C14	C15	39.2649	0.5788
H13	C13	C14	C15	9.0875	0.7846
				170.0885	3.4271

TOTAL NO OF ATOMS 20
MEANPLANE ON DMD 9FEB89

ORIGINAL COORDINATES AND THEIR E.S.D.S

ATOM NO.	X/A	Y/B	Z/C	SYG X/A	SYG Y/B	SYG Z/C
C1	-0.12323	-0.30426	0.15217	0.00096	0.00090	0.00043
C2	0.06845	-0.24573	0.18191	0.00099	0.00094	0.00046
C3	0.22860	-0.09406	0.14409	0.00087	0.00091	0.00040
C4	0.21424	0.00554	0.06736	0.00071	0.00076	0.00039
C5	0.36695	0.16449	0.02741	0.00085	0.00082	0.00043
C13	-0.34251	-0.26220	0.04807	0.00080	0.00085	0.00043
C14	-0.15472	-0.21665	0.07346	0.00077	0.00074	0.00039
C15	0.02275	-0.07989	0.01363	0.00065	0.00067	0.00036
C16	0.05443	-0.21615	-0.09067	0.00099	0.00098	0.00047
C5'	-0.36695	-0.16449	-0.02741	0.00085	0.00082	0.00043
C13'	0.34251	0.26220	-0.04807	0.00080	0.00085	0.00043
C15'	-0.02275	0.07989	-0.01363	0.00065	0.00067	0.00036
H1	-0.23074	-0.40485	0.18499	0.00757	0.00714	0.00386
H2	0.09239	-0.30705	0.24291	0.00799	0.00819	0.00462
H3	0.36715	-0.00778	0.16720	0.00677	0.00634	0.00337
H5	0.49654	0.21191	0.05913	0.00726	0.00664	0.00362
H13	-0.44773	-0.35957	0.07904	0.00713	0.00688	0.00361
H161	0.07759	-0.33086	-0.07524	0.00697	0.00760	0.00365
H162	0.15095	-0.13824	-0.13381	0.00815	0.00777	0.00421
H163	-0.04353	-0.27079	-0.14002	0.00929	0.00911	0.00513

MEANPLANE ON DMD 9FEB89

PLANE 1 IS (0.3622)X + (-0.5633)Y + (-0.7326)Z - (0.0795) = 0

CHI SQUARED = 19.7452

ATOMS IN PLANE

ATOM NO.	X	Y	Z	P	ESD(P)	P/ESD(P)
C1	0.3765	-2.3571	1.9132	-0.0094	0.0061	1.556
C2	1.6828	-2.0085	2.2871	0.0195	0.0064	3.057
C3	2.3122	-0.9011	1.8116	-0.0153	0.0058	2.642
C4	1.7244	-0.0817	0.8469	0.0051	0.0052	0.973
C14	-0.2945	-1.6253	0.9367	0.0006	0.0052	0.116
			SUM OF P(I)	0.0005		

OTHER ATOMS

C5	2.2700	1.0794	0.3446	-0.0724	0.0057	12.697
C13	-1.6153	-1.8837	0.6044	-0.0786	0.0058	13.651
C15	0.4585	-0.5721	0.1714	0.2924	0.0047	62.258
C16	0.9282	-1.3214	-1.1400	1.8546	0.0056	332.906
C5'	-2.2700	-1.0794	-0.3446	-0.0866	0.0057	15.081
C13'	1.6153	1.8837	-0.6044	-0.0804	0.0058	13.975
C15'	-0.4585	0.5721	-0.1714	-0.4515	0.0047	96.113
H1	-0.0350	-3.1053	2.3259	-0.0475	0.0510	0.933
H2	2.1858	-2.5375	3.0541	-0.0521	0.0587	0.887
H3	3.1164	-0.3504	2.1022	-0.2310	0.0440	5.140
H5	3.1511	1.3483	0.7434	-0.1792	0.0479	3.744
H13	-2.0233	-2.6065	0.9933	-0.1123	0.0482	2.340
H161	1.5065	-2.1355	-0.9460	2.3923	0.0500	47.823
H162	1.3104	-0.7106	-1.6824	2.0540	0.0554	37.061
H163	0.2719	-1.6054	-1.7605	2.2200	0.0660	33.659

MEANPLANE ON DMD 9FE989

PLANE 2 IS (0.3837)X + (-0.5635)Y + (-0.7316)Z - (0.0813) = 0

CHI SQUARED = 47.1953

ATOMS IN PLANE

ATOM NO.	X	Y	Z	P	ESD(P)	P/ESD(P)
C1	0.3765	-2.3571	1.9132	-0.0059	0.0061	1.471
C2	1.6826	-2.0085	2.2871	0.0233	0.0064	3.478
C3	2.3122	-0.9011	1.8116	-0.0113	0.0058	2.133
C4	1.7244	-0.0617	0.8469	0.0061	0.0052	1.168
C14	-0.2945	-1.6253	0.9867	-0.0009	0.0052	0.171
H1	-0.0350	-3.1053	2.3259	-0.0471	0.0510	0.924
H2	2.1856	-2.5375	3.0541	-0.0473	0.0537	0.814
H3	3.1164	-0.3504	2.1022	-0.2287	0.0450	5.043
			SUM OF P(I)	-0.3193		

OTHER ATOMS

C5	2.2700	1.0794	0.3446	-0.0213	0.0057	12.412
C13	-1.6153	-1.8837	0.6044	-0.0833	0.0058	14.295
C15	0.4585	-0.5721	0.1714	0.2811	0.0047	61.952
C16	0.9282	-1.3214	-1.1400	1.8589	0.0066	282.576
C5'	-2.2700	-1.0794	-0.3446	-0.0234	0.0057	16.076
C13'	1.6153	1.8837	-0.6044	-0.0814	0.0058	14.131
C15'	-0.4585	0.5721	-0.1714	-0.4483	0.0047	96.790
H5	3.1511	1.3483	0.7434	-0.1765	0.0479	3.687
H13	-2.0238	-2.6065	0.9938	-0.1136	0.0482	2.419
H161	1.5068	-2.1355	-0.9460	2.3917	0.0500	47.802
H162	1.3104	-0.7106	-1.6824	2.0932	0.0554	37.017
H163	0.2719	-1.6084	-1.7605	2.2283	0.0660	33.603

ANGLES BETWEEN NORMALS TO PLANES

PLANE(1)	DIRECTION COSINES			PLANE(2)	DIRECTION COSINES			ANGLE
1	0.3822	-0.5633	-0.7326	2	0.3837	-0.5635	-0.7316	0.11

TORSION ANGLES ON DMD

A	B	C	ALPHA	BETA	GAMMA
7.4950	7.5930	12.8590	101.1000	80.9200	115.4100

LABEL	X	Y	Z
C21	0.336010	0.522080	0.325310
C21	0.000870	0.001340	0.000470
C22	0.424330	0.721190	0.335320
C22	0.000890	0.001270	0.000500
C23	0.351660	0.842430	0.407510
C23	0.000850	0.001140	0.000490
C24	0.187490	0.760330	0.478400
C24	0.000680	0.000760	0.000390
C25	0.100630	0.867530	0.551650
C25	0.000970	0.000970	0.000480
C33	0.064990	0.222050	0.381940
C33	0.000900	0.001010	0.000520
C34	0.169650	0.423570	0.390660
C34	0.000720	0.000680	0.000370
C35	0.113810	0.544980	0.488060
C35	0.000590	0.000660	0.000320
C36	0.220210	0.534200	0.580280
C36	0.000870	0.001080	0.000460
C25'	-0.100630	0.132470	0.448350
C25'	-0.000940	0.000970	0.000480
C33'	-0.064990	0.777950	0.618060
C33'	0.000900	0.001010	0.000520
C35'	-0.113810	0.455020	0.511940
C35'	0.000590	0.000660	0.000320
H21	0.367170	0.433990	0.266220
H21	0.006440	0.006590	0.003720
H22	0.545410	0.792470	0.291940
H22	0.011220	0.010480	0.005620
H23	0.412470	0.993310	0.412100
H23	0.009530	0.009300	0.004590
H25	0.155870	0.995220	0.555900
H25	0.006130	0.006670	0.003070
H33	0.088320	0.137480	0.328600
H33	0.008170	0.008790	0.004530
H361	0.177640	0.393610	0.587500
H361	0.006480	0.007290	0.003340
H362	0.194290	0.615020	0.649620
H362	0.005940	0.006080	0.003750
H363	0.349930	0.607220	0.568810
H363	0.007130	0.006440	0.003330

TORSION ANGLES

C25'	C33	C34	C21	179.2038	0.7621
H33	C33	C34	C21	6.6930	5.6991
C33	C34	C21	H21	5.3706	3.8974
C33	C34	C21	C22	176.3191	0.7561
C34	C21	C22	C23	3.0388	1.2416
C34	C21	C22	H22	177.0553	6.1844
H21	C21	C22	C23	166.7767	4.0422
C21	C22	C23	H23	175.7306	4.7244
C21	C22	C23	C24	4.0359	1.1840
H22	C22	C23	C24	174.0974	5.4785
C22	C23	C24	C25	178.3743	0.6905
C22	C23	C24	C35	10.3883	0.9307
H23	C23	C24	C35	169.8287	4.3736
H23	C23	C24	C33	1.4063	4.4779
C23	C24	C25	C33'	178.2776	0.6992
C23	C24	C33	C35'	146.9369	0.4916
C23	C24	C33	C34	23.8471	0.7010
H361	C36	C33	C35'	61.6982	2.8722
H362	C36	C33	C35'	69.9320	2.2523
H363	C36	C33	C35'	169.4972	3.3316
H361	C36	C33	C24	178.4756	2.2428
H362	C36	C33	C24	56.8948	2.2159
H363	C36	C33	C24	49.6703	3.3647
H361	C36	C33	C34	56.7681	3.3571
H362	C36	C33	C34	178.6032	2.1915
H363	C36	C33	C34	72.0367	3.3562
C24	C35	C34	C33	163.0294	0.5789
C24	C35	C34	C21	24.5479	0.8044
C21	C34	C35	C35'	147.9742	0.6134
C33	C34	C35	C35'	39.6077	0.7623
C25'	C33	C34	C35	9.0460	1.0658
H33	C33	C34	C35	178.4443	5.0281

TOTAL NO OF ATOMS 20
MEANPLANE ON DMD 9FEB89

ATOM NO.	ORIGINAL COORDINATES AND THEIR E.S.D.S X/A	Y/B	Z/C	SYG X/A	SYG Y/B	SYG Z/C
C21	0.33601	0.52205	0.32531	0.00087	0.00134	0.00047
C22	0.42433	0.72119	0.33532	0.00089	0.00127	0.00050
C23	0.35.66	0.84243	0.40751	0.00085	0.00114	0.00049
C24	0.15749	0.76033	0.47840	0.00066	0.00076	0.00039
C25	0.10063	0.56753	0.55165	0.00097	0.00097	0.00045
C33	0.06499	0.22205	0.38194	0.00090	0.00101	0.00052
C34	0.16965	0.42[illegible]7	0.39066	0.00072	0.00088	0.00037
C35	0.11381	0.54498	0.48606	0.00059	0.00066	0.00032
C36	0.22021	0.53420	0.58028	0.00087	0.00108	0.00046
C25'	-0.10063	0.13247	0.44835	0.00096	0.00097	0.00048
C33'	-0.06499	0.77795	0.61806	0.00090	0.00101	0.00052
C35'	-0.11381	0.45502	0.51194	0.00059	0.00066	0.00032
H21	0.36717	0.43399	0.26622	0.00644	0.00659	0.00372
H22	0.54541	0.79247	0.29194	0.01122	0.01048	0.00562
H23	0.41247	0.99331	0.41210	0.00853	0.00930	0.00459
H25	0.15587	0.99522	0.55590	0.00613	0.00667	0.00307
H33	0.08832	0.13748	0.32360	0.00817	0.00879	0.00453
H361	0.17764	0.39361	0.58750	0.00648	0.00729	0.00334
H362	0.19429	0.61502	0.64962	0.00594	0.00608	0.00375
H363	0.34993	0.60722	0.56881	0.00713	0.00644	0.00333

MEANPLANE ON DMD 9FEB89

PLANE 1 IS (-0.7462)X + (0.0638)Y + (-0.6627)Z - (-3.6263) = 0

CHI SQUARED = 14.1334

ATOMS IN PLANE ATOM NO.	X	Y	Z	P	ESD(P)	P/ESD(P)
C21	1.4776	3.0027	4.0901	0.0050	0.0071	0.706
C22	1.5111	4.3505	4.2160	-0.0174	0.0072	2.398
C23	0.7179	5.0537	5.1236	0.0179	0.0069	2.589
C24	-0.1012	4.3647	6.0149	-0.0055	0.0054	1.030
C34	0.6343	2.2109	4.9117	0.0019	0.0055	0.348
			SUM OF P(I)	0.0019		
OTHER ATOMS						
C25	-0.9528	4.9696	6.9359	0.0583	0.0072	8.103
C33	0.5387	0.8443	4.8021	0.0959	0.0071	13.442
C35	0.0678	2.8706	6.1363	-0.3075	0.0046	67.280
C36	1.0876	2.6328	7.2958	-1.8520	0.0068	273.150
C25'	-0.2760	0.1119	5.6371	0.1038	0.0071	14.520
C33'	-1.7675	4.2374	7.7708	0.0661	0.0071	9.260
C35'	-1.2966	2.2111	6.4366	0.4696	0.0046	102.734
H21	1.8782	2.5035	3.3472	0.1665	0.0505	3.295
H22	2.0983	4.9164	3.6705	-0.0580	0.0829	0.700
H23	0.6914	6.0804	5.1813	0.0650	0.0657	0.989
H25	-0.9462	5.8380	6.9893	0.0733	0.0461	1.592
H33	0.8809	0.3591	4.1315	0.2541	0.0635	4.002
H361	1.2412	1.6557	7.3866	-2.0891	0.0494	42.313
H362	0.7707	3.0639	8.1676	-2.1657	0.0484	44.792
H363	1.7986	3.1540	7.1516	-2.2537	0.0514	43.875

MEANPLANE ON DHD 9FE589

PLANE 2 IS (-0.7469)X + (0.0640)Y + (-0.6618)Z - (-3.6213) = 0

CHI SQUARED = 26.3516

ATOMS IN PLANE ATOM NO.	X	Y	Z	P	ESD(P)	P/ESD(P)
C21	1.4776	3.0027	4.0901	0.0029	0.0071	0.404
C22	1.5111	4.3505	4.2160	-0.0193	0.0073	2.656
C23	0.7179	5.0537	5.1236	0.0175	0.0069	2.529
C24	-0.1012	4.3647	6.0149	-0.0047	0.0054	0.869
C34	0.6843	2.2199	4.9117	0.0010	0.0055	0.174
H21	1.8782	2.5035	3.3472	0.1634	0.0506	3.232
H22	2.0983	4.9164	3.6705	-0.0607	0.0829	0.732
H23	0.6914	6.0804	5.1613	0.0645	0.0657	0.986
			SUM OF P(I)	0.1648		
OTHER ATOMS						
C25	-0.9528	4.9698	6.9359	0.0606	0.0072	8.429
C33	0.5387	0.8443	4.8021	0.0946	0.0071	13.280
C35	0.0678	2.8706	6.1363	-0.3069	0.0046	67.127
C36	1.0876	2.6328	7.2958	-1.8511	0.0068	272.953
C25'	-0.2760	0.1119	5.6371	0.1039	0.0071	14.527
C33'	-1.7675	4.2374	7.7708	0.0697	0.0071	9.760
C35'	-1.2966	2.2111	6.4366	0.4714	0.0046	103.107
H25	-0.9462	5.8380	6.9893	0.0759	0.0461	1.646
H33	0.8809	0.3591	4.1315	0.2521	0.0635	3.969
H361	1.2412	1.6557	7.3866	-2.0885	0.0494	42.288
H362	0.7707	3.0639	8.1676	-2.1638	0.0484	44.751
H363	1.7986	3.1540	7.1516	-2.2535	0.0514	43.856

ANGLES BETWEEN NORMALS TO PLANES

PLANE(1)	DIRECTION COSINES			PLANE(2)	DIRECTION COSINES			ANGLE
1	-0.7462	0.0638	-0.6627	2	-0.7469	0.0640	-0.6618	0.07